Small Molecule Chemistry of Molybdenum and Titanium Tris Amido Complexes

by

Jonas Christopher Peters
B. Sc. Chemistry
University of Chicago
1993

Submitted to the Department of Chemistry
in Partial Fulfillment of the Requirements
for the Degree of

DOCTOR OF PHILOSOPHY
at the
MASSACHUSETTS INSTITUTE OF TECHNOLOGY
June 1998

Signature of Author_____
Department of Chemistry
May 18, 1998

Certified by_____
Christopher C. Cummins
Thesis Supervisor

Accepted by_____
Dietmar Seyferth
Chairman, Departmental Committee on Graduate Students

This doctoral thesis has been examined by a Committee of the Department of Chemistry as follows:

Professor Richard R. Schrock.....

Chairman

Professor Christopher C. Cummins.....

Thesis Supervisor

Professor Dietmar Seyferth.....

To My Parents
Mayleen Mendelson and
James Peters

– We'll drink to tonight, to hearts as light
To Love, as gay and fleeting.
As bubbles that swim, on the beaker's brim,
And break on the lips while meeting –

Herman Melville, Moby Dick

TABLE OF CONTENTS

Small Molecule Chemistry of Molybdenum and Titanium Tris Amido Complexes

Jonas Christopher Peters

Submitted to the Department of Chemistry, May 1998
Massachusetts Institute of Technology
in Partial Fulfillment of the Requirements for the Degree of
Doctor of Philosophy of Chemistry

Thesis Supervisor: Christopher C. Cummins

Title: Professor of Chemistry

Abstracts

Chapter 1. Dinitrogen Chemistry: Redox Facilitated Cleavage and Functionalization of N_2 using $Mo(N[R]Ar)_3$ and One Electron Reductants.

Enhancement of an N_2 cleavage reaction by $Mo(N[R]Ar)_3$ (R = $C(CH_3)(CD_3)_2$, Ar = 3,5-dimethylphenyl), and Na/Hg amalgam is presented. The reaction is facile at 25 °C and atmospheric dinitrogen pressure. The elusive terminal N_2 complex $(N_2)Mo(N[R]Ar)_3$ is trapped by Ti(N[*t*-Bu]-Ph)$_3$ to afford (Ph[*t*-Bu]N)$_3$Ti(μ-N_2)Mo(N[R]Ar)$_3$, which has been structurally characterized. The reactive dinitrogen complexes [Na(12-crown-4)$_2$][Mo(N_2)(N[R]Ar)$_3$] and [Na(THF)$_3$][(N_2)Mo(N[Ad]Ar)$_3$] (Ad = 1-adamantyl) have been isolated and structurally characterized. Oxidation of these complexes, both chemically and electrochemically, unequivocally establishes that $(N_2)Mo(N[R]Ar)_3$ dissociates readily into $Mo(N[R]Ar)_3$ and N_2 under one atmosphere of N_2. [Na][(N_2)Mo(N[Ad]Ar)$_3$] is used to form N-Si and N-C bonds in the syntheses of the silyldiazenido complex (Me_3SiNN)Mo-(N[Ad]Ar)$_3$ and the benzoyldiazenido complex (PhC(O)NN)Mo(N[Ad]Ar)$_3$. Synthetic and electrochemical data are presented to explain the observed redox enhancement of the N_2 cleavage reaction.

Chapter 2. Cyanide Chemistry: Reduction and Functionalization of Cyanide Bound to $Mo(N[R]Ar)_3$.

Cyanide anion is investigated as a potential synthon for the delivery of a carbido substituent to $Mo(N[R]Ar)_3$. (NC)Mo(N[R]Ar)$_3$ was prepared from (I)Mo(N[R]Ar)$_3$ and subsequently used to access the key dinuclear complex (μ-CN)[Mo(N[R]Ar)$_3$]$_2$ by direct condensation with $Mo(N[R]Ar)_3$. Reduction of (μ-CN)[Mo(N[R]Ar)$_3$]$_2$ by Na/Hg amalgam effects C-N bond cleavage at an anilido ligand and generates (Ar[R]N)$_2$(ArN)Mo(μ-NC)Mo(N[R]Ar)$_3$ by loss of a *tert*-butyl substituent. (Ar[R]N)$_2$(ArN)Mo(μ-NC)Mo(N[R]Ar)$_3$ has been structurally characterized. Direct deposition of cyanide anion to sterically encumbered $Mo(N[Ad]Ar)_3$ is accomplished cleanly with [N(*n*-Bu)$_4$][CN] to generate [N(*n*-Bu)$_4$][(NC)Mo(N[Ad]Ar)$_3$. This complex is used in the construction of a μ-CN linkage by direct reaction with IV(N[R]Ar_F)$_2$ (R = $C(CD_3)_2CH_3$, Ar = 2-fluoro-5-methylphenyl) in the synthesis of (Ar_F[R]N)$_2$V(μ-NC)Mo(N[Ad]Ar)$_3$, which has been structurally characterized.

Chapter 3. CO Chemistry: The Synthesis and Study of a Molecular Molybdenum Carbide Complex Featuring One-Coordinate Carbon.

CO is investigated as a potential synthon for the delivery of a carbido substituent to Mo(N[R]Ar)$_3$. (OC)Mo(N[R]Ar)$_3$ is prepared by addition of CO to Mo(N[R]Ar)$_3$. Reduction by Na/Hg amalgam cleanly generates [Na][(OC)Mo(N[R]Ar)$_3$], which has been structurally characterized as $\{(OEt_2)Na(OC)Mo(N[R]Ar)_3\}_2$. Functionalization of [(OC)Mo(N[R]Ar)$_3$]$^-$ with pivalylchloride, ClC(O)^{t}Bu, affords ^{t}BuC(O)-O-C≡Mo(N[R]Ar)$_3$, whose characterization includes an X-ray study. Metallic sodium effects C-O bond rupture in ^{t}BuC(O)-O-C≡Mo(N[R]Ar)$_3$ at the Mo–*C*–*O* linkage. This reaction is used synthetically to convert ^{t}BuC(O)-O-C≡Mo(N[R]Ar)$_3$ directly to HC≡Mo(N[R]Ar)$_3$. Subsequent deprotonation of HC≡Mo(N[R]Ar)$_3$ by *tert*-butyllithium and benzylpotassium provides the metallated carbides [Li][C≡Mo(N[R]Ar)$_3$] and [K][C≡Mo(N[R]Ar)$_3$], respectively, which are obtained as solvent free ion-pair complexes. [K][C≡Mo(N[R]Ar)$_3$] has been structurally characterized. Addition of 2.2.2-cryptand and 2 eq of benzo-15-crown-5 to [K][C≡Mo(N[R]Ar)$_3$] produces the terminal carbido complexes [K(2.2.2-crypt)][C≡Mo(N[R]Ar)$_3$] and [K(Benzo-15-crown-5)$_2$][C≡Mo(N[R]Ar)$_3$], respectively. [K(Benzo-15-crown-5)$_2$][C≡Mo(N[R]Ar)$_3$] has been structurally characterized and shown to be a discrete salt consisting of distinct [K(Benzo-15-crown-5)$_2$]$^+$ cations and [C≡Mo(N[R]Ar)$_3$]$^-$ anions. ^{13}C NMR data are presented showing that these carbide complexes feature signature ^{13}C NMR shifts in a range from 475 to 500 ppm. The chemical reactivity of [K][C≡Mo(N[R]Ar)$_3$] is explored in the synthesis of a variety of novel organometallic complexes including Cl_2PC≡Mo(N[R]Ar)$_3$, [K][S-CH_2CH_2C≡Mo(N[R]Ar)$_3$], [S-C≡Mo(N[R]Ar)$_3$]$^-$, [Se-C≡Mo(N[R]Ar)$_3$]$^-$, and [Te-C≡Mo(N[R]Ar)$_3$]$^-$. Anionic [Se-C≡Mo(N[R]Ar)$_3$]$^-$ has been structurally characterized as the discrete salt complex [K(Benzo-15-crown-5)$_2$][Se-C≡Mo(N[R]Ar)$_3$].

Abbreviations Used in the Text

Å	Angstrom (10^{-10} m)
Anal.	Analysis (Elemental)
Ar	3,5-dimethylphenyl
R	deuterated *tert*-Butyl group $C(CD_3)_2(CH_3)$
Ar_F	2-fluoro-5-methylphenyl
-N[R]Ar	anilido ligand where R = $C(CD_3)_2(CH_3)$ and Ar = 3,5-dimethylphenyl
-N[Ad]Ar	anilido ligand where Ad = 1-adamantyl and Ar = 3,5-dimethylphenyl
-N[R]Ar_F	anilido ligand where R = $C(CD_3)_2(CH_3)$ and Ar_F = 2-fluoro-5-methylphenyl
atm	Atmosphere
br	broad
Bu	Butyl
calcd.	calculated
cm^{-1}	wavenumber
Cp	C_5H_5 (cyclopentadienyl)
d	doublet
deg (°)	degrees
d^n	number of *d* electrons
eq	equivalents
eqn	equation
Et	Ethyl
$Cp_2Fe^{+/0}$	Ferrocene/Ferrocenium
G	Gauss
g	grams
h	hours
^1H	proton
^2H	deuteron
HOMO	Highest Occupied Molecular Orbital
Hz	Hertz (sec^{-1})
i-Pr	*iso*-Propyl
IR	Infrared
J	coupling constant in Hertz
K	degrees kelvin

LUMO	Lowest Unoccupied Molecular Orbital
m	multiplet
Me	Methyl
min	minutes
MO	Molecular Orbital
NMR	Nuclear Magnetic Resonance
ORTEP	Oak Ridge Thermal Elipsoid Plot
OTf	O_3SCF_3, triflate, trifluoromethanesulfonate
Ph	phenyl
ppm	parts per million
Pr	Propyl
q	quartet
s	singlet
SQUID	Superconducting QUantum Interference Device
t	triplet
t-Bu	*tert*-Butyl
THF	tetrahydrofuran
UV/vis	Ultra Violet-Visible
X	anionic One-Electron Donor Ligand
δ	chemical shift downfield from tetramethylsilane
$\Delta\nu_{1/2}$	peak width at half height
ν	stretching frequency
ε	extinction coefficient at wavelength of maximum optical absorption
λ_{max}	wavelength of maximum optical absorption
μ	magnetic moment, or bridging ligand
μ_B	Bohr magneton
μ_{eff}	effective magnetic moment

Chapter 1. N_2 Chemistry: Redox Facilitated Cleavage and Functionalization of Dinitrogen Using $Mo(N[R]Ar)_3$ and One Electron Reductants.

by Jonas C. Peters

MIT Department of Chemistry room 6-332
Massachusetts Institute of Technology

May 18, 1998

Contents

List of Figures

1 Introduction

Dinitrogen and related small nitrogenous molecules engender widespread interest in the inorganic community.[1] Our group's own interest in this regard was initiated by Laplaza and Cummins' report in 1995 on the isolation and characterization of $Mo(N[R]Ar)_3$, **1**.[2] This communication revealed a first glance at the unusual "azophilicity" of **1**. An exciting array of reactions were elucidated soon thereafter demonstrating that **1** was an avid N-atom acceptor, reacting with a variety of substrates such as aryl azides,[2] nitrous oxide,[2] Chisholm's $N{\equiv}Mo(O\mathit{t}Bu)_3$,[3] and molecular N_2[4] to afford a robust molybdenum nitrido complex characterized by a very strong Mo-N triple bond, $N{\equiv}Mo(N[R]Ar)_3$ **2**. The latter reaction, in which N_2 is the N-atom donor molecule, proceeds through the dinuclear complex $(\mu\text{-}N_2)\{Mo(N[R]Ar)_3\}_2$, **3**, featuring a linear dinitrogen ligand bridging two molybdenum centers. Dinuclear **3** is thermally unstable and at 25 °C splits apart into two equivalents of **2** with clean first order kinetics and a $t_{1/2}$ of approximately 30 minutes. This reaction is depicted below in eqn 3. A full manuscript detailing the dinitrogen cleavage reaction was published in 1996.[5] A variety of questions was motivated by this work, both with regard to the formation of the bridged intermediate **3** and with respect to the channeling of N_2 uptake along reaction pathways other than that ultimately leading to the thermodynamic sink **2**. With regard to the formation of dinuclear **3** the following points merit emphasis. When **1** was stirred at 25 °C under a dinitrogen atmosphere in solvents such as benzene, OEt_2 or tetrahydrofuran (THF), no build-up of intensely purple **3** was observed. In fact, at ambient temperatures **1** was stable in solution under a dinitrogen atmosphere and, by ^2H NMR spectroscopy, was the only detectable species in solution over a 24 h period. Infrared and Raman spectroscopy[5] corroborated this point in that no ν_{NN} stretch was observed when solution spectra of **1** were acquired under a dinitrogen atmosphere at 25 °C. The putative *terminal* dinitrogen complex $(N_2)Mo(N[R]Ar)_3$, **4**, shown in eqn 1, was not observed spectroscopically at temperatures ranging from -78 °C to 25 °C under one atmosphere of N_2. Incubation of **1** at -35 °C over a period of many hours effected the build-up of a significant concentration of dinuclear **3** that carried on cleanly to formation of **2** over a period of approximately 3 days. Dinuclear **3** showed a ^2H NMR signal at 13 ppm and featured a centrosymmetric ν_{NN} stretch at 1630 cm^{-1} in a Raman spectrum. No other species were spectroscopically observed. We have assumed that the mononuclear terminal dinitrogen complex **4** necessarily precedes formation of the dinuclear complex **3**. Because **4** has not been spectroscopically observable at low or ambient temperatures, we believe dinitrogen uptake by **1** to generate **4** is a reversible process, as indicated in eqn 1, lying far to the side of the two dissociated species ($K_{eq} \ll 1$). The irreversible production of intermediate **3** results from the bimolecular reaction between **4** and **1**, shown in eqn 2.

$$\underset{\mathbf{1}}{Mo(N[R]Ar)_3} + N_2 \rightleftharpoons \underset{\mathbf{4}}{(N_2)Mo(N[R]Ar)_3} \tag{1}$$

$$\underset{\mathbf{1}}{Mo(N[R]Ar)_3} + \underset{\mathbf{4}}{(N_2)Mo(N[R]Ar)_3} \longrightarrow \underset{\mathbf{3}}{(\mu\text{-}N_2)[Mo(N[R]Ar)_3]_2} \tag{2}$$

$$\underset{\mathbf{3}}{(\mu\text{-}N_2)[Mo(N[R]Ar)_3]_2} \longrightarrow 2\ \underset{\mathbf{2}}{N{\equiv}Mo(N[R]Ar)_3} \tag{3}$$

Against this backdrop we initiated an investigation to trap elusive $(N_2)Mo(N[R]Ar)_3$ **4** by reductants other than **1** itself with an eye on elaborating the dinitrogen chemistry of the reducing $Mo(N[R]Ar)_3$ template.

2 Results and Discussion

2.1 $Mo(N[R]Ar)_3$ + Na/Hg amalgam under a dinitrogen atmosphere. Observation of redox acceleration of the dinitrogen cleavage reaction.

Stirring THF solutions of **1** over stoichiometric Na/Hg under a dinitrogen atmosphere resulted in a rapid transformation at 25 °C. Initially displaying the bright orange color of **1**, these solutions acquired an intense purple color reminiscent of intermediate **3** within one hour. ^{2}H NMR spectroscopy revealed that a steady consumption of orange **1** coincided with the formation of the neutral dinuclear complex **3**. A new, sharper peak at 1.5 ppm, indicative of a diamagnetic species, was also observed. Fig 1 shows an FTIR spectrum of this solution featuring an intense ν_{NN} vibration at 1761 cm^{-1}. Other stretches appearing in this spectrum are typical of complexes bearing the –N[R]Ar ligand. The most prominent are those at 1596 and 1583 cm^{-1} arising from aryl ν_{CC} vibrations. An FTIR spectrum of pure **1** is shown in Fig 2 for comparison. As the reaction mixture was stirred over a period of several hours the intense purple color gradually diminished, and the final solution settled to a red-brown. ^{2}H NMR spectroscopy of the reaction products revealed complete consumption of both the starting material **1** and intermittently formed **3**. A ^{1}H NMR spectrum of this crude product mixture indicated that nitride **2** had formed in 85 % yield. Approximately 10 % of a new diamagnetic side product was also present, displaying one set of anilido ligand resonances in addition to those for solvated THF. A solution FTIR spectrum of this mixture still showed the presence of the ν_{NN} at 1761 cm^{-1}, its intensity diminished when compared to spectra acquired at earlier reaction times. Based in part on literature precedent provided by Schrock[6] and coworkers we tentatively assigned the new diamagnetic side product as an anionic dinitrogen complex $[(N_2)Mo(N[R]Ar)_3]^-$, [**5**], with a THF-solvated sodium cation $[Na^+(THF)_x]$. These observations are depicted in eqn 4. The anionic N_2 containing species will be referred to as the ion-pair complex $[Na][(N_2)Mo(N[R]Ar)_3]$, or more simply as [Na][**5**].

$$\underset{\mathbf{1}}{Mo(N[R]Ar)_3} \xrightarrow{N_2,\ Na/Hg} 85\ \%\ \underset{\mathbf{2}}{N{\equiv}Mo(N[R]Ar)_3} + 10\ \%\ \underset{[Na][\mathbf{5}]}{[Na][(N_2)Mo(N[R]Ar)_3]} \quad (4)$$

These observations were reproducible with the following caveat: the product ratio of neutral **2** to anionic [**5**] was variable and depended on factors such as the rate of stirring of the heterogeneous solution and the concentration of unreacted **1** present throughout the reaction. Individual experiments resulted in virtually quantitative formation of **2** without appreciable quantities of [**5**], as well as in significantly higher yields (25 – 50 %) of the anionic dinitrogen species [**5**]. This suggested that the overall reaction pathway depended heavily on both the concentration of unreacted **1** present in solution during the reaction, as well as on the rate of reduction by the sodium

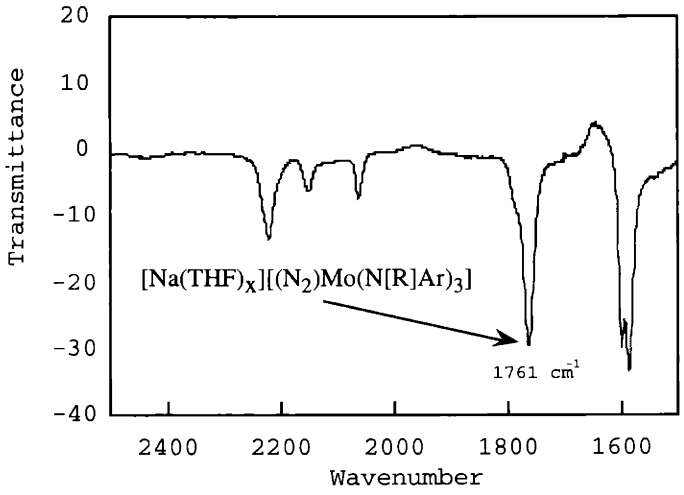

Figure 1: IR spectrum of an aliquot taken from a THF solution of $Mo(N[R]Ar)_3$ stirring over Na/Hg amalgam for 1 h under N_2 showing the intense ν_{NN} band of $[Na][(N_2)Mo(N[R]Ar)_3]$, [Na][**5**].

amalgam. Importantly, when product mixtures containing a significant percentage of [Na][**5**] were exposed to *additional* $Mo(N[R]Ar)_3$ under an N_2 atmosphere the *neutral* bridged complex **3** was generated rapidly. These qualitative observations are summarized below:

- Under an N_2 atmosphere $[(N_2)Mo(N[R]Ar)_3]^-$, [**5**], is capable of rapidly generating **3** from **1** at *room temperature.*
- The overall reaction pathway, i.e. that pathway leading to appreciable yields of [**5**] versus the cleavage product $N{\equiv}Mo(N[R]Ar)_3$, **2**, dramatically depended on two factors.
  1. The concentration of unreacted **1** present in solution.
  2. The rate of reduction by the sodium amalgam.

The redox-facilitated cleavage/functionalization reaction of eqn 4, initially confusing and unpredictable, provided an interesting chemical puzzle to which the rest of this chapter is devoted.

2.2 $Mo(N[R]Ar)_3$ + Na/Hg amalgam under argon.

$Mo(N[R]Ar)_3$ **1** proved stable to excess Na/Hg amalgam under an argon atmosphere. Very little decay of **1** was observed in THF over a period of 24 h at 25 °C when stirred over a 0.4 % Na/Hg amalgam. The amount of decay was consistent with typical decomposition of **1** in THF solution in the absence of the Na/Hg reductant. *Na/Hg amalgam does not appear to reduce* **1** *directly.* Initially we considered the possibility that Na/Hg reduced **1** to generate an anionic $[Mo(N[R]Ar)_3]^-$ species, which was subsequently and rapidly trapped by N_2 to generate [**5**]. This is outlined in eqns 5 and 6, respectively. The lack of reactivity between **1** and Na/Hg amalgam, as well as the electrochemical

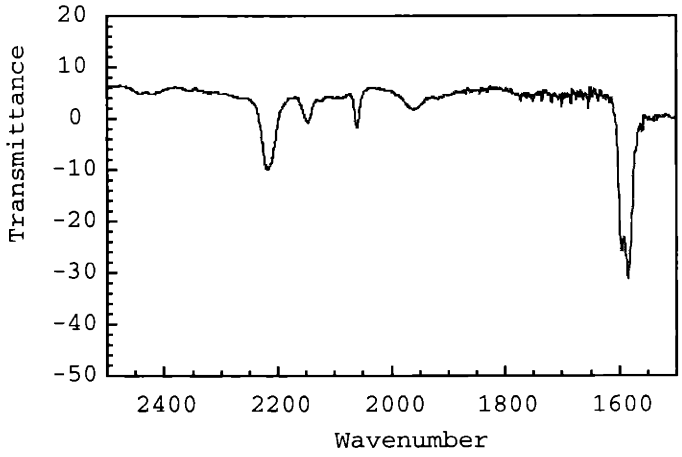

Figure 2: IR spectrum of $Mo(N[R]Ar)_3$, in THF solution under N_2.

stability of **1** at potentials as low as -2.8 V in THF (*vide infra*), renders this model an unlikely explanation for the generation of [**5**] by Na/Hg amalgam under N_2. It seemed likely that neutral $(N_2)Mo(N[R]Ar)_3$, present in low but significant concentration, was the electron accepting species as shown in eqn 7. Notably, in a full manuscript which included electrochemical data Floriani and coworkers recently reported that the anionic species $[(THF)V(Mes)_3]^-$ (Mes = 2,4,6-$Me_3C_6H_2$), isoelectronic to neutral $Mo(N[R]Ar)_3$, binds N_2 readily.[7]

$$\underset{\mathbf{1}}{Mo(N[R]Ar)_3} \underset{}{\overset{Na/Hg}{\rightleftharpoons}} [Mo(N[R]Ar)_3]^- \tag{5}$$

$$[Mo(N[R]Ar)_3]^- + N_2 \longrightarrow \underset{[\mathbf{5}]}{[(N_2)Mo(N[R]Ar)_3]^-} \tag{6}$$

$$\underset{\mathbf{4}}{(N_2)Mo(N[R]Ar)_3} \xrightarrow{Na/Hg} \underset{[Na][\mathbf{5}]}{[Na][(N_2)Mo(N[R]Ar)_3]} \tag{7}$$

2.3 Synthesis of $(Ph[t\text{-}Bu]N)_3Ti(\mu\text{-}N_2)Mo(N[R]Ar)_3$.

Once generated, $[(N_2)Mo(N[R]Ar)_3]^-$ was stable in solution in the *absence* of $Mo(N[R]Ar)_3$. In the *presence* of $Mo(N[R]Ar)_3$, $[(N_2)Mo(N[R]Ar)_3]^-$ was a viable precursor to $(\mu\text{-}N_2)\{Mo(N[R]Ar)_3\}_2$ by way of a bimolecular pathway. We reasoned that a bulky one electron reductant might yield a dinitrogen complex that is sterically inaccessible to **1**, thereby prohibiting bimolecular reaction pathways subsequent to the reduction step. $Ti(N[t\text{-}Bu]Ph)_3$, **6**, was a viable candidate for this task. Green **6** and its analogue $Ti(N[R]Ar)_3$ have shown facile and clean solution chemistry in their ability to act as soluble and sterically encumbered one electron reductants.[8,9] When stoichiometric

amounts of **1** and **6** were stirred in OEt_2 under a dinitrogen atmosphere at 25 °C, the initially olive green solution gradually lightened in color, and over the course of a 15 h period, deposited a deep orange solid. The product $(Ph[t\text{-}Bu]N)_3Ti(\mu\text{-}N_2)Mo(N[R]Ar)_3$, **7**, was isolated and characterized in 81 % yield. This reaction is shown in eqn 8.

$$\underset{\mathbf{1}}{Mo(N[R]Ar)_3} + \underset{\mathbf{6}}{Ti(N[t\text{-}Bu]Ph)_3} \xrightarrow{N_2} \underset{\mathbf{7}}{(Ph[t\text{-}Bu]N)_3Ti(\mu\text{-}N_2)Mo(N[R]Ar)_3} \quad (8)$$

Complex **7** is robust in both solution and in the solid state and, as expected, does not react with $Mo(N[R]Ar)_3$. ^1H NMR spectroscopy supported the formulation of a complex containing two independent ligand environments, with one unique set for the three –N[R]Ar ligands coordinating the molybdenum center and another unique set for the three –N[*t*-Bu]Ph ligands surrounding titanium. That **7** was sterically crowded was manifested by a significant broadening of the resonances corresponding to protons both in the *ortho* positions of the aryl rings and in the *tert*-butyl groups of the respective anilido ligands. These signals sharpened upon warming. An FTIR spectrum of **7** confirmed the presence of the bridging dinitrogen ligand with a ν_{NN} at 1575 cm^{-1}. Because this region of the spectrum was complicated by the presence of rather intense anilido ν_{CC} vibrations, a $^{15}N_2$ labeled derivative, $(Ph[t\text{-}Bu]N)_3Ti(\mu\text{-}^{15}N_2)Mo(N[R]Ar)_3$, was prepared. A shift in ν_{NN} from 1575 cm^{-1} to 1524 cm^{-1} was consisent with a simple harmonic oscillator model (ca. 1522 cm^{-1}). The difference FTIR spectrum of the labeled and unlabeled complexes is shown in Fig 3. The ^{15}N NMR spectrum of $(Ph[t\text{-}Bu]N)_3Ti(\mu\text{-}^{15}N_2)Mo(N[R]Ar)_3$ showed doublets at 437.15 and 433.09 ppm relative to liquid ammonia (0 ppm) with a $^1J_{NN}$ of 12.6 Hz. **7** was recrystallized from pentane, and single crystals suitable for an X-ray diffraction study were obtained from a pentane solution stored at -35 °C. A thermal ellipsoid representation of **7** is shown in Figure 4. The complex displays a dinitrogen ligand sandwiched linearly with respect to the Mo-N-N-Ti axis. Each metal center adopts a pseudo-tetrahedral geometry, and the N_2 ligand rests in the aliphatic pocket provided by the *tert*-butyl groups of the respective anilido ligands. The *tert*-butyl groups are all directed in the usual "upward" fashion towards what may be regarded as the center of the molecule. They adopt a staggered conformation with an average N-Ti-Mo-N dihedral angle of ca. 18°. The Mo-N(7) bond length of 1.787(3)Å is indicative of strong π-bonding to the dinitrogen ligand by the $Mo(N[R]Ar)_3$ portion of the complex. This distance is significantly shorter than the Mo-N bonding distances to the anilido ligands (avg. = 1.968Å). The Ti-N(8) distance of 1.880(3)Å suggests a lesser degree of π-bonding by the $Ti(N[t\text{-}Bu]Ph)_3$ portion of the molecule to the N_2 ligand. The N(8)-N(7) bond length of 1.229(4)Å manifests an appreciable degree of cooperative dinitrogen reduction by the respective *tris*-anilido molybdenum and titanium complexes.

Most importantly, the *tris*-anilido complexes **6** and **1** did not react when stirred in OEt_2 at 25 °C under an argon atmosphere. While several reports in the literature show that low valent amido complexes of titanium can exhibit dinitrogen chemistry,[10,11] studies of the solution chemistry of **6** and related $Ti(N[R]Ar)_3$ have not revealed any independent propensity for reactivity with dinitrogen. Similarly, dinitrogen chemistry was not reported for Wolczanski's related $Ti(O\text{-}Si^tBu_3)_3$.[12,13] Taken collectively, these results indicate that the formation of **7** results from the capture of $(N_2)Mo(N[R]Ar)_3$, **4**, by reactive $Ti(N[t\text{-}Bu]Ph)_3$, **6**, in a classical inner-sphere electron transfer reaction as first described by Taube.[14] Like the reductant Na/Hg amalgam, **6** *reacts readily*

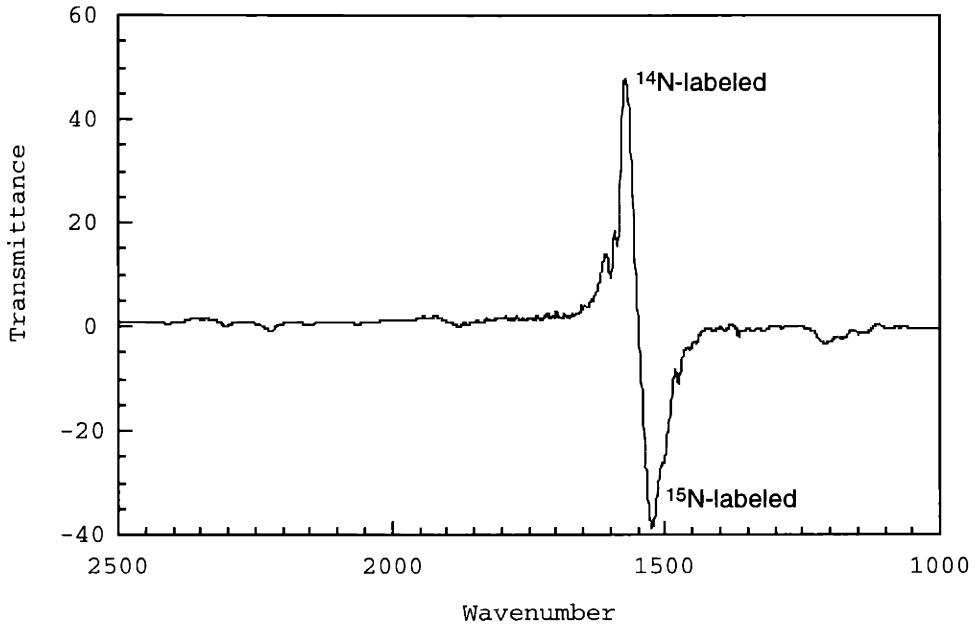

Figure 3: Difference FTIR spectrum (KBr/CH_2Cl_2) showing the intense ν_{NN} stretching vibration for (Ph[*t*-Bu]N)$_3$Ti(μ-N_2)Mo(N[R]Ar)$_3$, **7**, and its ^{15}N-labeled analogue (Ph[*t*-Bu]N)$_3$Ti($^{15}\mu$-N_2)Mo(N[R]Ar)$_3$.

with **4** at 25 °C whereas three-coordinate Mo(N[R]Ar)$_3$ itself *does not.*

2.4 Dinitrogen Chemistry of *tris*-anilido Molybdenum Complexes Bearing Bulky –N[Ad]Ar Substituents.

The successful trapping of elusive (N_2)Mo(N[R]Ar)$_3$ by the bulky Ti(N[*t*-Bu]Ph)$_3$ reductant encouraged us to focus on the clean isolation of an anionic "MoN_2^-" species. Because the clean generation of [(N_2)Mo(N[R]Ar)$_3$]$^-$ was hampered by bimolecular chemistry that eventually led to N≡Mo(N[R]Ar)$_3$ as the dominant reaction product (eqn 4), it seemed that providing the anilido ligands with an even greater degree of steric bulk might allow the clean generation of a MoN_2^- species stable to bimetallic decomposition pathways. Replacement of the *tert*-butyl groups of –N[R]Ar with bulkier 1-adamantyl (Ad) substituents, –N[Ad]Ar, afforded a three-coordinate molybdenum complex Mo(N[Ad]Ar)$_3$, **8**, where bimolecular dinitrogen chemistry seemed unlikely on steric grounds. Ryan Sutherland was the first to prepare and study **8**.[15] Its synthesis was difficult in comparison to that of **1** and was not highly reproducible. In setting out to use **8** in the dinitrogen chemistry described here, it was first necessary to find a reproducible synthesis and to elucidate its complete characterization.

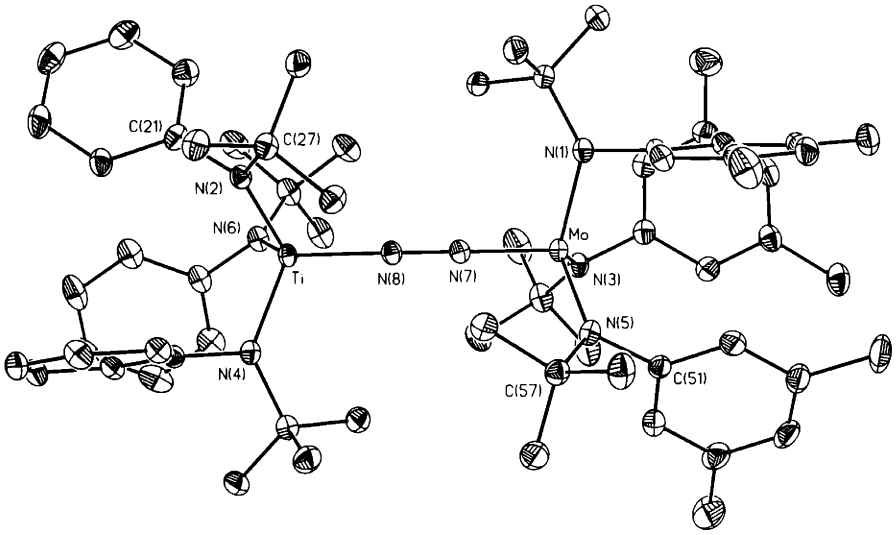

Figure 4: 35 % thermal ellipsoid representation of (Ph[*t*-Bu]N)$_3$Ti(μ-N$_2$)Mo(N[R]Ar)$_3$, **7**, from X-ray coordinates. Selected distances (Å) and angles (°): Mo-N(7), 1.787(3); Ti-N(8), 1.880(3); N(7)-N(8), 1.229(4); Mo-N(1), 1.969(3); Mo-N(3), 1.971(3); Mo-N(5), 1.963(3); Ti-N(2), 1.956(3); Ti-N(4), 1.951(3); Ti-N(6), 1.954(3); N(7)-Mo-N(1), 102.59(13); N(7)-Mo-N(3), 103.17(13); N(7)-Mo-N(5), 104.03(13); N(5)-Mo-N(1), 113.23(13); N(5)-Mo-N(3), 115.22(13); N(1)-Mo-N(3), 116.25(13). N(8)-Ti-N(6), 109.87(87); N(8)-Ti-N(2), 111.11(13); N(8)-Ti-N(4), 109.98(13); N(4)-Ti-N(6), 109.09(13); N(4)-Ti-N(2), 108.80(13); N(6)-Ti-N(2), 107.93(13).

2.5 Synthesis of Mo(N[Ad]Ar)$_3$.

The synthesis of **8**, shown in eqn 9, followed a protocol similar to that originally described for **1**, whereby addition of 2 eq of the lithium salt Li(N[Ad]Ar) to $MoCl_3(THF)_3$ in OEt_2 effected the desired transmetallation reaction.[2] Undesired side reactions required that the resulting crude product be further purified. Analytically pure **8** is bright yellow-orange in color, significantly lighter in shade than Mo(N[R]Ar)$_3$. The crude product, initially isolated in darker shades, was extracted into a pentane–benzene mixture and further filtered through Celite to remove residual HN[1-Ad]Ar impurities—the use of benzene serving to selectively solubilize **8**, helping to separate it from the HN[Ad]Ar impurities. This was somewhat problematic because both **8** and HN[Ad]Ar have limited solubility in pentane and in OEt_2. Multigram quantities of **8** were obtained reproducibly in yields typically ranging from 35–50 % based on the starting lithium salt. Like that obtained for Mo(N-[R]Ar)$_3$, a solution magnetic susceptibility measurement obtained by the method of Evans for **8** was consistent with a quartet ground state (μ_{eff} = 2.96 μ_B).[16,17] Infrared spectra (CaF_2, THF) of **8** showed two signature bands at 1597 and 1583 cm^{-1} resulting from the aryl ν_{CC} vibrations of the –N[Ad]Ar ligands. **8** was stable in the solid state for long periods at 25 °C and, once properly purified, provided a sturdy manifold for the molybdenum(III) dinitrogen chemistry of interest. Single crystals of **8** deposited from an OEt_2 solution on standing at 25 °C and a thermal ellipsoid representation of **8** is shown in Figure 5. As anticipated, the molybdenum center adopts a trigonal planar geometry and is well-caged by the extremely encumbering *tris*-anilido ancillary ligands. In stark contrast to Mo(N[R]Ar)$_3$, three-coordinate **8** did not react in a bimolecular fashion with dinitrogen (eqn 10) to form a dinuclear species (μ-N_2)[Mo(N[Ad]Ar)$_3$]$_2$. Solutions of **8** were indefinitely stable under a dinitrogen atmosphere at -35 °C.

$$2\ \text{LiN[Ad]Ar} + \text{MoCl}_3(\text{THF})_3 \longrightarrow \underset{\mathbf{8}}{\text{Mo(N[Ad]Ar)}_3} \qquad (9)$$

$$\underset{\mathbf{8}}{\text{Mo(N[Ad]Ar)}_3} \xrightarrow{N_2} \textbf{No Rxn} \qquad (10)$$

2.6 Mo(N[Ad]Ar)$_3$ + Na/Hg amalgam under N_2. Isolation of anionic [(N_2)Mo-(N[Ad]Ar)$_3$]$^-$.

As shown in eqn 11, when a THF solution of **8** was stirred over a 0.4 % Na/Hg amalgam under a dinitrogen atmosphere at 25 °C, the anionic dinitrogen complex [Na][(N_2)Mo(N[Ad]Ar)$_3$], [Na][**9**], was the major species produced. This species may be equivalently formulated as [Na(THF)$_x$][**9**] when THF is present to solvate the Na^+ cation (*vide infra*). While the lack of deuterium incorporation in the –N[Ad]Ar ligands removed ^{2}H NMR spectroscopy as a viable spectroscopic probe, it was found that the formation of [**9**] was easily monitored by IR spectroscopy. [**9**] displayed two distinct ν_{NN} bands at 1783 and 1757 cm^{-1} in THF solution, as shown in Fig 6, and its formation was complete within several hours. The observation of two distinct ν_{NN} bands for [**9**] was surprising since only one band at 1761 cm^{-1} was observed under similar conditions in the Mo(N[R]Ar)$_3$ system

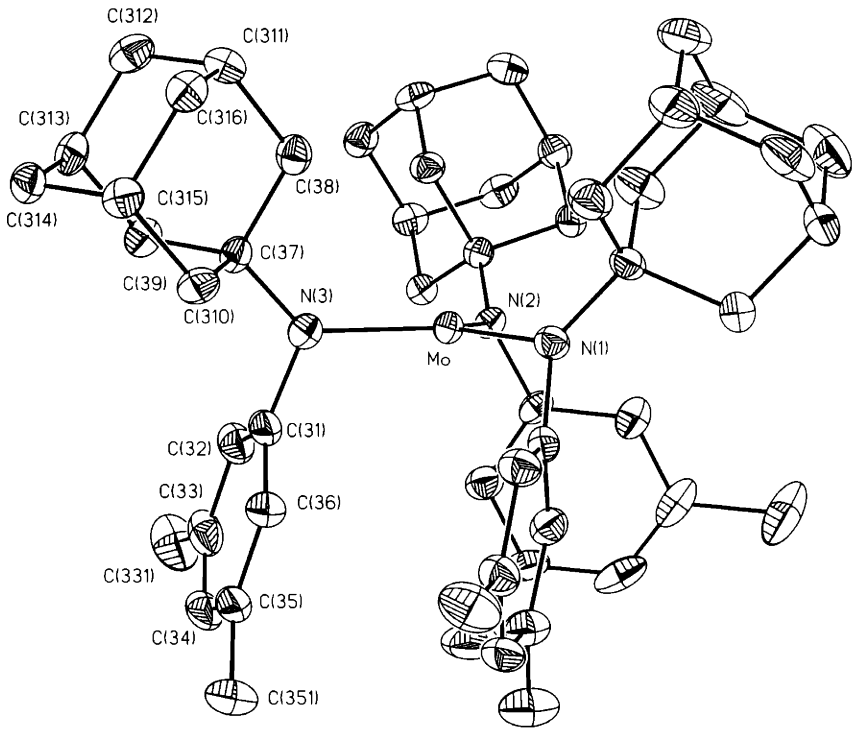

Figure 5: 35 % thermal ellipsoid representation of Mo(N[Ad]Ar)$_3$, **8**, from X-ray coordinates. Selected distances (Å) and angles (°): Mo-N(1), 1.989(3); Mo-(N2), 1.974(3); Mo-N(3), 1.958(3); N(1)-C(11), 1.429(5); N(1)-C(17), 1.485(5); N(2)-C(21), 1.435(5); N(2)-C(27), 1.481(5); N(3)-C(31), 1.450(5); N(3)-C(37), 1.484(5); N(3)-Mo-N(2), 121.55(13); N(3)-Mo-N(1), 118.01(14); N(2)-Mo-N(1), 120.17(13); C(11)-N(1)-C(17), 122.3(3); C(11)-N(1)-Mo, 109.5(2); C(17)-N(1)-Mo, 128.1(2); C(21)-N(2)-C(27), 117.9(3); C(21)-N(2)-Mo, 109.9(2); C(27)-N(2)-Mo, 132.2(2); C(31)-N(3)-C(37), 118.9(3); C(31)-N(3)-Mo, 110.0(2); C(37)-N(3)-Mo, 131.0(3).

(Fig 1). Curiously, this phenomenon has been a somewhat general result for complexes containing the –N[Ad]Ar ligand set. For example, the neutral carbonyl complex (OC)Mo(N[Ad]Ar)$_3$ exhibits two ν_{CO} stretches, whereas (OC)Mo(N[R]Ar)$_3$ exhibits only one. Similarly, the anionic cyanide complex [Li][(NC)Mo(N[Ad]Ar)$_3$], discussed in Chapter 2, shows two ν_{CN} stretches in THF. It is tempting to suggest that this phenomenon arises from conformational isomers present in solution, easily detectable on the fast time scale of IR spectroscopy. For instance, it is possible that complexes bearing the adamantyl anilido ligands are perturbed from their typical "upward" arrangement, as manifested in the X-ray structure of Mo(N[Ad]Ar)$_3$ (Fig 5), when dissolved in solvents such as OEt_2 and THF. Stated more simply, if solution structures of both C_3 and C_s symmetry are possible for complexes with an Mo(N[Ad]Ar)$_3$ core, one would anticipate *two* distinct vibrations for complexes bearing *one* N_2, CN, or CO ligand. However, it must be noted that *all* of the solid state structures obtained for complexes bearing the –N[Ad]Ar ligand show an upward, pseudo-C_3 arrangement of the three adamantyl substituents. Hence, although it seems plausible, we lack structural data supporting an explanation which invokes conformational isomerism in solution.

[Na][**9**] is scarlet in the presence of donor solvents such as THF or OEt_2 but precipitates as an orange solid when submerged in hydrocarbons such as pentane or benzene. ^{1}H NMR spectroscopy showed that this color change coincided with complete or near complete loss of the donor solvent molecules which solvate the Na^+ cation. The orange solid was virtually insoluble in pentane, and its isolation and purification as the solvent-free complex [Na][(N_2)Mo(N[Ad]Ar)$_3$] in ca. 64 % yield was straightforward. Orange [Na][**9**] is stable in the solid state, both under a dinitrogen atmosphere and under vacuum. Its scarlet color returned upon dissolution in OEt_2 and THF. Like Mo(N[R]-Ar)$_3$, three-coordinate **8** did not react with 0.4 % Na/Hg under an argon atmosphere, suggesting that the N_2 binding step precedes reduction in the generation of [**9**].

$$\underset{\mathbf{8}}{\text{Mo(N[Ad]Ar)}_3} \xrightarrow{\text{Na/Hg, THF}} \text{[Na(THF)}_x\text{][(N}_2\text{)Mo(N[Ad]Ar)}_3\text{]} \qquad (11)$$

2.7 X-ray Structure of [Na(THF)$_3$][(N_2)Mo(N[Ad]Ar)$_3$].

An X-ray diffraction study on a single crystal of [Na(THF)$_3$][**9**], grown from heptane–THF, revealed an ion-paired dinitrogen complex in which a Na^+ cation is coordinated by three THF molecules, in addition to the β-nitrogen atom of the N=N=Mo(N[Ad]Ar)$_3$ core at a Na-N(5) distance of 2.21(2)Å (Fig 7). The dinitrogen ligand itself sits symmetrically on the pseudo-C_3 axis of the *tris*-anilido molybdenum fragment and does not extend beyond the pocket provided by the three adamantyl substituents. Its structural elucidation provides a simple pictorial explanation of how the steric inaccessibility of the bridged N_2 complex (μ-N_2)[Mo(N[Ad]Ar)$_3$]$_2$, makes the synthesis of [**9**] straightforward.

While bimetallic complexes featuring a bridging dinitrogen ligand are prominent in the literature,[5] structurally characterized examples in which one of the metal centers is an alkali metal are rare.[18–21] Schrock et al. reported in 1994[6] that, under the appropriate conditions, Na/Hg effected the transformation of a molybdenum(IV) triflato complex, [($C_6F_5NCH_2CH_2$)$_3$N]Mo(OTf), to an anionic dinitrogen complex formulated as [($C_6F_5NCH_2CH_2$)$_3$N]Mo(N_2)][Na(OEt_2)$_x$]. Although structural

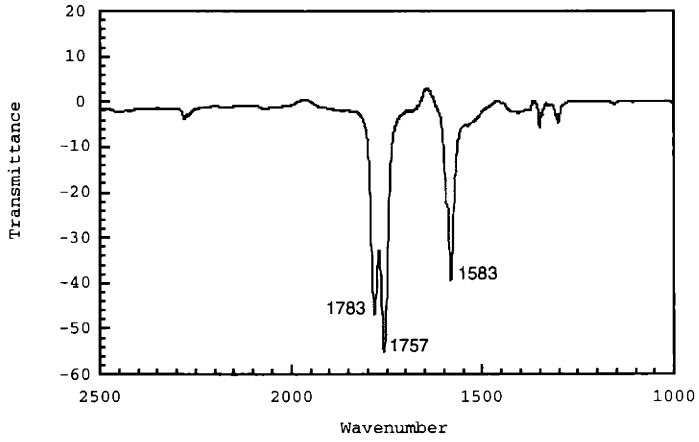

Figure 6: IR spectrum of a direct aliquot taken from a THF solution of $Mo(N[Ad]Ar)_3$ stirring over Na/Hg for 1 h under N_2. Two intense ν_{NN} bands for $[Na(THF)_x][(N_2)Mo(N[Ad]Ar)_3]$, [Na][**9**], are apparent at 1783 and 1757 cm^{-1}.

data was not reported for this complex, its reaction chemistry revealed nucleophilic character at the β-nitrogen atom. Hence, $[(C_6F_5NCH_2CH_2)_3N]$Mo-N=N-Si(iPr)$_3$ and $[(C_6F_5NCH_2CH_2)_3N]$Mo-N=N-$SnBu_3$ were obtained by treatment of $[(C_6F_5NCH_2CH_2)_3N]Mo(N_2)][Na(OEt_2)_x]$ with ClSi(i-Pr)$_3$ and $ClSnBu_3$, respectively. Recently, O'Donoghue and Schrock have extended this work to a host of related dinitrogen complexes bearing a "$[(Me_3SiNCH_2CH_2)_3N]Mo(N_2)$" core.[22,23]

2.8 Reaction of $[(N_2)Mo(N[Ad]Ar)_3]^-$ with $ClSiMe_3$. Synthesis of $(Me_3SiNN)Mo(N[Ad]Ar)_3$.

Addition of $ClSiMe_3$ to an ethereal solution of [Na][**9**] unveiled the nucleophilic nature of the anionic core. A change in color from the scarlet of solvated $[Na(OEt_2)_x]$[**9**] to bright yellow occurred instaneously at 25 °C. Following salt removal a ^1H NMR spectrum of the crude product mixture showed the expected resonance for a –SiMe_3 group and confirmed a nearly quantitative conversion to the anticipated silyldiazenido complex $(Me_3SiNN)Mo(N[Ad]Ar)_3$, **10**, as shown in eqn 12. An IR spectrum of **10** showed a dramatic shift from the intense ν_{NN} vibration at 1761 cm^{-1} of [**9**] to a very broad absorbance centered at 1646 cm^{-1}.

$$\underset{[Na][\mathbf{9}]}{[Na][(N_2)Mo(N[Ad]Ar)_3]} + ClSiMe_3 \xrightarrow{-\ NaCl} \underset{\mathbf{10}}{(Me_3SiNN)Mo(N[Ad]Ar)_3} \qquad (12)$$

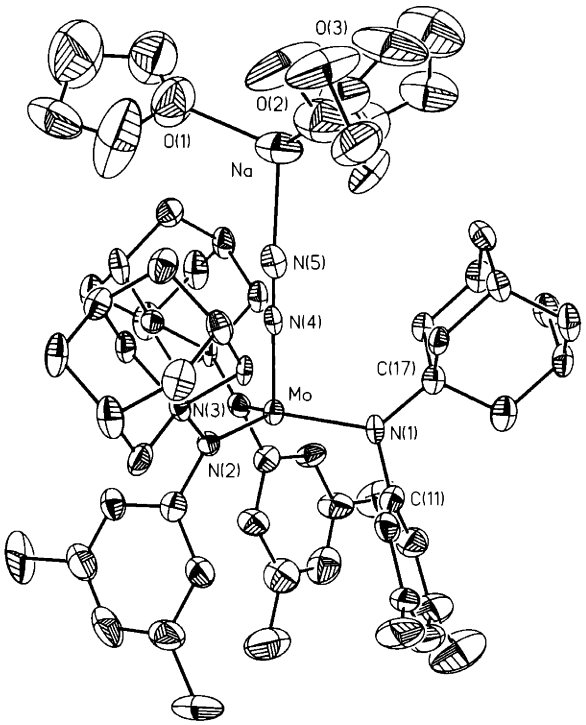

Figure 7: 35 % thermal ellipsoid representation of $[Na(THF)_3][(N_2)Mo(N[Ad]Ar)_3]$, $[Na(THF)_3][\mathbf{9}]$, from X-ray coordinates. Selected bond distances (Å) and angles (°): Mo-N(1), 2.005(10); Mo-(N2), 2.011(11); Mo-N(3), 2.043(11); Mo-N(4), 1.85(2); N(4)-N(5), 1.16(2); Na-O(1), 2.20(2); Na-O(2), 2.26; Na-O(3), 2.20(2); Na-N(5), 2.21(2); N(1)-Mo-N(3), 115.6(4); N(1)-Mo-N(2), 119.1(4); N(2)-Mo-N(3), 119.9(4); N(4)-Mo-N(1), 98.5(5); N(4)-Mo-N(2), 97.1(5); N(4)-Mo-N(3), 97.8; N(4)-N(5)-Na, 177.1(11); N(5)-N(4)-Mo, 179.2(11); O(1)-Na-N(5), 110.6(7); O(2)-Na-N(5), 109.5(7); O(3)-Na-N(5), 113.8(7).

2.9 Reaction of $[(N_2)Mo(N[Ad]Ar)_3]^-$ with PhC(O)Cl. Synthesis of $(PhC(O)NN)Mo(N[Ad]Ar)_3$.

The addition of benzoyl chloride to a cold ethereal solution of [Na][**9**] effected N-C bond formation with concomitant salt elimination (eqn 13). The reaction was not quantitative, and the orange, crystalline benzoyldiazenido product $(PhC(O)NN)Mo(N[Ad]Ar)_3$, **11**, was obtained in 45 % yield from the greenish reaction solution that resulted upon mixing. By analogy to the Curtius rearrangement we wondered whether **11** might exhibit a tendency to thermally rearrange to phenylisocyanate and $N{\equiv}Mo(N[Ad]Ar)_3$.[24] No $N{\equiv}Mo(N[Ad]Ar)_3$ was generated from a benzene solution of **11** maintained at 75 °C for 2 hours.

$$\underset{[Na][\mathbf{9}]}{[Na][(N_2)Mo(N[Ad]Ar)_3]} + PhC(O)Cl \xrightarrow{-NaCl} \underset{\mathbf{11}}{(PhC(O)NN)Mo(N[Ad]Ar)_3} \quad (13)$$

The reactions shown in equations 12 and 13 suggest that $[^-N{=}N{=}Mo(N[Ad]Ar)_3]$ is an appropriate resonance description for the anionic core of [**9**]. The β-nitrogen atom should be regarded as nucleophilic with localized partial negative charge.

The use of transition metals to coordinate and activate dinitrogen gas, thereby making it a more reactive and more easily functionalized molecule, remains a challenging area of interest.[25] The construction of N-C and N-Si bonds from nitrogen bound to zero-valent, d^6 Mo and W cores has been reported for metal centers bearing phosphine and macrocyclic thioether coligands.[25] Chatt and coworkers reported the first examples of N-C bond formation from metal-coordinated dinitrogen in 1972.[26] Hidai has reported the molecular structure of the benzoyldiazenido complex *trans*-$[Mo(Cl)(NNC(O)Ph)(Ph_2PCH_2CH_2PPh_2)_2]$.[27] Noteworthy for comparison, the complexes *trans*-$[M(N_2)_2(Ph_2PCH_2CH_2PPh_2)_2]$ (M = Mo,W) reacted with *iodotrimethylsilane* at 50 °C in benzene to afford silyldiazenido complexes *trans*-$[M(I)(NNSiMe_3)(Ph_2PCH_2CH_2PPh_2)_2]$, but no direct reaction was observed with *chlorotrimethylsilane* under analogous conditions.[25] As described above, $[(N_2)Mo(N[Ad]Ar)_3]^-$ reacts readily and cleanly with chlorotrimethylsilane. Some of the salient features of the dinitrogen chemistry of $Mo(N[Ad]Ar)_3$ are summarized in Fig 8.

2.10 Synthesis and Isolation of $[(N_2)Mo(N[R]Ar)_3]^-$.

The success of the titanium(III) trapping of $(N_2)Mo(N[R]Ar)_3$ to give **7**, and the clean isolation and structural characterization of $[Na(THF)_3][(N_2)Mo(N[Ad]Ar)_3]$ encouraged us to re-focus our efforts on understanding the redox-facilitated dinitrogen cleavage reaction of $Mo(N[R]Ar)_3$ shown in eqn 4. Inevitably, the clean isolation of [**5**] relied upon circumventing a subsequent bimolecular reaction between unreacted **1** and [**5**]. This requirement was met in part by the utilization of a large excess of Na/Hg amalgam. Additionally, a low concentration of **1** should disfavor the bimolecular decomposition pathway of [**5**]. This latter requirement was fulfilled by a slow addition of **1** to an amalgam containing solvent mixture. In a typical experiment, a dilute solution of **1** was added dropwise, very slowly, to a vigorously stirring mixture of Na/Hg in THF under a dinitrogen atmosphere. The rate of addition was determined empirically by an array of attempts until conditions were found in which the intense purple color of the undesired bridged species **3** was

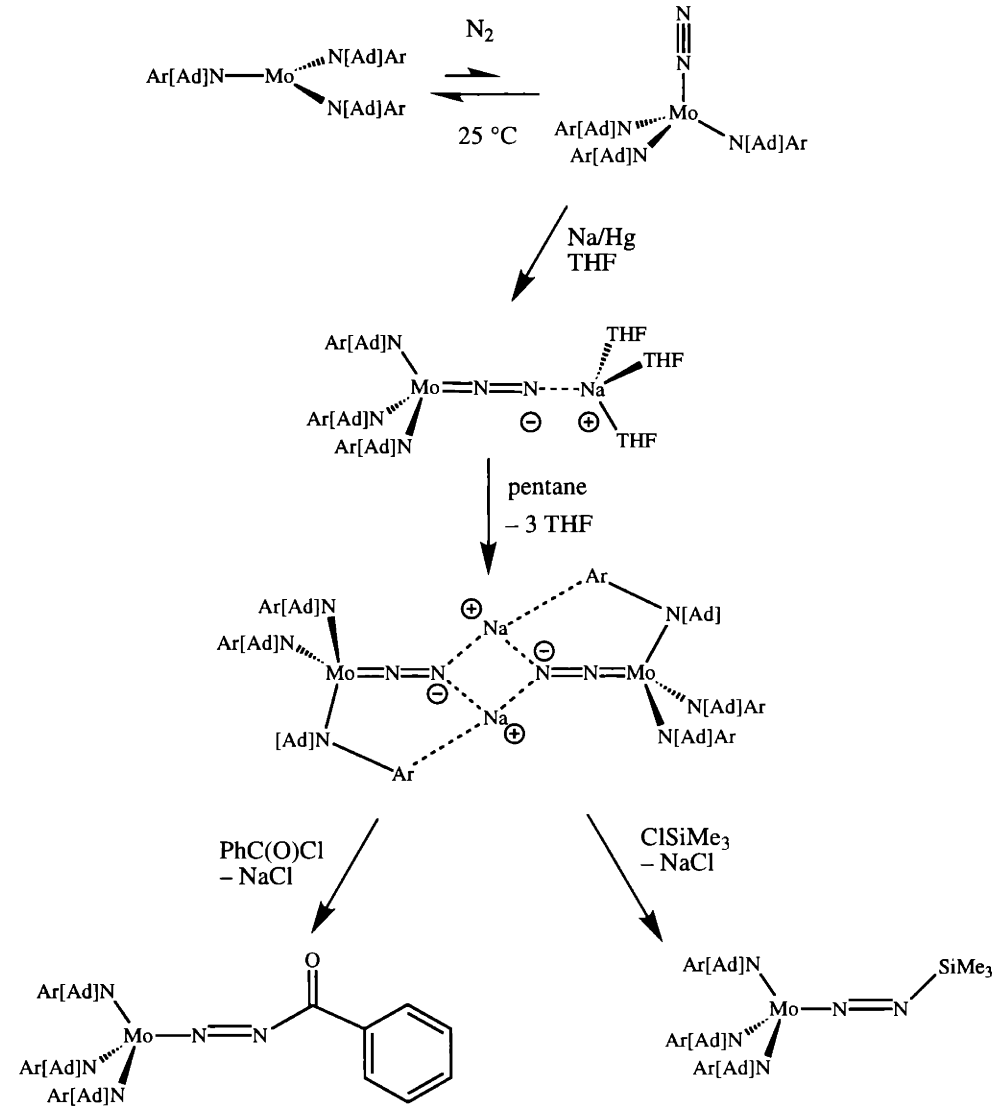

Figure 8: Dinitrogen Chemistry of $Mo(N[Ad]Ar)_3$ showing the generation of anionic $[(N_2)Mo(N[Ad]Ar)_3]^-$, [**9**], and its utilization in N-C and N-Si bond formation to afford the complexes $(PhC(O)NN)Mo(N[Ad]Ar)_3$, **11**, and $(Me_3SiNN)Mo(N[Ad]Ar)_3$, **10**.

no longer noticeable throughout the addition. A 10 h dropwise addition of **1** to a stirring amalgam under N_2 reproducibly converted ca. 0.01 mmol of **1** to [Na][**5**] in good yield (eqn 14).

$$\underset{\mathbf{1}}{Mo(N[R]Ar)_3} + N_2 \xrightarrow{Na/Hg} \underset{[Na][\mathbf{5}]}{[Na][(N_2)Mo(N[R]Ar)_3]} \quad (14)$$

A ^{1}H NMR spectrum of the crude product mixture showed that the target anion had formed in ca. 96 % yield under *these* conditions with only trace impurities of nitride **2** and HN[R]Ar. Consistent with earlier observations, [Na][**5**] showed an intense ν_{NN} at 1761 cm^{-1} in THF. Like $[(N_2)Mo(N[Ad]Ar)_3]^-$, $[(N_2)Mo(N[R]Ar)_3]^-$ was scarlet in the presence of donor solvents such as THF and OEt_2 and is best formulated as $[Na(THF)_X][\mathbf{5}]$ or $[Na(OEt_2)_X][\mathbf{5}]$ when such solvents are present. On triturating pentane solutions of $[Na(THF)_X][\mathbf{5}]$ the solvent molecules were effectively removed. Recrystallization from pentane afforded the stable, solvent-free derivative $[Na][(N_2)Mo(N[R]Ar)_3]$ in 69 % yield. This complex is likely dimeric in nature, exhibiting an Na_2N_2 square whereby the sodium cations are stabilized by intramolecular aryl interactions provided by the anilido ligands.[28] The ion pair [Na][**5**] was moderately soluble in pentane but precipitated immediately on addition of two eq of 12-crown-4. An intensely violet solid was easily isolated which was insoluble in pentane, benzene, and OEt_2, reflecting its distinctly ionic nature. It was solubilized by tetrahydrofuran, and a single crystal suitable for an X-ray diffraction study was obtained by storing a THF–pentane solution at -35 °C. The solid state structure confirmed its assignment as the discrete salt complex $[Na(12\text{-crown-}4)_2][\mathbf{5}]$ (eqn 15). An thermal ellipsoid representation of $[Na(12\text{-crown-}4)_2][\mathbf{5}]$ is shown in Figure 9. The terminally bound dinitrogen complex adopts the expected geometry in which the dinitrogen ligand sits on the pseudo-C_3 axis of the $Mo(N[R]Ar)_3$ template and is centered within the C_3 propeller of the *tert*-butyl substituents. The N(4)-N(5) bond distance of 1.171(14)Å is appreciably shorter than that found in $(Ph[t\text{-}Bu]N)_3Ti(\mu\text{-}N_2)Mo(N[R]Ar)_3$ **7** (1.229(4)Å). This reflects a greater degree of N_2 reduction in **7**, further manifested by the respective ν_{NN} stretching frequencies for the two complexes: 1761 cm^{-1} for $[Na(12\text{-crown-}4)_2][\mathbf{5}]$ vs. 1575 cm^{-1} for **7**.

$$\underset{[Na][\mathbf{5}]}{[Na][(N_2)Mo(N[R]Ar)_3]} \xrightarrow{2\ 12\text{-crown-}4} [Na(12\text{-crown-}4)_2][(N_2)Mo(N[R]Ar)_3] \quad (15)$$

2.11 Oxidation of $[(N_2)Mo(N[R]Ar)_3]^-$ by Cp_2FeOTf.

With key precursor [**5**] in hand an attempt at the direct synthesis of the elusive neutral dinitrogen complex $(N_2)Mo(N[R]Ar)_3$, **4**, by the chemical oxidation of [**5**] became possible. Ferrocenium triflate (Cp_2FeOTf)[29] was chosen as an appropiate one electron oxidant. Fast addition of a scarlet solution of [Na][**5**] to an intensely blue THF solution of Cp_2FeOTf effected the rapid oxidation of [**5**] as shown in eqn 16.

$$\underset{[Na][\mathbf{5}]}{[Na][(N_2)Mo(N[R]Ar)_3]} \xrightarrow{Cp_2FeOTf} \underset{\mathbf{1}}{Mo(N[R]Ar)_3} + N_2 \quad (16)$$

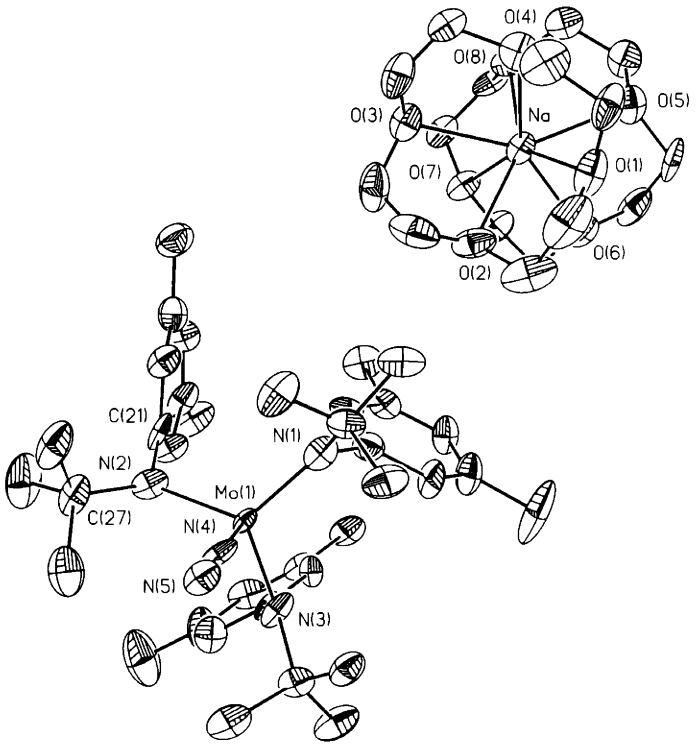

Figure 9: 35 % Thermal ellipsoid representation of $[Na(12\text{-crown-}4)_2][(N_2)Mo(N[R]Ar)_3]$, $[Na(12\text{-crown-}4)_2]$[**5**], from X-ray coordinates. Selected bond distances (Å) and angles (°): Mo(1)-N(1), 1.994(12); Mo(1)-(N2), 2.016(11); Mo(1)-N(3), 1.999(11); Mo(1)-N(4), 1.840(11); N(4)-N(5), 1.171(14); N(4)-Mo(1)-N(3), 98.8(4); N(4)-Mo(1)-N(1), 97.1(5); N(4)-Mo-N(2), 96.7(4); N(3)-Mo(1)-N(2), 118.8(5); N(3)-Mo(1)-N(1), 116.5(5); N(1)-Mo(1)-N(2), 119.6(5).

Effervescence was observed quickly upon mixing, indicating dissociation of the coordinated dinitrogen ligand upon oxidation. IR spectra of the crude mixtures acquired just after mixing showed that the intense ν_{NN} band of [**5**] at 1761 cm^{-1} had completely decayed to baseline. No stretches were observed which might have corresponded to the neutral dinitrogen complex **4** in question. A ^2H NMR spectrum of the crude mixture corroborated this by showing that $Mo(N[R]Ar)_3$ was produced cleanly and quantitatively by the chemical oxidation. The oxidation proceeded analogously at -35 °C. It is apparent that [**5**] spontaneously and rapidly loses dinitrogen upon chemical oxidation and that neutral **4** *is not a chemically isolable species.* Interestingly, O'Donoghue and Schrock reported that oxidation of the related complex $\{[(Me_3SiNCH_2CH_2)_3N]Mo(N_2)\}_2Mg(THF)_2$ gave a moderately stable dinitrogen adduct $[(Me_3SiNCH_2CH_2)_3N]Mo(N_2)$.[22] This complex was structurally characterized and formulated as a low spin neutral dinitrogen complex of molybdenum(III). Apparently, the apical donor atom, provided by the triamidoamine ligand and absent in our *tris*-amido system, provides just enough electron density at the metal center to make the N_2 adduct of the $(Me_3SiNCH_2CH_2)_3N$-Mo core stable. Recent electrochemical experiments by Baraldo comparing the two systems suggest that the trianionic $(Me_3SiNCH_2CH_2)_3N$ ancillary ligand set is appreciably more reducing than the *tris*-anilido ligand set employed here.[30] For example, Baraldo measured the reduction potential of $N{\equiv}Mo(N[R]Ar)_3$ in THF to be -2.7 V whereas the reduction potential for the related complex $[(Me_3SiNCH_2CH_2)_3N]Mo{\equiv}N$ was measured to be -2.9 V in THF ($[N(n\text{-}Bu)_4][PF_6]$, versus $Cp_2Fe^{+/0}$).

2.12 Chemical oxidation of $[(N_2)Mo(N[Ad]Ar)_3]^-$.

As was the case for [**5**], [**9**] was readily oxidized by Cp_2FeOTf. This propensity for oxidation was also manifested in a brief study of its chemistry. We were interested in using simple salt elimination reactions as a means to install "(Ar[Ad]N)$_3$Mo-N=N-" units effectively as bulky N_2-bridged assemblies around a central transition metal center such as Mo, Re, or W. Though this avenue remains to be explored in detail, initial probe reactions indicate that redox susceptible metal halides such as $MoCl_3(THF)_3$ can oxidize [**9**] to liberate N_2. Harder, less readily reduced metal centers such as titanium and zirconium are certainly worthwhile candidates for further investigation.[23] Baraldo recently obtained an X-ray structure of the complex $(Ar[R]N)_3Mo\text{-}N{=}N\text{-}Zr(Cl)Cp_2$ prepared by addition of [**5**] to $Cp_2Zr(H)(Cl)$, Schwartz's reagent.[30] Furthermore, in a collaborative effort, Aaron Odom found that stoichiometric $[Na][(N_2)Mo(N[Ad]Ar)_3]$ and $IU(N[R]Ar)_3$ reacted in OEt_2 to form the N_2-bridged complex $(Ar[Ad]N)_3Mo(\mu\text{-}N_2)U(N[R]Ar)_3$ by salt elimination (eqn 17). Odom characterized $(Ar[Ad]N)_3Mo(\mu\text{-}N_2)U(N[R]Ar)_3$ by X-ray crystallography and showed it to contain a linear N_2 ligand bridging the *tris*-anilido molybdenum and uranium centers, reminiscent of the structure determined for $(Ph[t\text{-}Bu]N)_3Ti(\mu\text{-}N_2)Mo(N[R]Ar)_3$.[31]

$$\underset{[Na][\mathbf{9}]}{[Na][(N_2)Mo(N[Ad]Ar)_3]} + U(I)(N[R]Ar)_3 \xrightarrow{OEt_2} (Ar[Ad]N)_3Mo(\mu\text{-}N_2)U(N[R]Ar)_3 \quad (17)$$

The few attempts made to protonate [**9**], in the hope of generating a parent diazenido species "(HNN)Mo(N[Ad]Ar)$_3$," resulted in undesired redox chemistry. Addition of sterically hindered

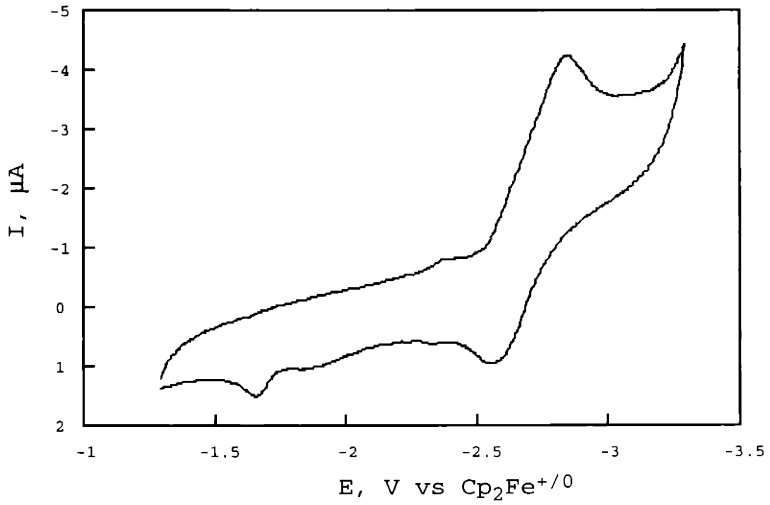

Figure 10: Cyclic Voltammogram of $Mo(N[R]Ar)_3$ **1** in 0.5 M THF solution of $[N(n\text{-}Bu)_4][PF_6]$. Scan rate = 0.1 V/s.

2,6-di-*tert*-butylphenol to an ethereal solution of [Na][**9**] resulted in a gradual color change from scarlet to green. IR spectra showed full consumption of starting material [**9**] and no new ν_{NN} vibrations, consistent with redox triggered N_2 dissociation. *tert*-Butyliodide was also investigated as a potential proton source. It was found that addition of this reagent to [**9**] also effected undesired N_2 loss.

2.13 Electrochemistry of $Mo(N[R]Ar)_3$ and $[(N_2)Mo(N[R]Ar)_3]^-$.[30]

The inherent instability of neutral $(N_2)Mo(N[R]Ar)_3$, **4**, prompted us to utilize another technique for its study. Due to the inherent redox nature of the Na/Hg facilitated N_2 cleavage reaction an electrochemical study was deemed appropriate. The cyclic voltammetry of a THF solution of $[(N_2)Mo(N[R]Ar)_3]^-$, [**5**], is shown in Fig 11 and displays a distinct oxidation wave at -1.7 V. No return wave was observable at scan rates ranging from 0.1–10 V/s, indicating that the oxidation product was unstable and had decayed completely before the scan was reversed. This irreversible proccess is assigned to the oxidation of $[(N_2)Mo(N[R]Ar)_3]^-$, [**5**], to generate neutral $(N_2)Mo(N[R]Ar)_3$, **4**, which quickly decays through dissociation of N_2 to afford $Mo(N[R]Ar)_3$, **1**. Based on this result the $t_{1/2}$ for neutral **4** appears to be less than one second.

A reduction wave was observed at -2.9 V. Through successive scans it was found that the wave at -1.7 V gradually decayed while the wave at -2.9 V increased, confirming that the reduction wave belonged to the decomposition product of **4**. That this decomposition product corresponded to **1** was confirmed through the independent electrochemical inspection of a solution of **1**. This is shown in Fig 10. An irreversible reduction wave at -2.9 V was observed. The corresponding oxidation wave at -1.7 V was readily assigned to the oxidation of $[(N_2)Mo(N[R]Ar)_3]^-$. This experiment is suggestive of fast uptake of dinitrogen by a reduced molybenum(II) species "$[Mo(N[R]Ar)_3]^-$".

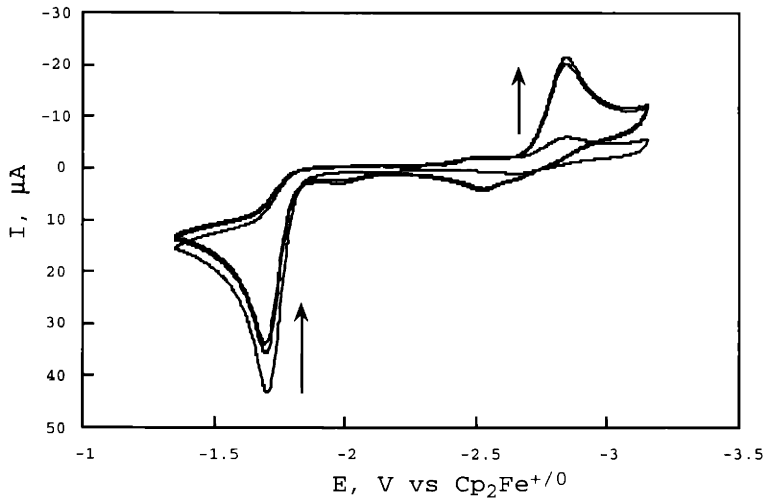

Figure 11: Cyclic Voltammogram of $[(N_2)Mo(N[R]Ar)_3]^-$, [**5**], in 0.5 M THF solution of [N(*n*-Bu)$_4$][PF_6]. Scan rate = 0.1 V/s.

Exhaustive electrolysis of a solution of **1** confirmed that the final product, under a dinitrogen atmosphere, was $[(N_2)Mo(N[R]Ar)_3]^-$. When a potential of -3.0 V was maintained for extensive periods, the solution color changed from the bright orange of **1** to the scarlet color of [**5**]. At this point the current had reached a plateau and one eq of electrons (based on **1**) had passed through the cell. The electrochemical response confirmed the presence of [**5**]. As expected, returning this solution to a potential of -1.3 V reverted the process, oxidizing [**5**] and regenerating the orange solution of **1**.

Attempts have been made to synthetically prepare a reduced *tris*-anilido molybdenum species " $Mo(N[R]Ar)_3^-$ " on a preparative scale in the absence of N_2 using solid sodium as the reductant. Despite considerable effort, an anionic *tris*-anilido molybdenum fragment of the form [Na][$Mo(N[R]Ar)_3$] has not been chemically confirmed (see experimental section for details).

2.14 Direct reaction of $Mo(N[R]Ar)_3$ and $[Na][(N_2)Mo(N[R]Ar)_3]$.

Equation 4 established that dinitrogen cleavage was dramatically accelerated at ambient temperatures by the presence of a Na/Hg amalgam. We presumed that the anionic species [**5**] reacted directly with **1** in solution to generate dinuclear **3**. With key [**5**] in hand this model could be tested directly. Mixing stoichiometic amounts of **1** and [Na][**5**] in THF under a dinitrogen atmosphere at 25 °C, resulted in a steady build-up of intensely purple **3** within one hour (^{2}H NMR). IR spectroscopy confirmed that a significant amount of [**5**] was present throughout the course of the reaction. Analysis of the final reaction products by ^{1}H NMR spectroscopy after 14 hours showed a mixture of N≡Mo(N[R]Ar)$_3$ and [$Na(THF)_x$][**5**] in a ca. 2:1 ratio. Inclusion of an internal integration standard indicated that ca. 90 % of the starting materials were accounted for by ^{1}H NMR spectroscopy. Additionally, a small amount of the ligand degradation byproduct HN[R]Ar was ob-

served. Notably, the reaction proceeded analogously regardless of whether or not the experiment was performed in the presence of added mercury. These reactions unequivocally demonstrate that $[(N_2)Mo(N[R]Ar)_3]^-$, [**5**], reacts readily with $Mo(N[R]Ar)_3$, **1**, to generate $(\mu\text{-}N_2)\{Mo(N[R]Ar)_3\}_2$, **3**, en route to the irreversible formation of $N{\equiv}Mo(N[R]Ar)_3$, **2**. This process is depicted by eqn 18 and eqn 3, respectively. Hence, reactions in which the redox catalyst $[(N_2)Mo(N[R]Ar)_3]^-$ is formed in the presence of **1** are likely to generate nitride product **2**.

$$\underset{\mathbf{1}}{Mo(N[R]Ar)_3} \xrightarrow{N_2/\ [Na][\mathbf{5}]} \underset{\mathbf{3}}{(\mu\text{-}N_2)\{Mo(N[R]Ar)_3\}_2} \qquad (18)$$

In our efforts to explore the diverse reaction chemistry of $Mo(N[R]Ar)_3$, a host of other one-electron reductants have been observed to facilitate the dinitrogen cleavage reaction. As shown in eqn 19, $NaEt_3BH$ offers a particularly clean example. When a homogeneous THF solution of $Mo(N[R]Ar)_3$ and an excess of $NaEt_3BH$ were stirred under an atmosphere of dinitrogen at 25 °C, nitride **2** was formed quantitatively over a period of 24 h. ^1H NMR and IR spectroscopies of the final crude mixture showed no $[(N_2)Mo(N[R]Ar)_3]^-$ nor any ligand degredation byproduct. As was the case for the Na/Hg facilitated cleavage reaction, the intense purple color of the N_2-bridged intermediate **3** was observed during the course of the reaction. The purple color dissipated gradually over 24 h, consistent with its decay to $N{\equiv}Mo(N[R]Ar)_3$. Undoubtedly, a variety of reaction pathways may be envisioned in order to account for the observed nitride product. An explanation which I favor is the following: The anion $[Et_3BH]^-$ reacts directly with $(N_2)Mo(N[R]Ar)_3$ by an inner-sphere redox pathway to generate $[(N_2)Mo(N[R]Ar)_3]^-$. A possible intermediate along this reaction coordinate is $[Na][(Ar[R]N)_3Mo\text{-}N{=}N\text{-}H\text{-}BEt_3]$. Intermediate $[Na][(Ar[R]N)_3Mo\text{-}N{=}N\text{-}H\text{-}BEt_3]$ may; (i) Split apart unproductively to $(N_2)Mo(N[R]Ar)_3$ and $NaEt_3BH$ or; (ii) Decompose to the molybdenum(II) complex $[Na][(N_2)Mo(N[R]Ar)_3]$ and oxidation products of $[HBEt_3]^-$, such as dihydrogen and triethylborane. The latter pathway is irreversible and should gradually funnel the starting material $Mo(N[R]Ar)_3$ to $[(N_2)Mo(N[R]Ar)_3]^-$. We have established that $[(N_2)Mo(N[R]\text{-}Ar)_3]^-$ rapidly generates $(\mu\text{-}N_2)\{Mo(N[R]Ar)_3\}_2$ in the presence of $Mo(N[R]Ar)_3$ and N_2. Hence, the gradual production of $[(N_2)Mo(N[R]Ar)_3]^-$ by $NaEt_3BH$, over a period of hours , should result in a high yield of $(\mu\text{-}N_2)\{Mo(N[R]Ar)_3\}_2$ and ultimately $N{\equiv}Mo(N[R]Ar)_3$ product.

$$\underset{\mathbf{1}}{Mo(N[R]Ar)_3} \xrightarrow{N_2\ /\ NaEt_3BH} \underset{\mathbf{2}}{N{\equiv}Mo(N[R]Ar)_3} \qquad (19)$$

2.15 Attempted Synthesis of anionic $(\mu\text{-}N_2)\{Mo(N[R]Ar)_3\}_2^-$.

An anionic N_2-bridged species of the form $[Na][(\mu\text{-}N_2)\{Mo(N[R]Ar)_3\}_2]$, [Na][**12**], seemed a likely intermediate in the generation of $(\mu\text{-}N_2)\{Mo(N[R]Ar)_3\}_2$ from the bimolecular reaction between **1** and [Na][**5**], as depicted in eqns 20 and 21 below. We wondered whether a dinitrogen-free THF mixture of [**5**] and $Mo(N[R]Ar)_3$ would contain detectable concentrations of $[Na][(\mu\text{-}N_2)\{Mo\text{-}(N[R]Ar)_3\}_2]$. To address this question, rigorously de-gassed THF was vacuum transferred into an NMR tube containing stoichiometric solids [Na][**5**] and **1**. ^2H NMR spectra aqcuired after

mixing showed no evidence for a new product assignable as $[Na][(\mu\text{-}N_2)\{Mo(N[R]Ar)_3\}_2]$. Both starting materials [Na][**5**] and **1** were present in addition to a small amount (<10 %) of the *neutral* bridged complex $(\mu\text{-}N_2)\{Mo(N[R]Ar)_3\}_2$. An analogous experiment carried out with the discrete salt complex $[Na(12\text{-crown-}4)_2][(N_2)Mo(N[R]Ar)_3]$ and $Mo(N[R]Ar)_3$ did not show signals consistent with a species of the form $[Na(12\text{-crown-}4)_2][(\mu\text{-}N_2)\{Mo(N[R]Ar)_3\}_2]$. A small amount of neutral **3** was again detected.

Though its intermediacy remains likely, $[Na][(\mu\text{-}N_2)\{Mo(N[R]Ar)_3\}_2]$ does not appear to be an isolable complex — at least under the reaction conditions of the redox-facilitated cleavage reaction. More probable is the notion that $[Na][(\mu\text{-}N_2)\{Mo(N[R]Ar)_3\}_2]$ dissociates readily to **1** and [Na][**5**] in the absence of a $(N_2)Mo(N[R]Ar)_3$ oxidant. Electrochemical data follows in support of this notion.

2.16 Electrochemistry of $(\mu\text{-}N_2)\{Mo(N[R]Ar)_3\}_2$.[30]

Fig 12 shows the cyclic voltamogram of a THF solution of $(\mu\text{-}N_2)\{Mo(N[R]Ar)_3\}_2$. A cathodic wave at -2.4 V is clearly observable. It was not possible to detect the corresponding anodic wave at scan rates between 0.1 and 10 V/s. A new anodic peak was detected at -1.7 V concomitant with this irreversible reduction process. The peak at -1.7 V was also irreversible and was readily assigned to the oxidation of $[(N_2)Mo(N[R]Ar)_3]^-$ (*vide supra*). Repetitive reductive scans effected a decrease in the magnitude of the wave at -2.4 V and a corresponding increase in the wave at -1.7 V. We assigned the wave at -2.4 V to the reduction of $(\mu\text{-}N_2)\{Mo(N[R]Ar)_3\}_2$ to generate $[(\mu\text{-}N_2)\{Mo(N[R]Ar)_3\}_2]^-$, [**12**], the bridged anion in question. Consistent with our inability to *synthetically generate and observe* this dinuclear anion, the species was unstable and split apart into $[(N_2)Mo(N[R]Ar)_3]^-$, [**5**], and $Mo(N[R]Ar)_3$, **1**, before it could be detected at the electrode. The anionic byproduct of decomposition, [**5**], was detected at -1.7 V after the succession of reductive scans. Based on its independent electrochemical investigation described above, we know that **1** itself is not electroactive through the potential window under consideration here (**1** is reduced at a potential of -2.9 V). When more anodic potentials were investigated a reversible wave at -1.2 V was detected (Fig 13). Its intensity synchronously decreased with the peak at -2.4 V. This behavior suggested oxidation of **3** to generate a dinuclear monocation stable enough for observation on the time scale of the electrochemical experiment. The electrochemical response of **3** confirms the following:

- $[(\mu\text{-}N_2)\{Mo(N[R]Ar)_3\}_2]^-$ is an unstable, reducing species.
- The redox potential for the reduction of $(N_2)Mo(N[R]Ar)_3$ by $[(\mu\text{-}N_2)\{Mo(N[R]Ar)_3\}_2]^-$, shown in eqn 21, should be a spontaneously favorable redox process with a $\Delta E \simeq 0.7$ V.

$$\mathbf{1} + [Na][\mathbf{5}] \rightleftharpoons \begin{matrix}[Na][(\mu\text{-}N_2)\{Mo(N[R]Ar)_3\}_2] \\ [Na][\mathbf{12}]\end{matrix} \tag{20}$$

$$\mathbf{4} + [Na][\mathbf{12}] \longrightarrow [Na][\mathbf{5}] + \mathbf{3} \tag{21}$$

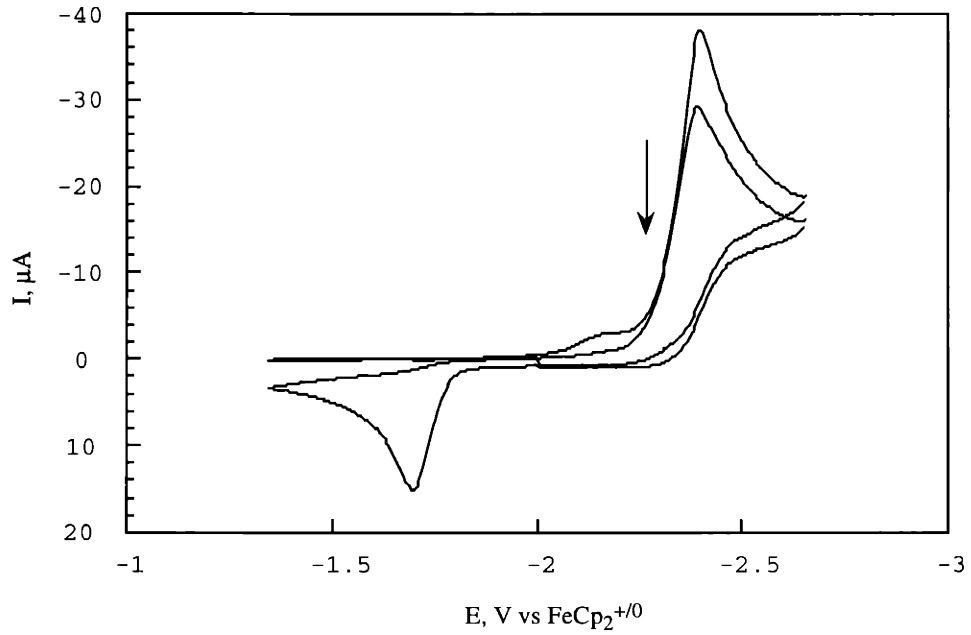

Figure 12: Cyclic Voltammogram of (μ-N_2){Mo(N[R]Ar)$_3$}$_2$ **3** in 0.5 M THF solution of [N(n-Bu)$_4$][PF_6]. Scan rate = 0.1 V/s.

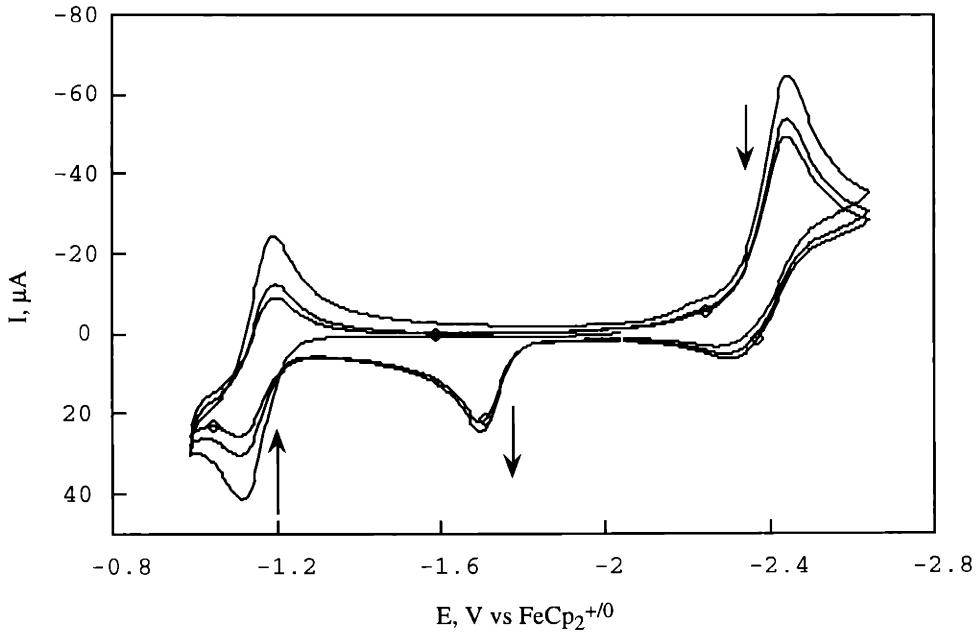

Figure 13: Cyclic Voltammogram of (μ-N_2){Mo(N[R]Ar)$_3$}$_2$ **3** in 0.5 M THF solution of [N(n-Bu)$_4$][PF_6]. Scan rate = 0.1 V/s.

2.17 Crossover experiment between Mo(N[R]Ar)$_3$ and Mo(N[*t*-Bu]Ar)$_3$ under vacuum.

Thwarted by our inability to prepare [Na][(μ-N$_2$){Mo(N[R]Ar)$_3$}$_2$] synthetically it was desirable to provide further indirect evidence for its intermediacy to corroborate our interpretation of the electrochemical data. Because the deutero-labeled anilido ligand –N[R]Ar can be readily prepared in its protio form, –N[*t*-Bu]Ar,[32] a crossover experiment was possible.[30] ^{2}H NMR spectroscopy clearly showed that Mo(N[R]Ar)$_3$ was generated on mixing a THF solution of stoichiomotetric Mo(N[*t*-Bu]Ar)$_3$ and [Na][**5**] under vacuum. Integration of the ^{2}H NMR signals for the respective –N[R]Ar ligands revealed that 38.5 % of the *deutero-labeled* [Na][**5**] was converted to *deutero-labeled* Mo(N[R]-Ar)$_3$. In accord with this observation, ^{1}H NMR spectroscopy confirmed that [Na(THF)$_x$][Mo(N$_2$)-(N[*t*-Bu]Ar)$_3$] was also generated. Control experiments have shown that [Na][**5**] is stable for days in THF at 25 °C with no appreciable decomposition to the three-coordinate Mo(N[R]Ar)$_3$ complex. Hence, transfer of the dinitrogen ligand from [Na][**5**] to Mo(N[*t*-Bu]Ar)$_3$ is best explained by the intermediate formation of an anionic bridged species, [(Ar[*t*-Bu]N)$_3$Mo(μ-N$_2$)Mo(N[R]Ar)$_3$]$^-$, susceptible to a degenerate dissociation pathway yielding the observed mixture, as depicted in eqn 22. Despite repeated attempts to generate an ideal 1:1 mixture of [Na][**5**] and [Na][(N$_2$)Mo(N[*t*-Bu]-Ar)$_3$], the ^{2}H NMR spectra of these solutions typically showed that a small amount of dinuclear **3** (ca. 7 %) had been generated. As mentioned above, this was also observed when [Na][**5**] was mixed with **1**.

$$[\text{Na}][\mathbf{5}] \;+\; \text{Mo(N[}t\text{-Bu]Ar)}_3 \;\underset{\longleftarrow}{\overset{\text{THF}}{\longrightarrow}}\; \mathbf{1} \;+\; [\text{Na}][\text{Mo(N}_2\text{)(N[}t\text{-Bu]Ar)}_3] \qquad (22)$$

3 Conclusions

Our research group's entry into dinitrogen chemistry began with Laplaza's remarkable discovery that the *tris*-anilido molybdenum complex, Mo(N[R]Ar)$_3$ **1**, was capable of binding and cleaving N$_2$.[4,5] We have attempted to approach a full understanding of this dramatic cleavage reaction, as well as to coax the Mo(N[R]Ar)$_3$ complex to provide a more diverse array of dinitrogen chemistry. This chapter presents one line of investigation whereby one electron reductants have been used to provide an informative overall picture. Eqn 4 introduced the initial observation that Na/Hg amalgam was capable of facilitating the N$_2$ cleavage reaction. It was shown definitively that (N$_2$)Mo(N-[R]Ar)$_3$, **4**, is present in low concentration at 25 °C in THF solution and that it is the species which is reduced by Na/Hg, as well as other one electron reductants including Ti(N[*t*-Bu]Ph)$_3$. The sterically encumbered complex Mo(N[Ad]Ar)$_3$ greatly simplified our efforts to isolate anionic dinitrogen complexes of molybdenum, and to begin a study of their diverse reaction chemistry. To date, our labs have used the complexes (N$_2$)Mo(N[R]Ar)$_3$, [Na][(N$_2$)Mo(N[Ad]Ar)$_3$], and [Na][(N$_2$)Mo(N[R]-Ar)$_3$] to synthesize species of the form (Ar[R]N)$_3$Mo=N=N-X where X = Na, Ti, Zr, U, Si, C. Hence, the goal to divert the chemistry of (N$_2$)Mo(N[R]Ar)$_3$ away from direct cleavage and towards a more diverse functionalization has been achieved. Using the *tris*-anilido molybdenum core as an N$_2$ template, dinitrogen has been delivered to an alkali metal (X = Na), transition metals (X =

Ti, Zr), an actinide element (X = U), and main group elements (X = C, Si). With these synthetic principles established, a rich coordination chemistry around the "Mo=N=N" core remains to be explored.

A second goal of this chapter was to establish the stability/instability of the neutral dinitrogen complex **4**. Complex **4** is unstable at ambient temerature and atmospheric dinitrogen pressure, dissociating readily to N_2 and $Mo(N[R]Ar)_3$. This was shown synthetically and electrochemically by the direct oxidation of $[(N_2)Mo(N[R]Ar)_3]^-$, [**5**]. Fortunately, $(N_2)Mo(N[R]Ar)_3$ is readily trapped by one electron reductants such that its inherent instablility does not prevent elaborating its chemistry. A schematic diagram displaying the relevant frontier orbitals of $Mo(N[R]Ar)_3$, $(N_2)Mo(N[R]Ar)_3$, and $[(N_2)Mo(N[R]Ar)_3]^-$ is shown in Fig 14 below. $Mo(N[R]Ar)_3$, a rigorously high spin complex with a quartet ground state,[5,33,34] interacts reversibly with N_2 to yield the unstable, low spin N_2 adduct $(N_2)Mo(N[R]Ar)_3$. This step constitutes a formal spin flip. One simplistic explanation to account for this spin forbidden reaction is that a small concentration of low spin $Mo(N[R]Ar)_3$ exists at 25 °C in solution. Such a low spin complex would have the appropriately available σ orbital oriented along the C_3 axis (predominantly d_{z^2} in character) to accept an incoming lone pair from the N_2 ligand. However, according to published calculations [33, 34] a low spin configuration for $Mo(N[R]Ar)_3$ is energetically inaccessible at 25 °C. Hence, this scenario is highly unlikey on theoretical grounds. More likely is the notion that the spin-flip occurs subsequent to a perturbation of the quartet ground state of $Mo(N[R]Ar)_3$ by the incoming N_2 ligand. The low spin $(N_2)Mo(N[R]Ar)_3$ adduct which forms is unstable toward dissociation, in stark contrast to its isolectronic and stable counterpart $(OC)Mo(N[R]Ar)_3$ (discussed in Chapter 3), reflecting the greater π acidity of the C≡O ligand versus the N≡N ligand. Alternatively, by moderately enhancing the π-donor ability of the molybdenum center a stable adduct becomes isolable, as in the case of Schrock's structurally characterized $[(Me_3SiNCH_2CH_2)_3N]Mo(N_2)$.[22] Finally, one electron reduction of low spin $(N_2)Mo(N[R]Ar)_3$ affords a singlet product, $[(N_2)Mo(N[R]Ar)_3]^-$, which is markedly stable to dissociation. The π donor character of the reduced d^4 core constitutes a much stronger Mo-N multiple bond for $[(N_2)Mo(N[R]Ar)_3]^-$, the core of which can be represented formally as $Mo{=}N{=}N^-$, in comparison to its neutral d^3 counterpart $(N_2)Mo(N[R]Ar)_3$, which should more closely correspond to Mo-N≡N.

The third goal of this chapter was to understand the redox-enhanced N_2 cleavage reaction of $Mo(N[R]Ar)_3$. Our initial approach in this vein was of a highly *synthetic* nature which relied upon control experiments in addition to the trapping, isolation, and characterization of the key complexes $(Ph[t\text{-}Bu]N)_3Ti(\mu\text{-}N_2)Mo(N[R]Ar)_3$, $[Na][(N_2)Mo(N[Ad]Ar)_3]$, and $[Na][(N_2)Mo(N[R]Ar)_3]$. This effort was largely mine. Luis Baraldo followed with a wealth of elegant electrochemical information, relevant aspects of which have been discussed here. In general we have found that those reactions which were initially studied *in the flask* can be appreciated from a simple picture based on relative reduction potentials. Fig 15, presented as a series of steps numbered (i)–(vi), summarizes our understanding of the redox-facilitated dinitrogen cleavage reaction.

- (i) Under N_2 at 25 °C three-coordinate $Mo(N[R]Ar)_3$ is in constant equilibrium with its unstable N_2 adduct, $(N_2)Mo(N[R]Ar)_3$.
- (ii) $(N_2)Mo(N[R]Ar)_3$ is irreversibly reduced by a 0.4 % Na/Hg amalgam to generate $[(N_2)Mo(N[R]Ar)_3]^-$. Importantly, $Mo(N[R]Ar)_3$ itself is not reduced by 0.4 % Na/Hg amalgam.

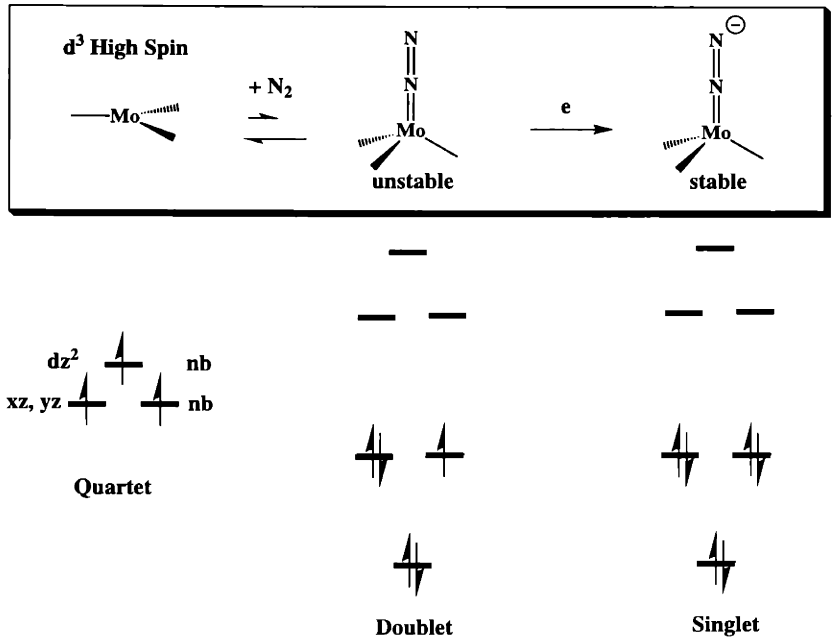

Figure 14: Important frontier orbitals for the complexes $Mo(N[R]Ar)_3$, $(N_2)Mo(N[R]Ar)_3$, and $[(N_2)Mo(N[R]Ar)_3]^-$. See main text for discussion.

- (iii) $[(N_2)Mo(N[R]Ar)_3]^-$ reacts in a bimolecular fashion with $Mo(N[R]Ar)_3$ present in solution to generate $[(\mu\text{-}N_2)\{Mo(N[R]Ar)_3\}_2]^-$, which itself is unstable and dissociates quickly to $Mo(N[R]Ar)_3$ and $[(N_2)Mo(N[R]Ar)_3]^-$. However, in the presence of $(N_2)Mo(N[R]Ar)_3$:
- (iv) $[(\mu\text{-}N_2)\{Mo(N[R]Ar)_3\}_2]^-$ is readily oxidized to afford the neutral product $(\mu\text{-}N_2)\{Mo(N[R]Ar)_3\}_2$ and to regenerate $[(N_2)Mo(N[R]Ar)_3]^-$.
- (v) $(\mu\text{-}N_2)\{Mo(N[R]Ar)_3\}_2$ cleaves spontaneously at 25 °C to afford to $N{\equiv}Mo(N[R]Ar)_3$, an irreversible thermodynamic sink in this system.
- (vi) $[(N_2)Mo(N[R]Ar)_3]^-$ generated in step (iv) can react with $(N_2)Mo(N[R]Ar)_3$ as in step (iii) to generate more $(\mu\text{-}N_2)\{Mo(N[R]Ar)_3\}_2$. Hence, most of the starting $Mo(N[R]Ar)_3$ is effectively funneled to the nitride product readily at ambient temperature and pressure.

A Redox-Facilitated Dinitrogen Cleavage Reaction

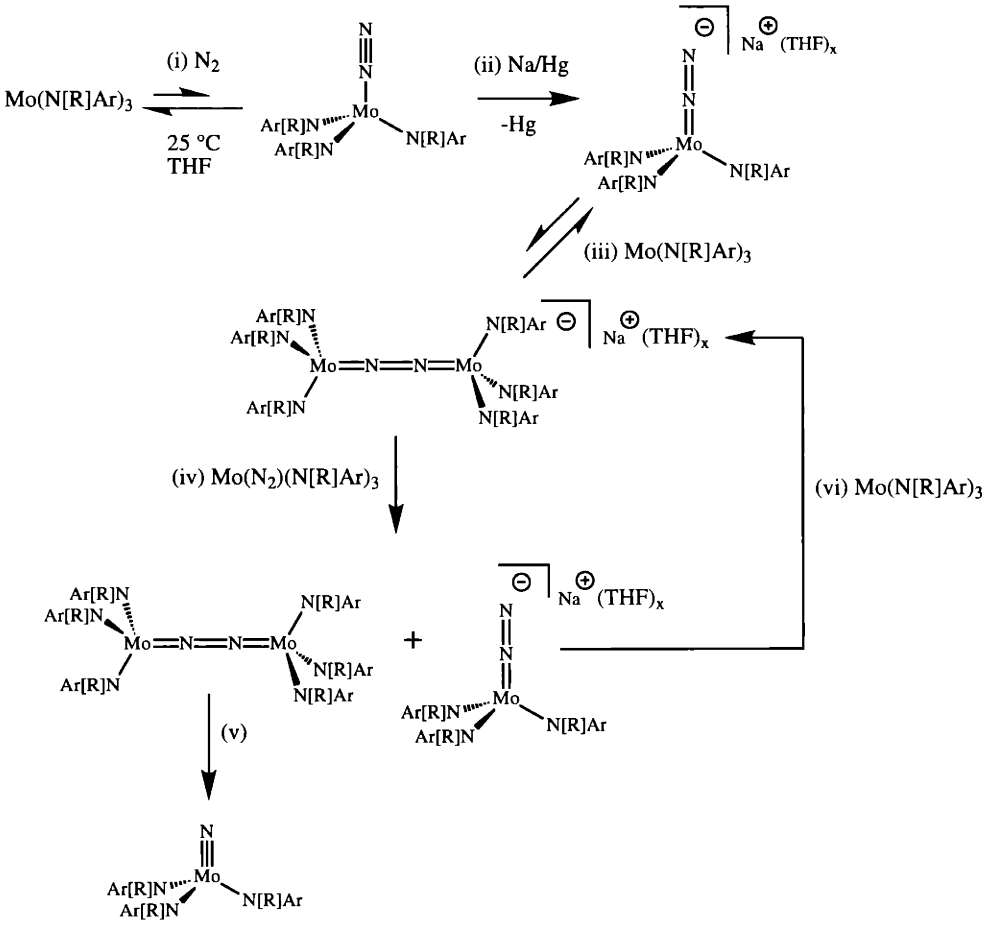

Figure 15: Reaction pathway for the facile conversion of $Mo(N[R]Ar)_3$ **1** to $N{\equiv}Mo(N[R]Ar)_3$ **2** by way of a Na/Hg amalgam reductant at 25 °C in THF solution, under a N_2 atmosphere.

4 Experimental Section

4.1 General Considerations

Unless stated otherwise, all operations were performed in a Vacuum Atmospheres dry box under an atmosphere of purified nitrogen, or using standard Schlenk techniques under an argon or dinitrogen atmosphere. Anhydrous OEt_2 and toluene were purchased from Mallinckrodt; *n*-pentane and *n*-hexane were purchased from EM Science. Ether was purified according to the procedure of Grubbs.[35] Aliphatic hydrocarbon solvents were distilled under a nitrogen atmosphere from very dark blue to purple sodium benzophenone ketyl solubilized with a small quantity of tetraglyme. Distilled solvents were transferred under vacuum into teflon-stopcocked glass vessels and stored, prior to use, in a Vacuum Atmospheres dry box. C_6D_6 was degassed and dried over activated 4 Å molecular sieves and transferred under vacuum into a storage vessel. 4 Å sieves, Celite and alumina were activated *in vacuo* overnight at a temperature above 180 °C. $Mo(N[R]Ar)_3$,[5] $Ti(N[R]Ar)_3$,[8] ferrocenium triflate,[29] and LiN[Ad]Ar[36] [37] were prepared according to published procedures. ^{15}N-labeled N_2 gas was purchased form Cambride Isotope Laboratory (CIL). $ClSiMe_3$ and benzoylchloride were degassed and dried over 4Å molecular sieves prior to use. Other chemicals were purified and dried by standard procedures or were used as received. Infrared spectra were recorded on a Bio-Rad 135 Series FTIR spectrometer. UV-visible spectra were recorded on a Hewlett-Packard 8453 diode-array spectrophotometer. ^1H and ^{13}C NMR spectra were recorded on Varian VXR-500, Varian XL-300, or Varian Unity-300 spectrometers. ^1H and ^{13}C NMR chemical shifts are reported with reference to solvent resonances (residual C_6D_5H in C_6D_6, 7.15 ppm; C_6D_6, 128.0 ppm; $CHCl_3$ in $CDCl_3$, 7.24 ppm; $CDCl_3$, 77.0 ppm). ^2H NMR chemical shifts are reported with respect to external C_6D_6 (7.15 ppm). Solution magnetic susceptibilities were determined by ^1H NMR at 300 MHz using the method of Evans.[16,17] Routine coupling constants are not reported. Combustion analyses (C, H, and N) were performed by Microlytics, Southdeerfield MA. X-ray diffraction data were collected on a Siemens Platform goniometer with a Charge Coupled Device (CCD) detector. Structures were typically solved by direct methods (SHELXTL V5.0, G.M Sheldrick and Siemens Industrial Automation, Inc., 1995) unless otherwise noted. Peaks in the ^1H and ^{13}C NMR spectra are denoted according to Fig 16.

4.2 Electrochemical Measurements.

The electrochemical measurements[30] were performed in THF solution containing the desired compounds and 0.5 M tetra-*n*-butylammonium hexafluorophosphate, $[N(n\text{-}Bu)_4][PF_6]$. In a typical procedure 5 mg of the complex was dissolved in 0.75 mL of clean THF. To this solution was added 0.75 mL of 1.0 M THF solution of tetra-*n*-butylammonium hexafluorophosphate. A platinum disk (1.6 mm diameter, Bioanalytical systems), a platinum wire, and a silver wire were employed as the working electrode, the auxiliary, and the reference, respectively. The electrochemical response was collected with the assistance of an Eco-Chemie Autolab potentiostat (pgstat20) and the GPES 4.3 software. An IR correction drop was always employed due to the high resistance of the solutions. A typical resistance value measured with the positive feedback technique for these solutions was 975 ohms. All of the potentials are reported against the ferrocenium/ferrocene couple measured in

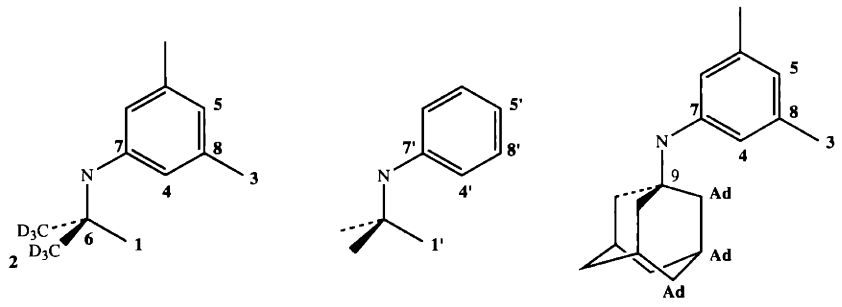

Figure 16: Labeling scheme for ^{1}H and ^{13}C NMR spectra. The positions on the adamantyl substituents have been designated generally as **Ad**.

the same solution.

4.3 $Mo(N[R]Ar)_3$ + 1 eq Na/Hg amalgam.

A 0.40 % Na/Hg was prepared by dissolving Na metal (5.7 mg, 0.2479 mmol) in 1.41 g Hg (7.03 mmol) in a 20 mL scintillation vial. THF was added (5 mL) and the amalgam was stirred for five minutes, followed by addition of solid orange $Mo(N[R]Ar)_3$ (173.4 mg, 0.2697 mmol) at 22 °C. Vigorous stirring was continued and within one hour the solution had acquired an intense purple color, indicative of $(\mu\text{-}N_2)\{Mo(N[R]Ar)_3\}_2$, confirmed by a ^{2}H NMR spectrum acquired at this time. Nearly all of $Mo(N[R]Ar)_3$ had been consumed after one hour (emphapprox. 3 % remaining). An FTIR spectrum showed a ν_{NN} band at 1761 cm^{-1} consistent with the presence of $[Na][(N_2)Mo(N[R]Ar)_3]$. Stirring was continued for 7 hours, by which time the purple color had faded and the solution had turned orange–red. The solution was filtered through Celite followed by removal of solvent *in vacuo*, yielding an orange–red solid. A ^{1}H NMR spectrum of this solid showed it to be 85 % $N{\equiv}Mo(N[R]Ar)_3$[2] and 15 % of $[Na][(N_2)Mo(N[R]Ar)_3]$, whose independent characterization is described below.

4.4 $Mo(N[R]Ar)_3$ + $NaEt_3BH$ under a dinitrogen atmosphere.

Solid orange $Mo(N[R]Ar)_3$ (61.8 mg, 0.0961 mmol) was dissolved in THF (2 mL) in a 20 mL scintillation vial equipped with a magnetic stir bar. Under a dinitrogen atmosphere 480 mL $NaEt_3BH$ (0.480 mmol, 1M solution in toluene) was added directly to the stirring orange solution at 22 °C. A gradual change in color resulting in an intensely purple solution was observed during the first few hours. After 24 h the purple color had dissipated and the solution was light brown. The volatiles were removed in vacuo and spectroscopic analysis (^{1}H NMR) showed quantitative formation of $N{\equiv}Mo(N[R]Ar)_3$ relative to an internal integration standard of $O(SiMe_3)_2$.

4.5 $Mo(N[R]Ar)_3$ + Na/Hg amalgam under argon.

A 0.4 % Na/Hg amalgam was prepared in a 50 mL RB-flask equipped with a side-arm and stopcock by dissolving solid sodium (22 mg, 0.957 mmmol) in Hg (5.44 g). THF (8 mL) was first added to the flask, followed by the addition of solid $Mo(N[R]Ar)_3$ under a counter-flow of argon, at once, to the stirring mixture. The vessel was sealed and stirring was continued under an argon atmosphere for 22 h at 25 °C. The reaction solution remained orange throughout. After 22 h the solvent was removed *in vacuo* and the resulting orange residue was extracted into pentane and filtered away from the amalgam. A ^2H NMR spectrum of this pentane solution showed only the starting material $Mo(N[R]Ar)_3$ and a small degree of decomposition to diamagnetic product (δ = 1.8 ppm). A ^1H NMR spectrum of the residue reconstituted into C_6D_6 showed that the diamagnetic product was HN[R]Ar, indicative of a small degree of ligand degradation (< 10 %).

4.6 $Mo(N[R]Ar)_3$ + Na(s) under argon.

Solid sodium metal (111 mg, 4.828 mmol) was weighed into a 50 mL RB-flask equipped with a side-arm and stopcock. The metal was spread around the base of the flask into a thin film so as to expose a high degree of surface area. THF (10 mL) was then added and the flask was stirred vigorously under argon for five minutes. $Mo(N[R]Ar)_3$ was added as a solid all at once under an argon counter-flow and the initially orange solution turned sienna in color within the first 30 minutes of stirring. After 2.5 h the mixture was dried *in vacuo* and the resulting residue was extracted into pentane, filtered through Celite, and again dried *in vacuo*. This step was repeated, and upon the second filtration 185 mg of a blackish, hydrocarbon insoluble solid was removed, affording a dark orange filtrate. This filtrate was stored at -35 °C and decanted 2x away from a small amount of precipitate which had settled out of solution. The filtrate was dried *in vacuo* and a ^1H NMR spectrum of the resulting orange-brown solid was acquired (C_6D_6) which showed resonances consistent with one -N[R]Ar ligand environment and solvated THF. A ^2H NMR spectrum showed a single resonance at 1.5 ppm. No ν_{NN} stretch was observed by infrared spectroscopy (THF, KBr). The solvated THF was not removable by lyophilization from a frozen benzene solution. An empirical formula for this orange-brown solid that is consistent with the ^1H NMR data obtained is *2.5 molecules of THF per 3 -N[R]Ar ligands, or a species such as "[Na(THF)$_{2.5}$][Mo(N[R]Ar)$_3$]"*. Analogous ^1H NMR spectra were obtained in several independent experiments. ^1H NMR (300 MHz, C_6D_6, 25 °C): δ = 6.24 (s, 4), 5.82 (5), 3.24 (t, THF), 2.25 (3), 1.45 (1), 1.23 (m, THF). No change was observed in the ^1H NMR spectrum of this material after exposure to air for a period of 1 h. Addition of 2 eq of 12-crown-4 to a sample of this solid in THF resulted in a complex mixture of products. An attempt to regenerate $Mo(N[R]Ar)_3$ by oxidation of the reduction product with stoichiometric ferrocenium triflate in OEt_2 led to a complex mixture of products including a large amount of HN[R]Ar. Upon addition of ca. stoichiometric $Mo(N[R]Ar)_3$ to this material, dissolved in THF under a dinitrogen atmosphere, fast reaction chemistry was observed leading, over a period of 24 h, to a mixture of $N{\equiv}Mo(N[R]Ar)_3$, $[(N_2)Mo(N[R]Ar)_3]$, and the starting material "$[Na(THF)_{2.5}][Mo(N[R]Ar)_3]$" in a 2:1:2 ratio, respectively. The ligand degradation byproduct HN[R]Ar was also produced in this reaction (ca. 14 %). The complex reacted slowly with carbon monoxide over a period of 30 minutes but did not afford the expected $[Na][(OC){\equiv}Mo(N[R]Ar)_3]$ which has been independently prepared (see Chapter 2). Additionally, the complex did not react independently with N_2 to form the known

species $[(N_2)Mo(N[R]Ar)_3]^-$. X-ray quality crystals of this material were never obtained. The nature of the reduction product remains unclear and its formulation simply as "$[Na(THF)_{2.5}][Mo(N[R]Ar)_3]$" is not likely to be correct.

4.7 Synthesis of $(Ph[t\text{-}Bu]N)_3Ti(\mu\text{-}N_2)Mo(N[R]Ar)_3$.

Solid orange $Mo(N[R]Ar)_3$ (187.5 mg, 0.293 mmol) and solid green $Ti(N[t\text{-}Bu]Ph)_3$ (144 mg, 0.293 mmol) were weighed into a 20 mL scintillation vial charged with a stir bar. 3.5 mL of OEt_2 were added to the vial and the contents was stirred at 25 °C, initially forming a dark, greenish orange solution. This solution was stirred under an atmosphere of dinitrogen for 36 h and monitored by ^2H NMR, showing a gradual depletion of paramagnetic $Mo(N[R]Ar)_3$ (δ = 64.5 ppm) and the formation of a single new resonance at δ = 1.8 ppm, indicative of a diamagnetic product. After 36 h all of the $Mo(N[R]Ar)_3$ had been consumed and a large amount of an orange precipitate was evident in the vial. This bright orange powder was collected on a sintered glass frit by filtration and the filtrate was pumped dry to a solid. The solids were combined and a ^1H NMR spectrum of the crude material showed a relatively clean transformation to one diamagnetic product displaying resonances for each ligand set in a 1:1 ratio (the amides on Ti being distinguishable from those on Mo). A small amount of HN[R]Ar and HN[*t*-Bu]Ph were also present. The crude material was extracted into pentane (15 mL) and recrystallized (two crops) to afford 267 mg (81 %) of a very deep orange, crystalline material. ^1H NMR (300 MHz, C_6D_6, 45 °C): δ = 7.20 (m, 8' and 5'), 7.09 (m, 8' and 5'), 7.00 (m, 8' and 5'), 6.73 (s, 5), 6.55 (br s, 4), 5.92 (br s, 4'), 2.11 (s, 3), 1.56 (s, 1), 1.49 (s, 1'). ^{13}C NMR (125.66 MHz, C_6D_6, 25 °C): 154.00 (aryl), 148.78 (aryl), 137.26 (aryl), 132.27 (aryl), 128.97 (aryl), 127.69 (aryl), 124.86 (aryl), 65.24 (6 or 6'), 62.25 (6 or 6'), 32.33 (2), 32.07 (2'), 21.86 (3). UV/vis (OEt_2): λ = 306 nm (ξ = 34 800), λ = 449 nm (ξ = 32 000). FTIR (CH_2Cl_2, CaF_2): ν_{NN} = 1575 cm^{-1}. Anal. Calcd for $C_{66}H_{78}D_{18}N_8MoTi$: C, 68.13; H, 8.32; N, 9.63. Found: C, 68.31; H, 8.40; N, 9.54.

4.8 Synthesis of $Ti(N[t\text{-}Bu]Ph)_3(\mu\text{-}^{15}N_2)Mo(N[R]Ar)_3$.

A 100 mL vessel containing $^{15}N_2$ gas at one atmosphere (approx. 4.1 mmol) was attached to a 50 mL round-bottom Schlenk flask containing a stir bar. The two vessels were separated by a break-seal. OEt_2 (8mL) was added to the Schlenk flask, which was subsequently degassed. Under a counter-flow of argon 200 mg of solid $Mo(N[R]Ar)_3$ (0.311 mmol) and 153 mg $Ti(N[t\text{-}Bu]Ph)_3$ were added to the Schlenk flask. The break seal was broken with the stir bar in order to expose the system to $^{15}N_2$. The reaction work-up followed the same protocol as that described above for $(Ph[t\text{-}Bu]N)_3Ti(\mu\text{-}N_2)Mo(N[R]Ar)_3$. FTIR ($CH_2Cl_2$, CaF_2): $\nu(^{15}NN)$ = 1524 cm^{-1} (calcd. 1522 cm^{-1}). ^{15}N NMR (50.65 MHz, C_6D_6, 25 °C): δ = 437.15 (d, $^1J_{NN}$ = 12.6 Hz), 433.09 (d, $^1J_{NN}$ = 12.6 Hz). $^{15}NH_2Ph$ was used as reference at 55 ppm relative to liquid ammonia at 0 ppm.

4.9 X-ray structure of (Ph[*t*-Bu]N)$_3$Ti(μ-N$_2$)Mo(N[R]Ar)$_3$.

Deep orange crystals were grown slowly from a pentane solution at -35 °C. The crystals were quickly moved from a scintillation vial to a microscope slide containing Paratone N (an Exxon product). Under the microscope an orange plate was selected and mounted on a glass fiber using wax. A total of 31317 reflections were collected ($-17 \leq h \leq 13$, $-21 \leq k \leq 21$, $-28 \leq l \leq 27$) in the θ range of 1.32 to 23.26° of which 11068 were unique ($R_{int} = 0.0616$). The structure was solved by direct methods in conjunction with standard difference Fourier techniques. All non-hydrogen atoms were placed in calculated ($d_{\text{C-H}} = 0.96$ Å) positions. The largest peak and hole in the difference map were 0.405 and -0.354 e·Å^{-3}, respectively. A semi-empirical absorption correction was applied based on pseudo-ψ-scans with maximum and minimum transmission equal to 0.1513 and 0.0954, respectively. A solvent pentane molecule was located in the difference map of the asymmetric unit and included during refinement. The least squares refinement converged normally with residuals of R (based on F) = 0.0579, wR (based on F^2) = 0.1326, and GOF = 1.086 based upon $I > 2\sigma(I)$. Crystal data for $C_{71}H_{107}MoN_8Ti$: monoclinic, space group = $P2_1/n$, $z = 4$, $a = 15.679(2)$ Å, $b = 19.580(4)$ Å, $c = 25.319(3)$ Å, $\alpha = 90°$, $\beta = 95.61(2)°$, $\gamma = 90°$, $V = 7736(2)$ Å^3, $\rho_{calc} = 1.045$ g·cm^{-3}, $F(000) = 2612$.

4.10 Synthesis and characterization of Mo(N[Ad]Ar)$_3$.

To a 500 mL flask was added 7.44 g Li(N[Ad]Ar) (2.85 mmol) and OEt_2 (150 mL). The mixture was stirred for 5 min at 25 °C and then $MoCl_3(THF)_3$ (5.96 g) was added in one portion. The reaction mixture darkened and attained a light brown color after 5 h, at which time it was filtered through Celite. The filtrate was stored at −35 °C to precipitate out a small quantity of solid. The mixture was then filtered through a sintered glass frit and the filter cake was washed with pentane until the washings were colorless. The orange washings and filtrate were combined and the cooling/filtration/extraction process was repeated. After solvent removal *in vacuo*, the residue was extracted into OEt_2 (50 mL). The solution was stored at ca. 28 °C until a light-orange solid precipitated. The solid (3.1 g) was collected on a frit and dried *in vacuo*. The ^{1}H NMR spectrum (C_6D_6) of the material revealed ≈ 2 % impurity of HN(Ad)Ar. The orange solid was dissolved in a 50:50 pentane–benzene mixture and the resulting solution was filtered through Celite. Solvent was removed from the filtrate *in vacuo*, affording 2.85 g of a light orange-yellow powder (35 %). μ_{eff} (C_6D_6) = 2.96 μ_B. Anal. Calcd for $C_{54}H_{72}MoN_3$: C, 75.49; H, 8.45; N, 4.89. Found: C, 75.33; H, 8.45; N, 4.68.

4.11 X-ray Structure of Mo(N[Ad]Ar)$_3$.

Orange rectangular crystals were grown slowly from an OEt_2 solution at 25 °C. The crystals were quickly moved from a scintillation vial to a microscope slide containing Paratone N (an Exxon product). Under the microscope an orange plate was selected and mounted on a glass fiber using wax. A total of 19029 reflections were collected ($-10 \leq h \leq 20$, $-14 \leq k \leq 13$, $-23 \leq l \leq 21$) in the θ range of 1.14 to 23.25° of which 6804 were unique ($R_{int} = 0.0469$). The structure was solved by direct methods in conjunction with standard difference Fourier techniques. All non-hydrogen atoms

were placed in calculated ($d_{C\text{-}H}$ = 0.96 Å) positions. The largest peak and hole in the difference map were 0.357 and −0.504 e·Å^{-3}, respectively. A semi-empirical absorption correction was applied based on pseudo-ψ-scans with maximum and minimum transmission equal to 0.6720 and 0.6191, respectively. The least squares refinement converged normally with residuals of R (based on F) = 0.0535, wR (based on F^2) = 0.1040, and GOF = 1.274 based upon $I > 2\sigma(I)$. Crystal data for $C_{47}H_{72}MoN_3$: monoclinic, space group = $P2_1/c$, z = 4, a = 18.874(3) Å, b = 12.6894(11) Å, c = 20.947(5) Å, α = 90°, β = 108.805(13)°, γ = 90°, V = 4749.0(13) Å^3, ρ_{calc} = 1.202 g·cm^{-3}, $F(000)$ = 1836.

4.12 Synthesis of [Na][(N$_2$)Mo(N[Ad]Ar)$_3$].

A 0.4 % Na/Hg amalgam was prepared by dissolving 100 mg Na metal (4.350 mmol) in 25 g Hg in a 50 mL RB-flask charged with a stir bar. THF (17 mL) was added to the amalgam and the mixture was stirred for five minutes, after which time orange Mo(N[Ad]Ar)$_3$ (895 mg, 1.045 mmol) was added directly to the vigorously stirring mixture as a solid. The reaction flask was plugged with a rubber septum fitted with a needle inlet, providing constant exposure to a dinitrogen atmosphere. The reaction solution acquired a scarlet color within 10 hours. The mixture was stirred for 35 hours after which time the deep scarlet supernatant was decanted away from the amalgam and dried *in vacuo*. The residue was subsequently extracted into OEt_2 (40 mL) and filtered through Celite. The filtrate was again dried *in vacuo*. Pentane (10 mL) was added to the resulting scarlet solid, effecting the precipitation of a bright orange solid from a solution which was now red-orange. The orange solid was collected on a sintered frit and washed twice with 10 mL of pentane. Pumping to dryness afforded 610 mg (64 %) of the solvent-free species [Na][(N$_2$)Mo(N[Ad]Ar)$_3$]. This solid was virtually insoluble in all hydrocarbons including benzene and was found to be unstable in CH_2Cl_2 and $CHCl_3$. Spectroscopic characterization was carried out on samples crystallized from OEt_2 at -35 °C, which produced a scarlet crystalline material in good yield. *Air-drying* of such a solid and subsequent extraction into C_6D_6 afforded homogeneous solutions which could be spectroscopically analyzed. A ^{1}H NMR spectrum of such a sample showed shifted OEt_2 resonances (there were approximately 9 molecules of OEt_2 per [Na][(N$_2$)Mo(N[Ad]Ar)$_3$]). ^{1}H NMR (300 MHz, C_6D_6, 25 °C): δ = 6.88 (s, 4), 6.63 (s, 5), 3.25 (q, OEt_2), 2.24 (s, 3), 2.18 (s, Ad), 1.93 (s, Ad), 1.67 (s, Ad), 1.11 (t, OEt_2). ^{13}C NMR (125.66 MHz, C_6D_6, 25 °C): δ = 136.89 (aryl), 131.45 (aryl), 121.76 (aryl), 118.11 (aryl), 68.24 (OEt_2), 66.3, 61.7, 45.9, 44.3, 37.80, 37.17, 32.63, 31.73, 30.55, 26.18, 23.46, 23.08, 21.93, 15.96 (OEt_2), 14.72 (OEt_2). FTIR (THF, KBr): ν_{NN} = 1783, 1757 cm^{-1}. UV/vis (OEt_2): λ_{max} = 465 nm (ξ = 4000). A sample appropriate for microanalysis was obtained as the discrete salt complex [Na(12-crown-4)$_2$][(N$_2$)Mo(N[Ad]Ar)$_3$] by addition of 2 eq of a benzene solution of 12-crown-4 to a scarlet solution of [Na][(N$_2$)Mo(N[Ad]Ar)$_3$] in THF–benzene. The resulting violet solution was dried *in vacuo* and washed thoroughly with pentane affording a violet powder. Recrystallization from a toluene–THF mixture at -35 °C afforded [Na(12-crown-4)$_2$][(N$_2$)Mo(N[Ad]Ar)$_3$] in good yield. Anal. Calcd for $C_{70}H_{104}N_5MoNaO_8$: C, 66.59; H, 8.30; N, 5.55. Found: C, 65.95; H, 8.41; N, 5.43.

4.13 X-ray Structure of $[Na(THF)_3][(N_2)Mo(N[Ad]Ar)_3]$.

Deep scarlet crystals were grown slowly by slow diffusion of heptane into a scarlet THF solution at 25 °C. The crystals were quickly moved from a scintillation vial to a microscope slide containing Paratone N (an Exxon product). Under the microscope a scarlet plate was selected and mounted on a glass fiber using wax. A total of 26843 reflections were collected ($-34 \leq h \leq 33$, $-31 \leq k \leq 34$, $-14 \leq l \leq 16$) in the θ range of 1.31 to 20.00° of which 7153 were unique (R_{int} = 0.0813). The structure was solved by direct methods in conjunction with standard difference Fourier techniques. All non-hydrogen atoms were placed in calculated ($d_{C\text{-}H}$ = 0.96 Å) positions. The largest peak and hole in the difference map were 1.246 and -0.907 e·Å^{-3}, respectively. A semi-empirical absorption correction was applied based on pseudo-ψ-scans with maximum and minimum transmission equal to 0.8158 and 0.6361, respectively. The least squares refinement converged normally with residuals of R (based on F) = 0.1443, wR (based on F^2) = 0.3792, and GOF = 1.297 based upon $I > 2\sigma(I)$. Crystal data for $C_{66}H_{72}MoN_5NaO_3$: trigonal, space group = $P\bar{3}$,z = 6,a=31.1129(8)Å,b=31.1129(8)Å,c=14.9633(6)Å,$\alpha = 90°$, $\beta = 90°$, $\gamma = 120°$, V = 12544.1(7) Å^3, ρ_{calc} = 0.875 g·cm^{-3}, $F(000)$ = 3480.

4.14 Synthesis of $(Me_3SiNN)Mo(N[Ad]Ar)_3$.

In a 20 mL scintillation vial solid orange $[Na][(N_2)Mo(N[Ad]Ar)_3]$ (34.5 mg, 0.0379 mmol) was dissolved in OEt_2 (2.5 mL) to form a scarlet solution. A separate OEt_2 solution (2 mL) of chlorotrimethylsilane (6 mg, 0.0552 mmol) was prepared and the solutions were then mixed at -35 °C. The stirring mixture turned to a bright yellow within five minutes. After 15 minutes the solution was filtered through Celite, removing a yellow cake which was washed with benzene (2 mL) until washings were colorless. The volatiles were removed *in vacuo* and the resulting yellow residue was recrystallized from pentane in two crops affording 21 mg (58 %) of the crystalline yellow solid $(Me_3SiNN)Mo(N[Ad]Ar)_3$. ^{1}H NMR (300 MHz, C_6D_6, 25 °C): δ = 6.89 (s, 5), 6.33 (s, 4), 2.16 (s, 5), 2.12 (s, Ad), 2.06 (s, Ad), 1.68 (dd, Ad), 0.39 (s, Si*Me*$_3$). ^{13}C NMR (125.66 MHz, C_6D_6, 25 °C): 137.31 (aryl), 131.74 (aryl), 121.78 (aryl), 118.13 (aryl), 66.77(9), 46.30(Ad), 44.33(Ad), 37.39(Ad), 37.16(Ad), 31.67(Ad), 30.54(Ad), 23.07(3), 21.95. FTIR (THF, KBr): ν_{NN} = 1646 cm^{-1} (br). Anal. Calcd for $C_{57}H_{81}N_5MoSi$: C, 71.29; H, 8.50; N, 7.29. Found: C, 71.22; H, 8.38; N, 7.19.

4.15 Synthesis of $(PhC(O)NN)Mo(N[Ad]Ar)_3$.

In a 20 mL scintillation vial solid orange $[Na][(N_2)Mo(N[Ad]Ar)_3]$ (92.3 mg, 0.101 mmol) was dissolved in OEt_2 (4mL) to form a scarlet solution. A separate OEt_2 solution (2 mL) of benzoylchloride (15.1 mg, 0.107 mmol) was prepared. Both solutions were chilled to -35 °C and the solution of benzoylchloride was then added quickly to the stirring solution of $[Na][(N_2)Mo(N[Ad]Ar)_3]$ causing a rapid color change to dark olive green. The solution was allowed to stir for an additional 24 h and then filtered through Celite. A bright orange solid was obtained by crystallization from pentane in several crops from the green filtrate (45 mg, 45 %). A benzene solution of this solid was thermally stable at 75 °C for 2 h. ^{1}H NMR (300 MHz, C_6D_6, 25 °C): δ = 8.73 (d, *para*-C_6H_5),

7.24 (m, *ortho, meta*-C_6H_5), 6.69 (5), 6.15 (4), 2.31 (Ad), 2.17 (Ad), 2.09 (3), 1.80 (Ad), 1.57 (Ad). ^{13}C NMR (125.66 MHz, C_6D_6, 25 °C): 146.98 (aryl), 137.79 (aryl), 131.58 (aryl), 129.61 (aryl), 129.34 (aryl), 121.77 (aryl), 118.13 (aryl), 65.74(9), 45.54(Ad), 44.31(Ad), 37.19(Ad), 31.74(Ad), 30.54(Ad), 21.84(3). Anal. Calcd for $C_{61}H_{77}N_5MoO$: C, 73.84; H, 7.82; N, 7.06. Found: C, 73.22; H, 7.88; N, 6.99.

4.16 Synthesis of [Na][(N_2)Mo(N[R]Ar)$_3$].

The following synthesis was carried out in a Dry-glove box under one atmosphere of dinitrogen. A 0.44 % Na/Hg amalgam was prepared by slowly dissolving Na (400mg, 0.0174 mol) in Hg (91 g, 0.454 mol) in a 250 mL RB-flask. The amalgam was allowed to cool to ambient temperature and THF (60 mL) was added to the flask. The contents were stirred vigorously for five minutes. Orange Mo(N[R]Ar)$_3$ (620 mg, 0.0965 mmol) was dissolved in THF (40 mL, 0.024M solution) and this solution was placed in a dropping funnel equipped with a stopcock. The orange solution of Mo(N[R]Ar)$_3$ was added dropwise, very slowly, to the vigorously stirring solution containing the amalgam at 25 °C. The rate was adjusted such that the addition took place over a period of ten hours. *Note: If the solution of Mo(N[R]Ar)$_3$ was added too quickly a side product, N≡Mo(N[R]Ar)$_3$, resulted in varying amounts depending on the rate of addition.* During the addition the solution acquired a scarlet color. The reaction mixture was stirred for an additional 12 h at 25 °C after which time the solvent was removed *in vacuo*. The resulting residue was extracted with pentane (30 mL) and decanted away from the amalgam. This orange solution was filtered through Celite and dried to a fine orange powder. Spectroscopic analysis (^1H NMR) revealed near quantitative conversion (96 % crude) to the desired product [Na][(N_2)Mo(N[R]Ar)$_3$] with only 2 % of amine HN[R]Ar and 2 % nitride N≡Mo(N[R]Ar)$_3$ present as side products. The orange powder was recrystallized from pentane in 69 % yield affording pure [Na][(N_2)Mo(N[R]Ar)$_3$] containing a trace amount of THF. ^1H NMR (300 MHz, C_6D_6, 25 °C): δ = 6.804 (s, 4), 6.63 (s, 5), 2.22 (s, 3), 1.38 (s, 1). ^{13}C NMR (125.66 MHz, C_6D_6, 25 °C): δ = 156.2 (aryl), 137.0 (aryl), 130.1 (aryl), 124.3 (aryl), 60.9 (6), 34.8 (1), 33.0 (2), 23.1 (3), 21.8 (3). FTIR (THF, KBr): ν_{NN} = 1761 cm^{-1}. Addition of two eq of 12-crown-4 afforded the discrete violet salt [Na(12-crown-4)$_2$][(N_2)Mo(N[R]Ar)$_3$]. This salt was highly insoluble in solvents such as pentane, diethyl ether, and benzene but was easily dissolved in THF and was recrystallized ca. quantitatively from a pentane–THF mixture. FTIR (THF, KBr): ν_{NN} = 1761 cm^{-1}. Elemental analysis. Anal. Calcd for $C_{52}H_{68}D_{18}N_5O_8MoNa$: C, 59.69; H, 8.28; N, 6.69. Found: C, 59.46; H, 8.26; N, 6.61.

4.17 X-ray Structure of [Na(12-crown-4)$_2$][(N_2)Mo(N[R]Ar)$_3$].

Deep violet crystals were grown slowly from a pentane–THF solution at -35 °C. The crystals were quickly moved from a scintillation vial to a microscope slide containing Paratone N (an Exxon product). Under the microscope a violet plate was selected and mounted on a glass fiber using wax. A total of 9132 reflections were collected ($-13 \leq h \leq 13, -16 \leq k \leq 18, -13 \leq l \leq 19$) in the θ range of 1.49 to 20.00° of which 5796 were unique ($R_{int} = 0.0690$). The structure was solved by direct methods in conjunction with standard difference Fourier techniques. All non-hydrogen atoms were placed in calculated ($d_{C\text{-}H}$ = 0.96 Å) positions. The largest peak and hole in the difference

map were 0.632 and -0.552 e·Å^{-3}, respectively. No absorption correction was applied. The least squares refinement converged normally with residuals of R (based on F) = 0.1156, wR (based on F^2) = 0.2431, and GOF = 1.117 based upon $I > 2\sigma(I)$. Crystal data for $C_{52}H_{86}MoN_5NaO_8$: triclinic, space group = P1, z = 2, a = 12.3630(8) Å, b = 16.2797(11) Å, c = 17.8547(12) Å, α = 71.3237(12)°, β = 87.1904(7)°, γ = 80.7164(12)°, V = 3359.7(4) Å^3, ρ_{calc} = 1.016 g·cm^{-3}, $F(000)$ = 1100.

4.18 [Na][(N_2)Mo(N[R]Ar)$_3$] + [Cp_2Fe][O_3SCF_3].

A scarlet solution of [Na][(N_2)Mo(N[R]Ar)$_3$] (36.0 mg, 0.0519 mmol) in 1.5 mL of THF was prepared in a small vial equipped with a stir bar. A separate deep blue solution of 17.4 mg ferrocenium triflate, [Cp_2Fe][O_3SCF_3] (0.0519 mmol), in 1.5 mL of THF was similarly prepared. The scarlet solution was added quickly at 25 °C to the intense blue solution of [Cp_2Fe][O_3SCF_3]. Effervescence was observed at once and the resulting homogeneous solution was orange-red in color. After filtration,the volatiles were removed *in vacuo* and spectroscopic analysis (FTIR, ^{1}H NMR, ^{2}H NMR) of the crude mixture confirmed complete consumption of [Na][(N_2)Mo(N[R]Ar)$_3$] and stoichiometric formation of Mo(N[R]Ar)$_3$ and Cp_2Fe. An analogous experiment carried out at low temperature (-35 °C) proceeded similarly.

4.19 Mo(N[R]Ar)$_3$ + [Na][(N_2)Mo(N[R]Ar)$_3$].

Scarlet [Na][(N_2)Mo(N[R]Ar)$_3$] (27 mg, 0.0390 mmol) was dissolved in THF (2mL) in a 20 mL scinitillation vial equipped with a stir bar. An orange solution of Mo(N[R]Ar)$_3$ (25 mg, 0.0389 mmol) in THF (1.5 mL) was added dropwise to the stirring scarlet solution over a period of ca. 30 seconds. No color change was observed after the first few minutes had passed. Within 30 minutes, however, the solution had acquired an intense purple color and a ^{2}H NMR spectrum of the reaction mixture after 1.5 h indicated the presence of the paramagnetic dinuclear complex (μ-N_2){Mo(N[R]Ar)$_3$}$_2$ (ca. 13 ppm) and a diamagnetic species (1.7 ppm) in a 1:7 ratio. All of the starting Mo(N[R]Ar)$_3$ had been consumed by this time. The reaction mixture was dried *in vacuo* after 7 h, by which time the intense purple color of (μ-N_2){Mo(N[R]Ar)$_3$}$_2$ had faded. A ^{1}H NMR spectrum of the crude mixture showed N≡Mo(N[R]Ar)$_3$ (62.4 %), [Na][(N_2)Mo(N[R]Ar)$_3$] (35.3 %), and HN[R]Ar (2.3 %).

4.20 Mo(N[R]Ar)$_3$ + [Na][(N_2)Mo(N[R]Ar)$_3$] + Hg under N_2.

In a 20 mL scintillation vial orange Mo(N[R]Ar)$_3$ (23.2 mg, 0.0360 mmol) was dissolved in THF (1.5 mL) and 207 mg of liquid mercury were added to the stirring solution at 25 °C. A solution of [Na][(N_2)Mo(N[R]Ar)$_3$] (25 mg, 0.0360 mmol) in THF (2 mL) was then added quickly via pipette. An intense purple color developed during the first hour of stirring. After 14 h, the solution was dried *in vacuo*. Addition of pentane (4 mL) to the dried residue resulted in an orange solution which was decanted away from a grey particulate at the base of the vial. The amalgam was washed further with pentane until the washings were colorless. The orange solution was dried

to a constant weight of 44.8 mg. ^{1}H NMR analysis of the crude orange solid (in C_6D_6 with an internal integration standard of hexamethyldisiloxane) showed the spectroscopically identifiable products to be N≡Mo(N[R]Ar)$_3$ (60 %), [Na][(N$_2$)Mo(N[R]Ar)$_3$] (28 %), and HN[R]Ar (6.5 %). A ^{2}H NMR spectrum of this solid (in THF) revealed that ca. 5 % of (μ-N$_2$){Mo(N[R]Ar)$_3$}$_2$ remained. The grey particulate which remained in the original reaction vial was tested for its activity to facilitate dinitrogen binding and cleavage by preparing a fresh solution of Mo(N[R]Ar)$_3$ (23.2 mg, 0.0360 mmol) in THF (2 mL) and adding it to the original reaction vial containing the grey particulate. The contents of the vial were stirred for several hours. The solution remained orange throughout and after 7 h a ^{1}H NMR spectrum of the crude mixture revealed only ca. 8 % N≡Mo-(N[R]Ar)$_3$. Starting Mo(N[R]Ar)$_3$ was the only other species detectable (ca. 90 % of the mixture).

4.21 Mo(N[R]Ar)$_3$ + [Na(12-crown-4)$_2$][(N$_2$)Mo(N[R]Ar)$_3$] under vacuum. Attempted synthesis of [Na(12-crown-4)$_2$](μ-N$_2$){Mo(N[R]Ar)$_3$}$_2$.

Solids violet [Na(12-crown-4)$_2$][(N$_2$)Mo(N[R]Ar)$_3$] (44.0 mg, 0.0421 mmol) and orange Mo(N[R]-Ar)$_3$ (27.1 mg, 0.0421 mmol) were weighed carefully into a sealable NMR tube. The tube was evacuated and rigorously degassed. THF (1.2 mL) was then vacuum distilled into the the tube at -196 °C. The tube was flame-sealed and transferred directly to a -78 °C dry-ice/isopropanol bath. The cold sample was then quickly analyzed by ^{2}H NMR spectroscopy. Both starting materials were present in near stoichiometric amounts (assignments at δ = 65 ppm for Mo(N[R]Ar)$_3$ and δ = 2.2 ppm for [Na(12-crown-4)$_2$][(N$_2$)Mo(N[R]Ar)$_3$]). A small amount of the neutral bridged complex (μ-N$_2$){Mo(N[R]Ar)$_3$}$_2$ was observed (δ = 13 ppm). No other resonances were observed. Upon standing at 25 °C the resonance at 13 ppm decayed to a new peak at 2 ppm, consistent with formation of N≡Mo(N[R]Ar)$_3$ (the signals for diamagnetic [Na(12-crown-4)$_2$][(N$_2$)Mo(N[R]Ar)$_3$] and N≡Mo(N[R]Ar)$_3$ are coincident by ^{2}H NMR spectroscopy). The relative ratios of starting Mo(N[R]Ar)$_3$ and [Na(12-crown-4)$_2$][(N$_2$)Mo(N[R]Ar)$_3$] remained constant over a period of 24 h at 25 °C. This experiment was repeated several times and always showed small but varying amounts of **3**. *A signal assignable to [Na(12-crown-4)$_2$][(μ-N$_2$){Mo(N[R]Ar)$_3$}$_2$] was not spectroscopically observed.* A similar experiment, performed with the ion-pair species [Na][(N$_2$)Mo(N[R]Ar)$_3$] and Mo(N[R]Ar)$_3$, behaved analogously.

4.22 Reaction of [Na][(N$_2$)Mo(N[R]Ar)$_3$] with Mo(N[*t*-Bu]Ar)$_3$ under vacuum.

Solid orange Mo(N[*t*-Bu]Ar)$_3$ (14.0 mg, 0.0224 mmol) and solid scarlet [Na][(N$_2$)Mo(N[R]Ar)$_3$] (17.1 mg, 0.0246 mmol) were carefully weighed into a sealable NMR tube. Rigourously de-gassed THF was subsequently vacuum distilled into the evacuated tube at -196 °C and the frozen vessel was flame-sealed. Upon thawing the mixture went homogeneous and ^{2}H NMR spectroscopy was used to analyze the deuterium-labeled species present. The spectra obtained clearly showed the presence of paramagnetic Mo(N[R]Ar)$_3$ at 65 ppm (ca. 38.5 %) as well as diamagnetic [Na][(N$_2$)Mo(N[R]-Ar)$_3$] at 1.0 ppm (ca. 54.5 %). A small amount of bridged (μ-N$_2$){Mo(N[R]Ar)$_3$}$_2$ was observed at 13 ppm (ca. 7 %). A ^{1}H NMR spectrum of the mixture, reconstituted in C_6D_6, confirmed that [Na(N$_2$)Mo(N[*t*-Bu]Ar)$_3$] had formed. This result was reproduced in two independent experiments.

References

[1] Sellmann, D.; Sutter, J. *Acc. Chem. Res.*, **1997**, *30*, 460. Richards, R. L. *Coord. Chem. Rev.*, **1996**, *154*, 83. Fryzuk, M. D.; Love, J. B.; Rettig, S. J.; Young, V. G. *Science*, **1997**, *275*, 1445. Leigh, G. J. *Acc. Chem. Res.*, **1992**, *25*, 177. Glassman, T. E.; Vale, M. G.; Schrock, R. R. *J. Am. Chem. Soc.*, **1992**, *114*, 8098. Cheng, T.-Y.; Ponce, A.; Rheingold, A. L.; Hillhouse, G. L. *Angew. Chem. Int. Ed. Engl.*, **1994**, *33*, 657. Arney, D. S. J.; Burns, C. J. *J. Am. Chem. Soc.*, **1995**, *117*, 9448. Albertin, G.; Antoniutti, S.; Bordignon, E.; Pattaro, S. *J. Chem. Soc. Dalton Trans.*, **1997**, 4445. Davies, S. C.; Hughes, D. L.; Janas, Z.; Jerzykiewicz, L.; Richards, R. L.; Sanders, J. R.; Sobota, P. *Chem. Comm.*, **1997**, 1261. Bercaw, J. E.; Rosenberg, E.; Roberts, J. D. *J. Am. Chem. Soc.*, **1974**, *96*, 612. Chatt, J.; Head, R. A.; Leigh, G. J.; Pickett, C. J. *J. Chem. Soc., Dalton Trans.*, **1978**, 1638. Desmangles, N.; Jenkins, H.; Ruppa, K. B.; Gambarotta, S. *Inorg Chim Acta*, **1996**, *250*, 1.

[2] Laplaza, C. E.; Odom, A. L.; Davis, W. M.; Cummins, C. C.; Protasiewicz, J. D. *J. Am. Chem. Soc.*, **1995**, *117*, 4999.

[3] Laplaza, C. E.; Johnson, A. R.; Cummins, C. C. *J. Am. Chem. Soc.*, **1996**, *118*, 709.

[4] Laplaza, C. E.; Cummins, C. C. *Science*, **1995**, *268*, 861.

[5] Laplaza, C. E.; Johnson, M. J. A.; Peters, J. C.; Odom, A. L.; Kim, E.; Cummins, C. C.; George, G. N.; Pickering, I. J. *J. Am. Chem. Soc.*, **1996**, *118*, 8623.

[6] Kol, M.; Schrock, R. R.; Kempe, R.; Davis, W. M. *J. Am. Chem. Soc.*, **1994**, *116*, 4382.

[7] Ferguson, R.; Solari, E.; Floriani, C.; Osella, D.; Ravera, M.; Re, N.; Chiesi-Villa, A.; Rizzoli, C. *J. Am. Chem. Soc.*, **1997**, *119*, 10104.

[8] Peters, J. C.; Johnson, A. R.; Odom, A. L.; Wanandi, P. W.; Davis, W. M.; Cummins, C. C. *J. Am. Chem. Soc.*, **1996**, *118*, 10175.

[9] Wanandi, P. W.; Davis, W. M.; Cummins, C. C.; Russell, M. A.; Wilcox, D. E. *J. Am. Chem. Soc.*, **1995**, *117*, 2110.

[10] Duchateau, R.; Gambarotta, S.; Beydoun, N.; Bensimon, C. *J. Am. Chem. Soc.*, **1991**, *113*, 8986.

[11] Beydoun, N.; Duchateau, R.; Gambarotta, S. *J. Chem. Soc., Chem. Comm.*, **1992**, 244.

[12] Covert, K. J.; Neithamer, D. R.; Zonnevylle, M. C.; Lapointe, R. E.; Schaller, C. P.; Wolczanski, P. T. *Inorg. Chem.*, **1991**, *30*, 2494.

[13] Covert, K. J.; Wolczanski, P. T.; Hill, S. A.; Krusic, P. J. *Inorg. Chem.*, **1992**, *31*, 66.

[14] Taube, H. *Electron Transfer Between Metal Complexes-Retrospective*; H. Taube, Ed.; World Scientific: Singapore, **1992**, 113.

[15] Sutherland, R. *Personal Communication*, **1996**.

[16] Evans, D. F. *J. Chem. Soc.*, **1959**, 2003.

[17] Sur, S. K. *J. Magnetic Resonance*, **1989**, *82*, 169.

[18] Yamamoto, A.; Miura, Y.; Ito, T.; Chen, H.-L.; Iti, K.; Ozawa, F. *Organometallics*, **1983**, *2*, 1429.

[19] Hammer, R.; Klein, H.-F.; Schubert, U.; Frank, A.; Huttner, G. *Angew. Chem., Int. Ed. Engl.*, **1976**, *15*, 612.

[20] Klein, H.-F. *Angew. Chem., Int. Ed. Engl.*, **1980**, *15*, 362.

[21] Gailus, H.; Woitha, C.; Rehder, D. *J. Chem. Soc., Dalton Trans.*, **1994**, 3471.

[22] O'Donoghue, M. B.; Zanetti, N. C.; Davis, W. M.; Schrock, R. R. *J. Am. Chem. Soc.*, **1997**, *119*, 2753.

[23] O' Donoghue M. B.; Schrock, R. R. *Personal Communication*, **1998**.

[24] March, J. M. *Advanced Organic Chemistry, 4th Ed.*; John Wiley & Sons: New York, 1992.

[25] Hidai, M.; Mizobe, Y. *Chem. Rev.*, **1995**, *95*, 1115.

[26] Chatt, J.; Heath, G. A.; Leigh, G. J. *J. Chem. Soc., Chem. Commun.*, **1972**, 44.

[27] Sato, M.; Kodama, T.; Hidai, M.; Uchida, Y. *J. Organomet. Chem.*, **1978**, *152*, 239.

[28] Fickes, M. G.; Odom, A. L.; Cummins, C. C. *Chem. Commun.*, **1997**, 1993.

[29] Schrock, R. R.; Sturgeoff, L. G.; Sharp, P. R. *Inorg. Chem.*, **1983**, *22*, 2801.

[30] Baraldo, L. *Personal communication*, **1998**.

[31] Odom, A. L.; Arnold, P. L.; Cummins, C. C. *J. Am. Chem. Soc.*, **1998**, *in press.*

[32] Johnson, M. J.; Mindiola, D.; Arnold, P. L. *Unpublished results*, **1998**.

[33] Cui, Q.; Musaev, D. G.; Svensson, M.; Sieber, S.; Morokuma, K. *J. Am. Chem. Soc.*, **1995**, *117*, 12366.

[34] Neyman, K. M.; Nasluzov, V. A.; Hahn, J.; Landis, C. R.; Rosch, N. *Organometallics*, **1997**, *16*, 995.

[35] Pangborn, A. B.; Giardello, M. A.; Grubbs, R. H.; Rosen, R. K.; Timmers, F. J. *Organometallics*, **1996**, *15*, 1518.

[36] Johnson, A. R.; Cummins, C. C. *Inorg. Synth.*, **1997**, *In Press.*

[37] Ruppa, K. B. P.; Desmangles, N.; Gambarotta, S.; Yap, G.; Rheinghold, A. L. *Inorg. Chem.*, **1997**, *36*, 1194.

Chapter 2. Cyanide Chemistry: Reduction and Functionalization of Cyanide Bound to $Mo(N[R]Ar)_3$.

by Jonas C. Peters

MIT Department of Chemistry room 6-332
Massachusetts Institute of Technology

May 18, 1998

Contents

List of Figures

1 General Introduction

1.1 Specific goals.

Recent efforts by our research group have unveiled new routes for generating strong metal to ligand triple bonds. The C_3 symmetric arrangement of the *tris*-anilido ligand set makes available three frontier orbitals, $a + e$, where the orbital of a symmetry is largely d_{z^2} in character and the degenerate e set is largely d_{xy} and d_{xz}.[1,2] Our group's interest derives, in part, from a fascination with new chemical transformations which install multiply bonded ligands, and the discovery of *new classes* of multiply bonded ligands. An early example which manifested both of these qualities was Laplaza's discovery that Mo(N[R]Ar)$_3$, **1**, reacted directly with white phosphorus to yield a complex containing one-coordinate phosphorus, P≡Mo(N[R]Ar)$_3$.[3] At the same time, Schrock and coworkers were forging ahead in the construction of a host of species which also featured C_3 symmetric metal centers containing strong metal to ligand triple bonds.[2] Their efforts resulted, "ca. simultaneously", in the synthesis of the terminal phosphido complex [(Me$_3$SiNCH$_2$CH$_2$)$_3$N]W≡P.[4] Within a short time it was clear that a molybdenum center surrounded by three highly reducing amido ligands, as in –N[R]Ar, could react voraciously with small molecule sources to generate a host of complexes containing multiply bonded ligands. Hence, N≡Mo(N[R]Ar)$_3$ had been prepared both from N$_2$[19] and from N$_2$O,[5] P≡Mo(N[R]Ar)$_3$ from P$_4$,[3] Mo(O)(N[R]Ar)$_3$ from a variety of O-atom sources,[20] Mo(S)(N[R]Ar)$_3$ from S$_8$,[20] Mo(Se)(N[R]Ar)$_3$ from Se,[20] and Mo(Te)(N[R]Ar)$_3$ from Te.[20] Excited by this wheel of reactivity, Professor Cummins and I set out to prepare a transition metal complex featuring a one coordinate carbon atom. Our hope was to furnish such a ligand to a *tris*-amido complex of Mo and/or Re. A search of the literature provided no examples of such a species, despite the vast wealth of complexes reported containing metal to carbon multiple bonds.[6] Hence, an appropriate choice for a "C-atom" synthon became immediately problematic. Examples of molecules containing rigorously one-coordinate carbon, of which we were aware, were C≡O and related isocyanides. Viewing the *tris*-anilido molybdenum fragment as isolobal with an N-atom and an analogous *tris*-anilido rhenium fragment as isolobal with an O-atom, we reasoned that delivery of a carbido ligand to such templates might afford stable d^0 complexes [$^-$(C)Mo(N[R]Ar)$_3$] and (C)Re(N[R]Ar)$_3$, isolobal with cyanide and carbon monoxide, respectively. By analogy to N≡Mo-(N[R]Ar)$_3$ prepared from dinitrogen, we looked to isoelectronic C≡O and $^-$C≡N as sources of a carbido functionality. Though the neutral (C)Re(N[R]Ar)$_3$ remains an unanswered question — to date our group has yet to access rhenium complexes bearing the –N[R]Ar substituents — these two chapters present a detailed investigation which ultimately lead to the synthesis and study of a molecular molybdenum carbide featuring one coordinate carbon, $^-$C≡Mo(N[R]Ar)$_3$.[13] The C-atom was derived from C≡O.

1.2 Background.

The dinitrogen cleavage reaction of Mo(N[R]Ar)$_3$ established that N$_2$ is a viable N-atom donor when the potential to form the dinuclear species (μ-N$_2$)[Mo(N[R]Ar)$_3$]$_2$ exists. Thermodynamics seemingly favors this cleavage reaction due to the two N≡Mo triple bonds generated. A logical extrapolation was that CN$^-$ might function similarly if sandwiched by two Mo(N[R]Ar)$_3$ fragments

and potentially split apart to generate one d^0 [$^-$C≡Mo(N[R]Ar)$_3$] fragment and one d^0 N≡Mo(N-[R]Ar)$_3$ fragment, as depicted in eqn 1.

$$[^-N{=}C{=}Mo(N[R]Ar)_3] \xrightarrow{Mo(N[R]Ar)_3} [^-C{\equiv}Mo(N[R]Ar)_3] + N{\equiv}Mo(N[R]Ar)_3 \quad (1)$$

By analogy, we envisioned similar routes to [C≡Mo(N[R]Ar)$_3$]$^-$ in which a CO ligand might be split by the direct reaction between [$^-$O-C≡Mo(N[R]Ar)$_3$] and a transition metal well-poised to accept an O-atom, such as V(mes)$_3$(THF).[7] While simple in principle, metal-mediated reactions resulting in the direct rupture of a strong C≡X triple bond (where X=O, N, NR) are relatively rare. Fig 1 shows five literature reactions which, when viewed together in conjunction with the N≡N cleavage of Mo(N[R]Ar)$_3$, provide a general framework from which the rational design of a terminal carbide complex may be approached.

Schrock established the direct six electron reduction of a nitrile by d^6 hexakis-*tert*-butoxy-ditungsten,[8] delivering carbyne and nitride functionalities to separate metal centers in the formation of distinct alkylidyne and nitride complexes (A). The cyanide cleavage strategy, presented in this chapter, bears a resemblance to the reaction shown in (A). Wolczanski has employed a related d^6 ditungsten center to expose C≡O and C≡NAr as simple sources of the carbide/oxo and carbide/imido functionalities, respectively (D). Notably, the carbide carbon atom bridges the two tungsten centers in the products. Prior to this work, Wolczanski and coworkers had shown that carbon monoxide could be cleaved cooperativley by three-coordinate tantalum centers (B). The bridged-acetylide product was thought to be derived from a ketenylide (OCC)Ta(OSi-*t*-Bu$_3$)$_3$ precursor, *not* from a terminal "(C)Ta(OSi-*t*-Bu$_3$)$_3$" species which subsequently underwent bimolecular coupling.[9,10] Chisholm and coworkers have studied a host of multinuclear tungsten complexes able to reductively cleave C≡X bonds,[11] an example of which is shown in (C).[12] Finally, reagent-based strategies have found utility in the stepwise cleavage of C≡X triple bonds.[13] Fehlhammer reported that phthaloyl dichloride reacts with an Fe-coordinated cyanide ligand as a means, in effect, to activate cyanide and deliver an N-atom to the organic substrate in the generation of a pthalimide byproduct (E).[14,15] A strategy of a reagent-based genre is presented in Chapter 3 .

2 Results and Discussion

2.1 Direct reaction of Mo(N[R]Ar)$_3$ with [N(*n*-Bu)$_4$][CN].

Our first attempt at cyanide cleavage involved the direct reaction of THF solutions of Mo(N[R]Ar)$_3$, **1**, with [N(*n*-Bu)$_4$][CN]. Addition of 1 eq of [N(*n*-Bu)$_4$][CN] to a stirring solution of **1** resulted in a rapid reaction in which a dramatic purple color appeared, persisting when stored cold but fading to brown when the solution was maintained at ambient temperatures. Spectroscopic monitoring by ^{2}H NMR reflected these color changes in that various resonances ranging from 0–7 ppm were observed to decay and to be replaced by new signals. A compound exhibiting a resonance at ca. 6 ppm appeared to be a likely candidate for the salt [N(*n*-Bu)$_4$][(NC)Mo(N[R]Ar)$_3$]. Repetitive pentane extraction of the brown residues which inevitably resulted removed pentane soluble impurities, leaving behind very small amounts of the intense blue salt [N(*n*-Bu)$_4$][(NC)Mo(N[R]Ar)$_3$], whose

C≡X Cleavage Reactions

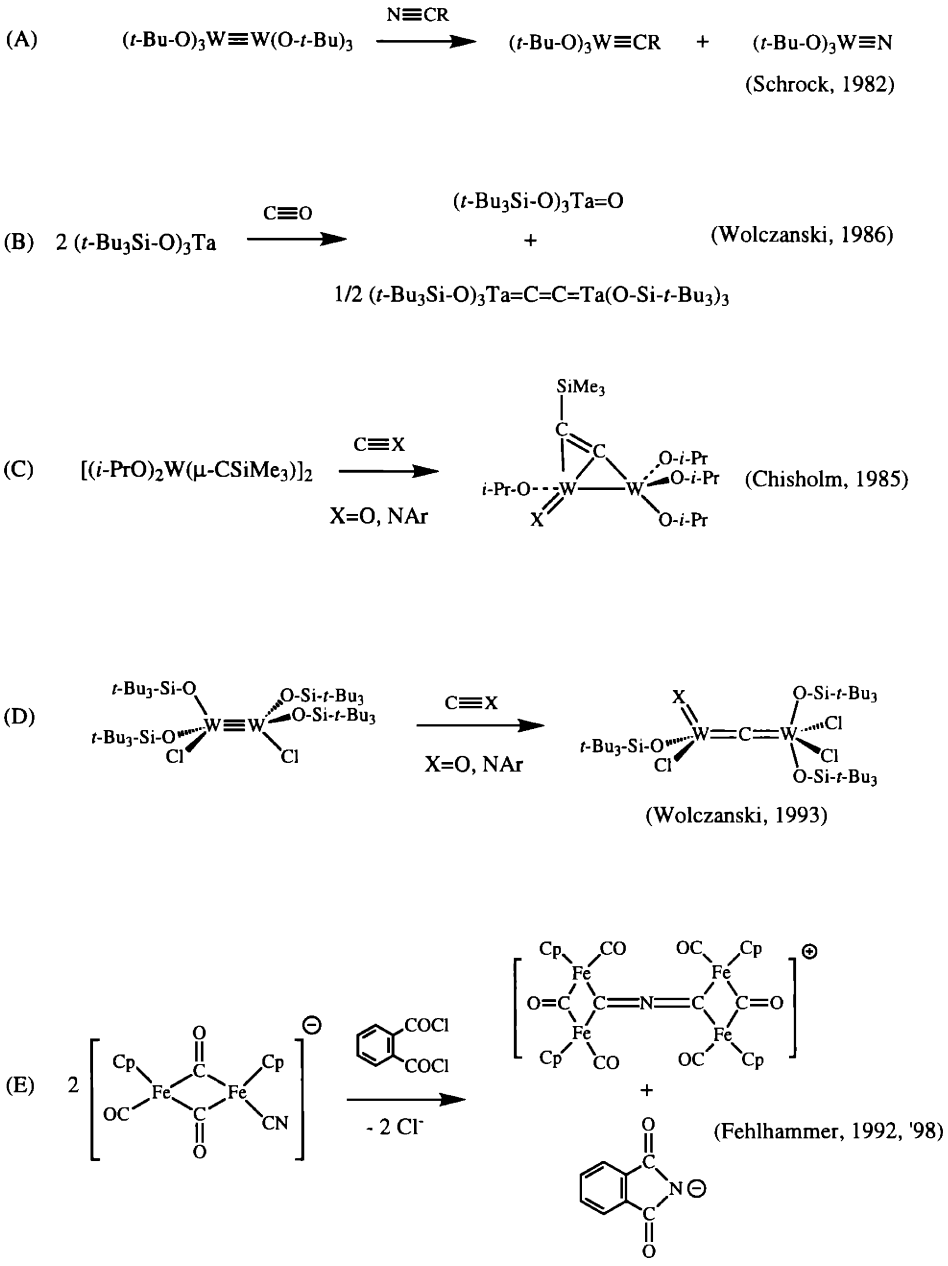

Figure 1: Illustrative examples of C≡X cleavage reactions.

IR spectrum in THF displayed an intense ν_{CN} stretch at 1941 cm^{-1}. This species showed a ^2H NMR signal at 6 ppm. Efforts to improve the synthesis of $[N(n\text{-}Bu)_4][NCMo(N[R]Ar)_3]$ by slow addition of **1** to a cold solution of $[N(n\text{-}Bu)_4][CN]$ were successful in part, but decomposition pathways remained problematic. Although slow addition of 1 eq of **1** to *1/2 eq* of $[N(n\text{-}Bu)_4][CN]$ was attempted as a direct route to the bridged species $[N(n\text{-}Bu)_4][(\mu\text{-}CN)\{Mo(N[R]Ar)_3\}_2]$, the reaction instead gave products which were not readily characterized and on work-up showed none of the anticipated $N{\equiv}Mo(N[R]Ar)_3$ which might have resulted from scission of the C–N bond of the bridged cyanide ligand.

2.2 Synthesis of $[(NC)Mo(N[Ad]Ar)_3]^-$.

The work described in Chapter 1 demonstrated that bimolecular bridged-N_2 complexes are sterically inaccessible when bulky –N[Ad]Ar ligands are employed. It was not surprising that the cyanide anion could be delivered cleanly to the more sterically encumbered $Mo(N[Ad]Ar)_3$ species. Hence, addition of a THF solution of $[N(n\text{-}Bu)_4][CN]$ to a stirring solution of $Mo(N[Ad]Ar)_3$ at 25 °C resulted in a rapid color change from orange to an intense blue. The blue color persisted, and an IR spectrum (Fig 2) of the crude mixture featured a band at 1929 cm^{-1}, indicating that the cyanide anion had been delivered to $Mo(N[Ad]Ar)_3$ as shown in eqn 2.

$$Mo(N[Ad]Ar)_3 \quad + \quad [N(n\text{-}Bu)_4][CN] \longrightarrow \begin{matrix} [N(n\text{-}Bu)_4][(NC)Mo(N[Ad]Ar)_3] \\ [N(n\text{-}Bu)_4][\mathbf{2}] \end{matrix} \qquad (2)$$

The resulting blue salt $[N(n\text{-}Bu)_4][(NC)Mo(N[Ad]Ar)_3]$, $[N(n\text{-}Bu)_4][\mathbf{2}]$, was isolated in 91 % yield by removal of the THF solvent and subsequent thorough washing of the crude salt with pentane. Initial probe experiments were performed in order to test the viability of $[N(n\text{-}Bu)_4][\mathbf{2}]$ as a direct precursor to a bridged anionic species of the form $[N(n\text{-}Bu)_4][(Ar[Ad]N)_3Mo(\mu\text{-}CN)\text{-}Mo(N[R]Ar)_3]$. Interestingly, addition of **1** to $[N(n\text{-}Bu)_4][(NC)Mo(N[Ad]Ar)_3]$ under a dinitrogen atmosphere resulted in chemistry reminiscent of that described in Chapter 1. IR spectra of such solutions revealed the gradual appearance of a band at 1766 cm^{-1}, likely indicative of the presence of $[N(n\text{-}Bu)_4][Mo(N_2)(N[R]Ar)_3]$ resulting from one electron redox chemistry. Chemical oxidation of $[N(n\text{-}Bu)_4][(NC)Mo(N[Ad]Ar)_3]$ with both ferrocenium triflate and silver triflate (*vide infra*) afforded the neutral molybdenum(IV) cyanide $(NC)Mo(N[Ad]Ar)_3$, **8**.

2.3 Direct Synthesis of $(NC)Mo(N[R]Ar)_3$ from $(I)Mo(N[R]Ar)_3$.

In order to make a *direct* electronic comparison to the well-studied N_2-cleavage reaction we required the synthesis of $(\mu\text{-}CN)\{Mo(N[R]Ar)_3\}_2$ in which all of the anilido ligands are substituted by *tert*-butyl substituents. A straightforward, and in retrospect "obvious" route, was achieved by preparation of the neutral cyanide complex $(NC)Mo(N[R]Ar)_3$, **4**, from $(I)Mo(N[R]Ar)_3$, **5**, followed by the direct condensation of **4** with a second equivalent of $Mo(N[R]Ar)_3$. Addition of a chilled solution of $[N(n\text{-}Bu)_4][CN]$ to an initially cold, brilliant green OEt_2 solution of **5** resulted, over a period of approx. 1h, in replacement of iodide with cyanide. ^2H NMR spectroscopy showed that the reaction was relatively clean. Compound **4** showed a single ^2H NMR signal at 31 ppm, readily distinguished from the resonance of **5** at 6 ppm. One eq of $[N(n\text{-}Bu)_4][I]$ precipitated from

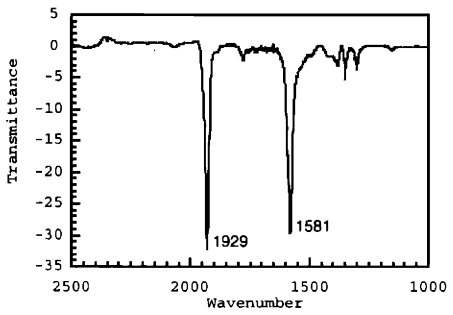

Figure 2: IR spectrum of [N(n-Bu)$_4$][(NC)Mo(N[Ad]Ar)$_3$], [N(n-Bu)$_4$][**2**] in THF solution showing an intense ν_{CN} at 1929 cm^{-1}.

the resulting red solution upon addition of pentane, and neutral **4** was obtained as a red, semi-crystalline solid in 77 % yield. Like **5**, **4** was sparingly soluble in pentane and OEt_2 when pure. Unlike its anionic analogue [(NC)Mo(N[Ad]Ar)$_3$]$^-$, the anticipated ν_{CN} stretch was not observed for **4** by IR spectroscopy. Notably, Myra O'Donoghue of the Schrock group recently prepared the neutral complex [($Me_3SiNCH_2CH_2$)$_3$N]Mo(CN) and did not observe a ν_{CN} stretch. The assignment of [($Me_3SiNCH_2CH_2$)$_3$N]Mo(CN) was justified based by on an X-ray crystallographic study.[16] SQUID magnetometry data (5–300K) were collected for **4** by Steven Klei, yielding a μ_{eff} of 2.81μ_B, consistent with two unpaired electrons for the formally molybdenum(IV) complex. A solution determination of the magnetic susceptibility by the method of Evans yielded a value of 2.46μ_B, somewhat low for the ideal spin only value of 2.83μ_B. The cyclic voltammetry of (NC)Mo(N[R]Ar)$_3$ showed reversible waves at -0.19 V and at -1.9 V (THF/[N(n-Bu)$_4$][PF_6], versus $Cp_2Fe^{+/0}$), assigned as the reversible oxidation and reduction of (NC)Mo(N[R]Ar)$_3$, respectively.[17] The reduction potential of -1.9 V for (NC)Mo(N[R]Ar)$_3$ should be compared with that of (N_2)Mo(N[R]Ar)$_3$ (-1.7 V), presented in Chapter 1. Apparently, it is measurably more difficult to reduce the neutral and stable cyanide complex of molybdenum than its neutral and unstable dinitrogen analogue.

$$\underset{\mathbf{5}}{\text{(I)Mo(N[R]Ar)}_3} + \text{[N(}n\text{-Bu)}_4\text{][CN]} \xrightarrow{\text{-[N(}n\text{-Bu)}_4\text{][I]}} \underset{\mathbf{4}}{\text{(NC)Mo(N[R]Ar)}_3} \qquad (3)$$

Interestingly, Gambarotta and coworkers have reported that a *tris*-amido complex of vanadium(IV) does not associate cyanide anion but rather is obtained as a discrete salt complex, [V{(NSiMe$_3$)$_2$}$_3$][CN], which was crystallographically characterized.[18] Our electrochemical and synthetic data suggest that cyanide complexes of *tris*-anilido molybdenum fragments are stable to oxidation and reduction, when pure. It is surprising that the cyanide anion does not find its way into the cationic pocket afforded to it by Gambarotta's [V{(NSiMe$_3$)$_2$}$_3$]$^+$. Notably, Fickes has isolated (NC)Nb(N[R]Ar)$_3$ by the reaction of (Cl)Nb(N[R]Ar)$_3$ with LiCN and presumes it to be a typical 4-coordinate complex of Nb(IV).[26] (NC)Nb(N[R]Ar)$_3$ has not been subjected to crystallographic scrutiny.

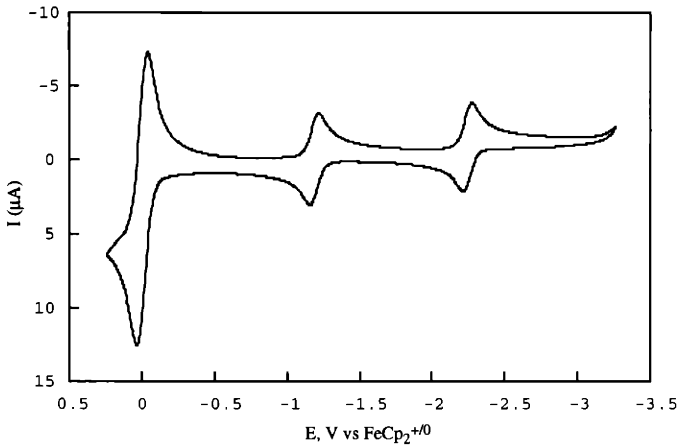

Figure 3: Cyclic Voltammogram of (μ-CN){Mo(N[R]Ar)$_3$}$_2$, **6**, in 0.5 M THF solution of [N(n-Bu)$_4$][PF$_6$]. The CV is referenced internally to $FeCp_2^{+/0}$. Scan rate = 0.1V/s.

2.4 Direct Synthesis of (μ-CN){Mo(N[R]Ar)$_3$}$_2$ from (NC)Mo(N[R]Ar)$_3$ and Mo(N[R]Ar)$_3$.

Access to the target molecule (μ-CN){Mo(N[R]Ar)$_3$}$_2$, **6**, was provided by simple addition of **1** to an ethereal solution of **4**. A rapid color change signaled condensation of the two complexes and the violet cyanide-bridged species **6** was eaily isolated and purified due to its low solubility in both OEt_2 and pentane. A ^{2}H NMR spectrum of **6** showed two distinct signals at 6.6 and 3.3 ppm, reflecting inequivalent molybdenum centers. Related (μ-N$_2$)[Mo(N[R]Ar)$_3$]$_2$, where both metal centers are chemically equivalent, exhibits a single resonace at 13 ppm.[19] A UV/vis spectrum of **6** showed a distinct absorbance at 530 nm, comparable to the characteristic absorbance at 547 nm for purple (μ-N$_2$)[Mo(N[R]Ar)$_3$]$_2$.[19] SQUID magnetometry data for **6** (5–300K) were consistent with one unpaired electron (μ_{eff} = 1.61μ_B). The cyclic voltammogram for **6**, shown in Fig 3, showed reversible waves at -1.2 V and -2.2 V assigned as the oxidation and reduction of (μ-CN)-{Mo(N[R]Ar)$_3$}$_2$, respectively. The reduction wave should be compared with that at -2.4 V for (μ-N$_2$)[Mo(N[R]Ar)$_3$]$_2$, discussed in Chapter 1. Cyanide-bridged **6** contains one less electron in its valence shell and should therefore be an easier species to reduce.

$$\underset{\mathbf{4}}{(NC)Mo(N[R]Ar)_3} + \underset{\mathbf{1}}{Mo(N[R]Ar)_3} \xrightarrow{OEt_2} \underset{\mathbf{6}}{(\mu\text{-}CN)\{Mo(N[R]Ar)_3\}_2} \quad (4)$$

2.5 Reaction of (μ-CN){Mo(N[R]Ar)$_3$}$_2$ with Na/Hg amalgam. Synthesis of (Ar[R]N)$_2$(ArN)Mo(μ-NC)Mo(N[R]Ar)$_3$, by C-N bond cleavage.

Paramagnetic (μ-CN){Mo(N[R]Ar)$_3$}$_2$ reacted with a slight excess of Na/Hg amalgam over a period of one hour, ultimately giving rise to a single diamagnetic product. Monitoring of the reaction

mixture by ^2H NMR spectroscopy over the first hour showed a rather rapid decay of the two signals corresponding to (μ-CN){Mo(N[R]Ar)$_3$}$_2$ and several new signals in the 0–10 ppm region reflective of one or more reduction products. After one hour a ^1H NMR spectrum of an aliquot of the crude reaction mixture revealed that one major diamagnetic species had been formed in approximately 90 % yield based on the (μ-CN){Mo(N[R]Ar)$_3$}$_2$ starting material. This deep orange species was pentane soluble and showed three distinct sets of resonances for the aryl groups of the anilido ligands in its ^1H NMR spectrum. That it did not react with 12-crown-4 and was rather lypophilic suggested that a Na^+ cation was not likely to be associated with the complex. This, along with the fact that the product was diamagnetic, suggested that the ion-pair product expected from reduction, [Na][(μ-CN){Mo(N[R]Ar)$_3$}$_2$], was not the species in hand. Single crystals were obtained from pentane, and an X-ray diffraction study was undertaken to confirm that the major product resulting from reduction was the neutral species (Ar[R]N)$_2$(ArN)Mo(μ-NC)Mo(N[R]Ar)$_3$, **7**, as shown in eqn 7. Complex **7** apparently results from the formal ejection of a *tert*-butyl radical, generating two diamagnetic molybdenum centers. Overall, the reaction appears to be catalytic in the Na/Hg amalgam reductant. It is likely that the reduction of (μ-CN){Mo(N[R]Ar)$_3$}$_2$ by Na/Hg is a reversible process. An attempt to identify products due to disproportionation and conproportionation of *tert*-butyl radical was carried-out by acquisition of the ^{13}C NMR spectrum of the volatile products of the reaction product mixture. Only THF solvent was observed. Because *tert*-butyl radical likely reacts with THF solvent more readily than undergoing disproportionation and conproportionation, reduction of (μ-CN){Mo(N[R]Ar)$_3$}$_2$ was attempted in C_6D_6 in the hope of identifying isobutane, isobutylene, and hexamethylethane. However, reduction did not occur in benzene over a 48 h period. Though the radical nature of the *tert*-butyl group loss has not been firmly established, C-N bond scission resulting in the elimination of *tert*-butyl radicals is a well-documented decomposition pathway for the –N[R]Ar ligand.[20] It is also noteworthy that C-N cleavage reactions thought to arise from the homolytic liberation of *tert*-butyl radical have been documented by several other groups, in particular for the *tert*-butylisocyanide ligand.[16,21,22]

$$\underset{\mathbf{6}}{(\mu\text{-CN})\{\text{Mo(N[R]Ar)}_3\}_2} \xrightarrow{\text{Na/Hg, } -\cdot[\text{C(CH}_3)(\text{CD}_3)_2]} \underset{\mathbf{7}}{(\text{Ar[R]N})_2(\text{ArN})\text{Mo}(\mu\text{-NC})\text{Mo(N[R]Ar)}_3} \quad (5)$$

Views of the X-ray structure of (Ar[R]N)$_2$(ArN)Mo(μ-NC)Mo(N[R]Ar)$_3$ are shown in figures 4 and 5. Its gross morphology can be described as a cyanide ligand bridging two molybdenum centers where the Mo-N-C-Mo linkage is bent at N with: (i) a pseudo-tetrahedral C-linked center encaged by three anilido ligands in the typical "upright" arrangement, where the *tert*-butyl substituents form a propeller about the Mo-C linkage; and (ii), a pseudo-tetrahedral N-linked center bearing two "upright" anilido ligands and a bent arylimido ligand derived from loss of the *tert*-butyl substituent. The cyanide C-N bond distance of 1.291(14) Å is suggestive of significant cyanide reduction/activation, to be compared with the C–N distance of 1.14 Å in free HCN.[23] Fehlhammer has tabulated a range of C-N bond distances for iron cyanide complexes in a recent paper titled "Activated Cyanide" that suggests the distance of 1.291(14) Å in **7** relects a rather activated cyanide ligand.[15] Holm and coworkers have structurally investigated a host of complexes wherein a cyanide ligand bridges Fe and Cu centers in a Fe-C-N-Cu linkage. This comprehensive study shows a short average C-N bond distance of 1.15(1) Å in some seven structures, despite a high variance in the

C-N-Cu angle (147°C to 147°C).[24] The N-linked molybdenum center in **7**, Mo(2), shows significant multiple bond character to both the cyanide nitrogen atom {Mo(2)-N = 1.846(11)Å} and to the imide nitrogen N(6) {Mo(2)-N(6) = 1.736(11)Å}. These values should be calibrated to the average Mo(2)-anilido distance of 1.987(10)Å. In effect, the Mo(2) center manifests a striking continuum of Mo-N bonding in its three chemically distinct nitrogenous ligands. The Mo(1)-cyanide carbon distance of 1.812(13)Å also reflects multiple bond character and the bent Mo(2)-N-C-Mo(1) linkage is probably best regarded as indicative of various degrees of multiple bonding at each respective linkage.

The cyclic voltammetry of $(Ar[R]N)_2(ArN)Mo(\mu\text{-}NC)Mo(N[R]Ar)_3$, **7**, was measured in order to compare it with its bridged precursor, $(\mu\text{-}CN)\{Mo(N[R]Ar)_3\}_2$ **6**. As shown in Fig 6, a completely *irreversible* wave was observed at -3.2 V ($THF/[N(n\text{-}Bu)_4][PF_6]$, versus $Cp_2Fe^{+/0}$) when scanning cathodically. We assigned this wave to the first reduction of **7** to generate the highly unstable anion $[(Ar[R]N)_2(ArN)Mo(\mu\text{-}NC)Mo(N[R]Ar)_3]^-$.

A *reversible* wave was observed at -2.2 V which we assigned to the oxidation of $(Ar[R]N)_2(ArN)Mo(\mu\text{-}NC)Mo(N[R]Ar)_3$ to generate the electrochemically observable cation $[(Ar[R]N)_2(ArN)Mo(\mu\text{-}NC)Mo(N[R]Ar)_3]^+$. That this wave corresponded to an oxidation of $(Ar[R]N)_2(ArN)Mo(\mu\text{-}NC)Mo(N[R]Ar)_3$ rather than a reduction was confirmed by the following rather simple experiment: Without allowing a freshly mixed solution of neutral $(Ar[R]N)_2(ArN)Mo(\mu\text{-}NC)Mo(N[R]Ar)_3$ to equilibrate we scanned cathodically from a starting potential of approximately -2.1 V. The reduction wave at -2.2 V showed only a partial reduction. As aniticipated, when the scan was reversed to the anode a full oxidation wave was observed. Reversing cathodically once more showed an increase in the intensity of the reduction wave at -2.2 V. This series of scans proved highly reproducible. We believe the experiment indicates that, on the first scan to the cathode, the solution at the electrode contained only a fraction of the oxidized species $[(Ar[R]N)_2(ArN)Mo(\mu\text{-}NC)Mo(N[R]Ar)_3]^+$ which was reduced at -2.2 V to nuetral $(Ar[R]N)_2(ArN)Mo(\mu\text{-}NC)Mo(N[R]Ar)_3$. Once the solution at the electrode was allowed to equilibrate by scanning anodically beyond the oxidation potential of $(Ar[R]N)_2(ArN)Mo(\mu\text{-}NC)Mo(N[R]Ar)_3$, reversing again to the cathode showed a more intense reduction wave. This is because the solution at the electrode had by then equilibrated and contained an appreciably higher concentration of the oxidized species.

The extremely low reduction potential of -3.2 V for **7** is approximately 1 V lower than that of its precursor **6**, which showed a *reversible* reduction at -2.2 V (*vide supra*). These electrochemical results allow us to formulate a model that explains the observed conversion of $(\mu\text{-}CN)\{Mo(N[R]Ar)_3\}_2$ to $(Ar[R]N)_2(ArN)Mo(\mu\text{-}NC)Mo(N[R]Ar)_3$ by Na/Hg amalgam in THF. Na/Hg amalgam is capable of reducing $(\mu\text{-}CN)\{Mo(N[R]Ar)_3\}_2$ to generate the anion $[(\mu\text{-}CN)\{Mo(N[R]Ar)_3\}_2]^-$, an electrochemically observable species. In the actual reaction mixture, this species undergoes a homolytic C-N bond cleavage reaction to generate $\cdot C(CD_3)_2(CH_3)$ and an extremely reducing anion, $[(Ar[R]N)_2(ArN)Mo(\mu\text{-}NC)Mo(N[R]Ar)_3]^-$. The anion $[(Ar[R]N)_2(ArN)Mo(\mu\text{-}NC)Mo(N[R]Ar)_3]^-$ should be spontaneously oxidized by any remaining $(\mu\text{-}CN)\{Mo(N[R]Ar)_3\}_2$ to generate more $[(\mu\text{-}CN)\{Mo(N[R]Ar)_3\}_2]^-$, as well as by Hg to regenerate Na/Hg amalgam. Hence, Na/Hg amalgam sets up a redox catalyzed conversion of $(\mu\text{-}CN)\{Mo(N[R]Ar)_3\}_2$ to $(Ar[R]N)_2(ArN)Mo(\mu\text{-}NC)Mo(N[R]Ar)_3$ in good yield. Fig 8 briefly summarizes the cyanide chemistry of $Mo(N[R]Ar)_3$.

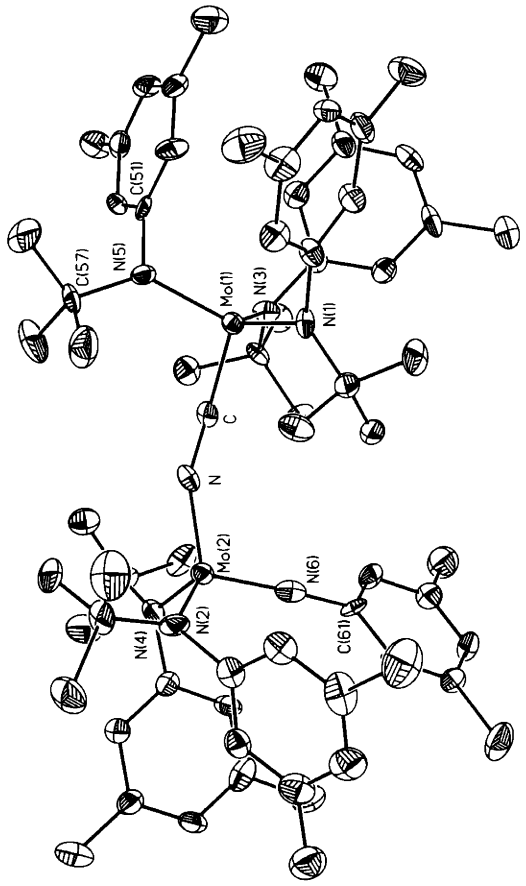

Figure 4: Thermal ellipsoid representation of $(Ar[R]N)_2(ArN)Mo(\mu\text{-}NC)Mo(N[R]Ar)_3$, **7**, from an X-ray study. Ellipsoids are at the 35% probability level. A molecule of OEt_2 crystallized in the asymmetric unit and has been omitted in the above figure. Selected bond distances (Å) and angles (°): Mo(1)-C, 1.812(13); Mo(2)-N, 1.846(11); C-N, 1.291(14); Mo(1)-N(1), 1.964(9); Mo(1)-N(3), 1.981(9); Mo(1)-N(5), 1.962(9); Mo(2)-N(2), 1.988(9); Mo(2)-N(4), 1.986(10); Mo(2)-N(6), 1.736(11); C-N-Mo(2), 156.1(8); N-C-Mo(1), 178.8(9); C-Mo(1)-N(1),N(2),N(3), avg. = 101.8(4); N-Mo(2)-N(2), 114.6(4), N-Mo(2)-N(4), 109.3(4); N-Mo(2)-N(6), 109.4(4); C(61)-N(6)-Mo(2), 164.8.

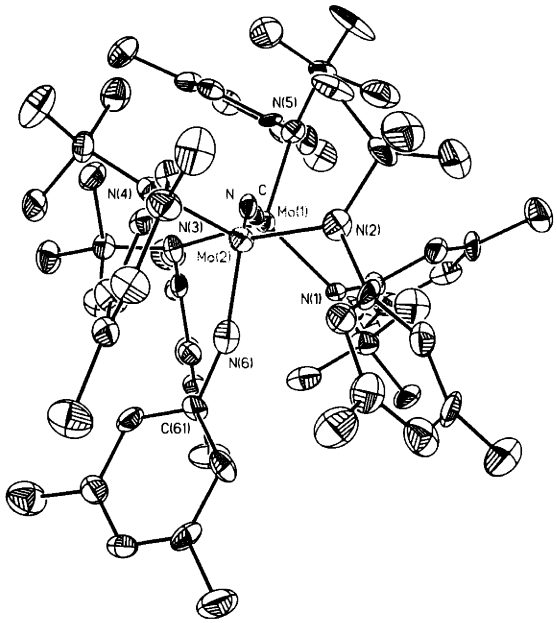

Figure 5: Thermal ellipsoid representation of $(Ar[R]N)_2(ArN)Mo(\mu\text{-}NC)Mo(N[R]Ar)_3$, **7**, from an X-ray study, with a view down the Mo(2)-N-C-Mo(1) axis. Ellipsoids are at the 35% probability level.

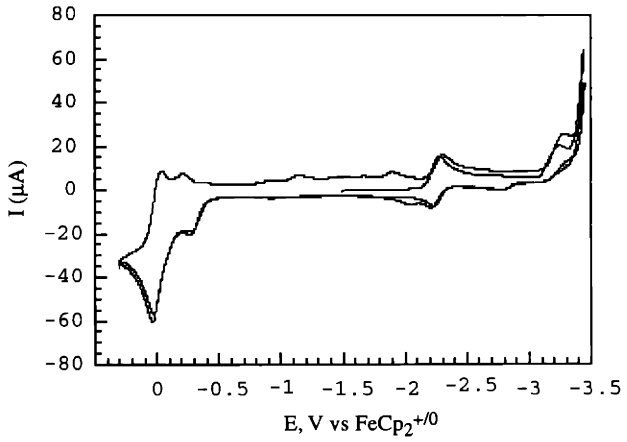

Figure 6: Cyclic Voltammogram of $(Ar[R]N)_2(ArN)Mo(\mu\text{-}NC)Mo(N[R]Ar)_3$, **6**, in 0.5 M THF solution of $[N(n\text{-}Bu)_4][PF_6]$. The CV is referenced internally to $FeCp_2^{+/0}$. Scan rate = 0.1V/s.

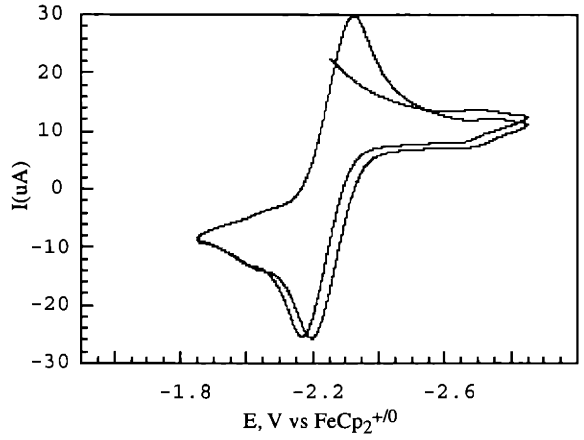

Figure 7: Cyclic Voltammogram of $(Ar[R]N)_2(ArN)Mo(\mu\text{-}NC)Mo(N[R]Ar)_3$, **6**, in 0.5 M THF solution of $[N(n\text{-}Bu)_4][PF_6]$, showing reversible oxidation. The CV is referenced to $FeCp_2^{+/0}$. Scan rate = 0.1V/s.

2.6 Synthesis of [Li][(NC)Mo(N[Ad]Ar)$_3$].

A Li^+ for $[N(n\text{-}Bu)_4]^+$ replacement was effected by addition of excess LiCl to a blue THF solution of $[N(n\text{-}Bu)_4][(NC)Mo(N[Ad]Ar)_3]$, $[N(n\text{-}Bu)_4][\mathbf{2}]$, as shown in eqn 6. A color change from blue to intense violet occurred gradually, concomitant with a change in the IR absorbance of the solution. Over a period of hours the stretch at 1929 cm^{-1} corresponding to $[N(n\text{-}Bu)_4][\mathbf{2}]$ decayed and was replaced by two distinct stretches at 1934 and 1915 cm^{-1}. An IR spectrum of the product is shown in Fig 9. The empirical observation of two ν_{CN} stretches is difficult to explain but is consistent with the solution IR spectra of two other complexes bearing the –N[Ad]Ar ligand set, namely the ion-pair complex $[Na][(N_2)Mo(N[Ad]Ar)_3]$ discussed in chapter 1 and the neutral carbonyl complex $(OC)Mo(N[Ad]Ar)_3$. These complexes also exhibit two distinct stretches in their IR spectra, assignable as ν_{NN} and ν_{CO} vibrations, respectively. The increased hydrocarbon solubility of $[Li(THF)_x][\mathbf{2}]$ compared with $[N(n\text{-}Bu)_4][\mathbf{2}]$ likely reflects tight ion-pairing in solution. An X-ray structural investigation of a crystal of the $[Li][(NC)Mo(N[Ad]Ar)_3]$ species grown from a pentane–THF solution showed a tetrahedral Li^+ cation bound to the β-N atom of the cyanide ligand and solvated by three molecules of THF. Although one of the THF molecules solvating the Li^+ cation was highly disordered, the structure adequately established the compound's gross connectivity as $(THF)_3Li\text{-}N{=}C{=}Mo(N[Ad]Ar)_3$. This species is structurally analogous to the $(THF)_3Na\text{-}N{=}N{=}Mo(N[Ad]Ar)_3$, which was discussed in Chapter 1.

$$[N(n\text{-}Bu)_4][\mathbf{2}] \xrightarrow{\text{THF, xs LiCl}} \underset{[Li][\mathbf{2}]}{(THF)_3Li\text{-}N{=}C{=}Mo(N[Ad]Ar)_3} \qquad (6)$$

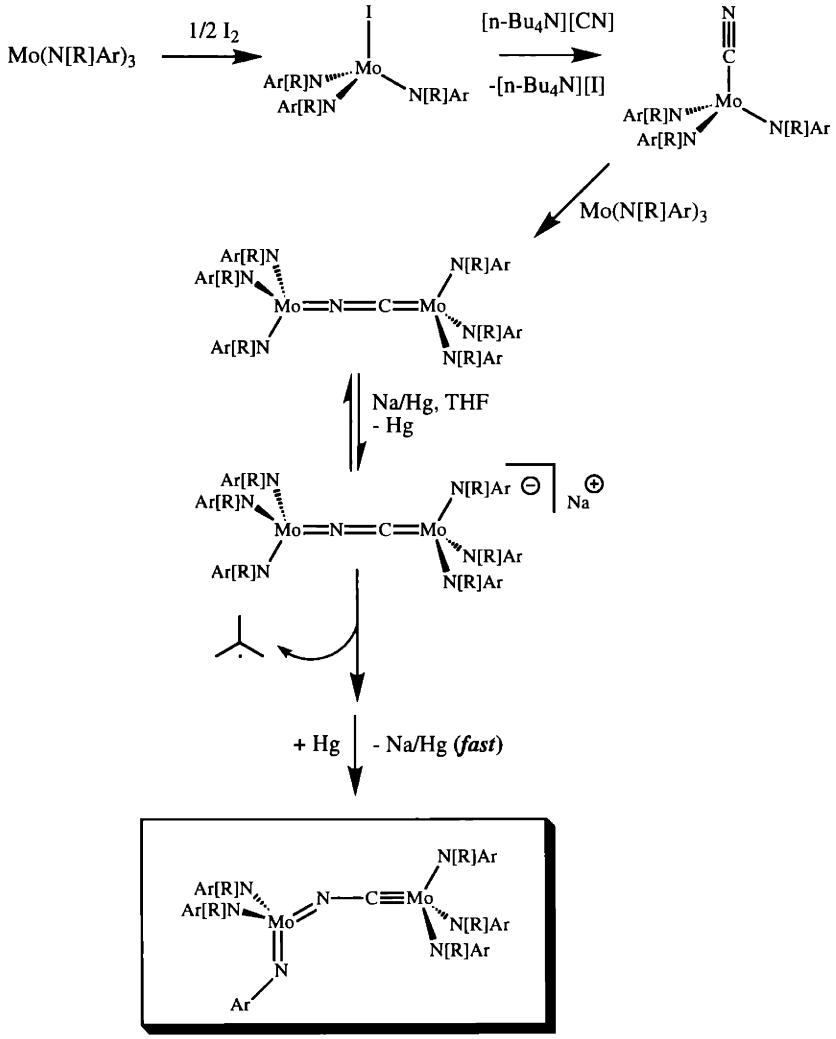

Figure 8: Reaction scheme showing the syntheses of (NC)Mo(N[R]Ar)$_3$, **4**, (μ-CN){Mo(N[R]Ar)$_3$}$_2$, **6**, and (Ar[R]N)$_2$(ArN)Mo(μ-NC)Mo(N[R]Ar)$_3$, **7**.

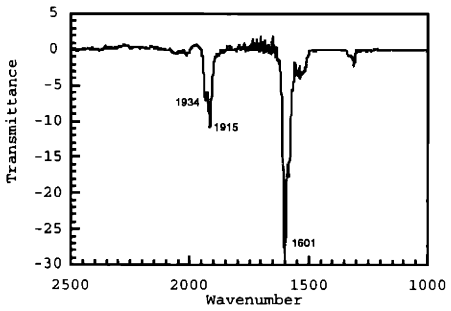

Figure 9: IR spectrum showing ν_{CN} bands of [Li][(NC)Mo(N[Ad]Ar)$_3$], [Li][**2**], at 1934 and 1915 cm^{-1} in THF solution. The intense band at 1601 cm^{-1} corresponds to an anilido aryl ν_{CC} vibration.

2.7 Oxidation of [(NC)Mo(N[Ad]Ar)$_3$]$^-$ by Cp$_2$FeOTf and AgOTf.

The oxidation of [N(*n*-Bu)$_4$][(NC)Mo(N[Ad]Ar)$_3$] by ferrocenium triflate resulted in the generation of ferrocene and the neutral cyanide complex (NC)Mo(N[Ad]Ar)$_3$, **8**, as shown in eqn 7. Like (NC)Mo(N[R]Ar)$_3$, **8** was reddish in color and was rather insoluble in pentane, making removal of ferrocene from the reaction mixture straightforward by pentane extraction. As was the case for neutral (NC)Mo(N[R]Ar)$_3$, an IR spectrum of neutral **8** did not show a ν_{CN} stretch.

2.8 (NC)Mo(N[Ad]Ar)$_3$ + Mo(N[R]Ar)$_3$. Synthesis of (Ar[Ad]N)$_3$Mo(μ-CN)-Mo(N[R]Ar)$_3$.

The ready synthesis of (μ-CN){Mo(N[R]Ar)$_3$}$_2$ and the ready synthesis of [N(*n*-Bu)$_4$][(NC)Mo-(N[Ad]Ar)$_3$] bring to light a delicate balance of steric control. (μ-CN){Mo(N[R]Ar)$_3$}$_2$ is sterically accessible and stable for R = *tert*-butyl. Conversely, the analogous species is sterically inaccessible when R = 1-Ad. This steric control allows direct deposition of the cyanide anion onto Mo(N[Ad]-Ar)$_3$ by preventing problematic bimolecular reaction pathways. Hence, while the direct isolation of [(NC)Mo(N[R]Ar)$_3$]$^-$ was problematic, [(NC)Mo(N[Ad]Ar)$_3$]$^-$ was readily obtained. These observations are reminiscent of those discussed in Chapter 1 involving related dinitrogen chemistry. We wondered whether the mixed ligand species (Ar[Ad]N)$_3$Mo(μ-CN)Mo(N[R]Ar)$_3$ would prove sterically accessible. When neutral (NC)Mo(N[Ad]Ar)$_3$ was mixed with a stoichiometric amount of **1** in THF an intensely violet solution resulted, analogous in color to (μ-CN){Mo(N[R]Ar)$_3$}$_2$. A ^{2}H NMR spectrum of this solution showed a single broad resonance at 6.8 ppm ($\Delta\nu_{1/2}$ = 60 Hz) reflecting that the deuterated Mo(N[R]Ar)$_3$ complex had condensed with the non-deuterated species (NC)Mo(N[Ad]Ar)$_3$ to form (Ar[Ad]N)$_3$Mo(μ-CN)Mo(N[R]Ar)$_3$, **9**. Complex **9** was sparingly soluble in hydrocarbon solvents.

$$\underset{[\mathrm{N}(n\text{-Bu})_4][\mathbf{2}]}{[\mathrm{N}(n\text{-Bu})_4][(\mathrm{NC})\mathrm{Mo}(\mathrm{N[Ad]Ar})_3]} + \mathrm{Cp_2FeOTf} \xrightarrow{-\ \mathrm{Cp_2Fe},\ -[\mathrm{N}(n\text{-Bu})_4][\mathrm{OTf}]} \underset{\mathbf{8}}{(\mathrm{NC})\mathrm{Mo}(\mathrm{N[Ad]Ar})_3} \quad (7)$$

$$\underset{\mathbf{8}}{(\mathrm{NC})\mathrm{Mo}(\mathrm{N[Ad]Ar})_3} + \underset{\mathbf{1}}{\mathrm{Mo}(\mathrm{N[R]Ar})_3} \xrightarrow{\mathrm{OEt_2}} \underset{\mathbf{9}}{(\mathrm{Ar[Ad]N})_3\mathrm{Mo}(\mu\text{-CN})\mathrm{Mo}(\mathrm{N[R]Ar})_3} \quad (8)$$

2.9 Reaction of $[\mathrm{N}(n\text{-Bu})_4][(\mathrm{NC})\mathrm{Mo}(\mathrm{N[Ad]Ar})_3]$ with $\mathrm{IV}(\mathrm{N[R]Ar}_F)_2$. Synthesis of $(\mathrm{Ar}_F\mathrm{[R]N})_2\mathrm{V}(\mu\text{-NC})\mathrm{Mo}(\mathrm{N[Ad]Ar})_3$.

The reaction chemistry of $[(\mathrm{NC})\mathrm{Mo}(\mathrm{N[Ad]Ar})_3]^-$ remains largely unexplored. The steric bulk of the anilido ligands should direct electrophiles to the anionic cyanide nitrogen. However, as in the case of $[\mathrm{Mo}(\mathrm{N_2})(\mathrm{N[R]Ar})_3]^-$, redox chemistry may prove problematic. Functionalization of the $[(\mathrm{NC})\mathrm{Mo}(\mathrm{N[Ad]Ar})_3]^-$ core by salt elimination was shown to be effective in the direct reaction of $[\mathrm{N}(n\text{-Bu})_4][(\mathrm{NC})\mathrm{Mo}(\mathrm{N[Ad]Ar})_3]$ with Fickes' vanadium complex $\mathrm{IVN[R]Ar_F}$ (Ar_F = 2-fluoro-5-methylphenyl),[25] generating the bridged-cyanide complex $(\mathrm{Ar}_F\mathrm{[R]N})_2\mathrm{V}(\mu\text{-NC})\mathrm{Mo}(\mathrm{N[Ad]Ar})_3$, **10**. The two complexes reacted rapidly at low temperature to generate **10** in ca. 60% yield, as estimated by a ^{2}H NMR spectrum of the crude reaction mixture. Complex **10** was isolated in 30 % yield by crystallization from $\mathrm{OEt_2}$. A magnetic susceptibility measurement by the method of Evans gave a μ_{eff} value of $1.70\mu_{\mathrm{B}}$, consistent with one unpaired electron for the dinuclear complex **10**. An X-ray structural investigation (Fig 10) of **10** showed a Mo-C-N-V linkage slightly bent at the N-atom. The structure was not of very high quality due to the disordered molecule of $\mathrm{OEt_2}$ present in the asymmetric unit and a disordered *tert*-butyl group at the vanadium center. One salient feature of the solid state structure of **10** is the unusually strong V-F(2) interaction at 2.147Å where F(2) is an *ortho*-fluorine of the –N[R]Ar$_{\mathrm{F}}$ ligand. Hence, the vanadium center should be regarded as rigorously 4-coordinate with a bond to F(2). Notably, a low temperature EPR spectrum of Fickes' related Ar'N=V(N[R]Ar$_{\mathrm{F}}$)$_2$ (Ar' = mesityl) showed splitting of the peaks of the eight-line spectrum, due to hyperfine coupling of ^{51}V (I=7/2, 99 %) into apparent doublets, presumed to result from a ^{19}F interaction in solution.[26] Sheree Stokes has observed varying degrees of Fe-F interactions in her widespread use of the N[R]Ar$_{\mathrm{F}}$ ligand (ranging from 2.258(5)–2.447(2)Å in the solid state).[27]

3 Conclusions

This chapter has presented a series of cyanide complexes based upon a *tris*-anilido molybdenum core. It has been shown that both neutral and anionic cyanide derivatives are accessible and that the neutral species provide access to key bimetallic bridged-cyanide species. Both the mononuclear and dinuclear cyanide complexes are redox active. The reduction potential of $(\mathrm{NC})\mathrm{Mo}(\mathrm{N[R]Ar})_3$

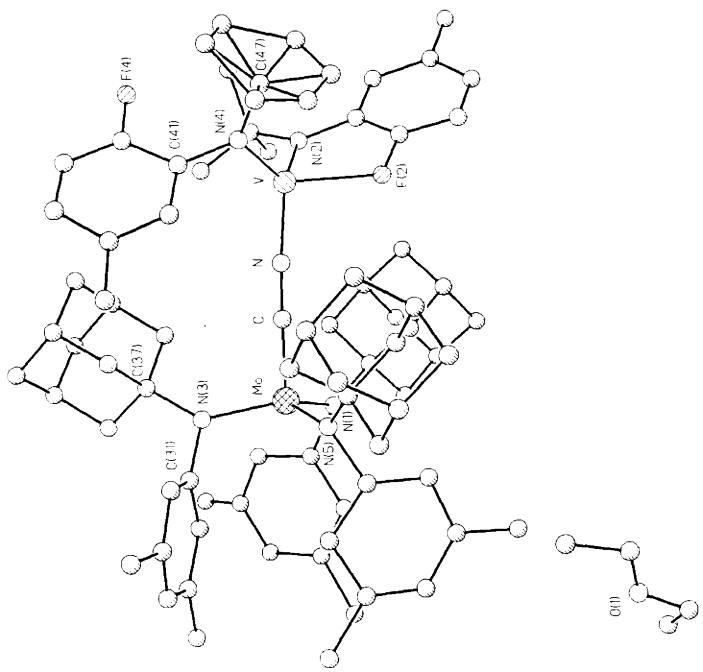

Figure 10: PLUTO structural drawing of $(Ar_F[R]N)_2V(\mu\text{-NC})Mo(N[Ad]Ar)_3$, **10**, from an X-ray study. One molecule of OEt_2 was present in the asymmetric unit and is included in the diagram. Selected bond distances (Å) and angles (°): Mo-C, 1.847(13); V-N, 1.799(11); C-N, 1.260(14); V-F(2), 2.148(7); Mo-N(1), 1.950(11); Mo-N(3), 1.933(12); Mo-N(5), 1.971(12); V-N(2), 1.962(10); V-N(4), 1.905(9); N-C-Mo, 176.1(9); C-N-V, 169.6(9); C-Mo-N(1),N(3),N(5), avg. = 100.8(4); N(2)-V-F(2), 78.9(4); N-V-N(2), 121.9(4); N-V-N(4), 115.0(5).

was measured to be -1.9 V in THF, a potential lower than its dinitrogen counterpart $(N_2)Mo(N[R]Ar)_3$ (-1.7 V). The reduction potential of the bridged complex $(\mu\text{-CN})\{Mo(N[R]Ar)_3\}_2$ was measured to be -2.2 V, a potential higher than its dinitrogen analogue $(\mu\text{-}N_2)[Mo(N[R]Ar)_3]_2$ (-2.4 V). The reduction potential of a 0.4 % Na/Hg amalgam in THF is reducing enough to reduce $(\mu\text{-CN})\{Mo(N[R]Ar)_3\}_2$.

The redox catalyzed formation of $(Ar[R]N)_2(ArN)Mo(\mu\text{-NC})Mo(N[R]Ar)_3$ by the reduction of $(\mu\text{-CN})\{Mo(N[R]Ar)_3\}_2$ with Na/Hg amalgam established a high degree of cyanide activation/reduction and a bonafied C-N cleavage reaction. However, the C-N bond cleaved was that of an anilido ligand rather than the bridged cyanide ligand itself. Hence, the cooperative direct cleavage of $^-C{\equiv}N$ by two $Mo(N[R]Ar)_3$ complexes was not a viable strategy for delivery of the C-atom from cyanide to generate a terminal carbido species $^-C{\equiv}Mo(N[R]Ar)_3$. Apparently, the reduction product $[Na][(\mu\text{-CN})\{Mo(N[R]Ar)_3\}_2]$, isoelectronic to its neutral and unstable N_2-analogue $(\mu\text{-}N_2)[Mo(N[R]Ar)_3]_2$, finds a viable reaction pathway to form the stable complex $(Ar[R]N)_2(ArN)Mo(\mu\text{-NC})Mo(N[R]Ar)_3$ via C-N cleavage at a peripheral anilido ligand and loss of Na/Hg amalgam. A dichotomy appears to exist between breaking the C-N sigma bond in cyanide versus the N-N sigma bond in dinitrogen. Along the reaction coordinate the isoelectronic and sterically similar species $(\mu\text{-}N_2)[Mo(N[R]Ar)_3]_2$ and $[(\mu\text{-CN})\{Mo(N[R]Ar)_3\}_2]^-$ choose different decomposition pathways, the former cleaving at the N-N bond of the bridging diatomic ligand. In the case where cyanide is the bridging ligand, the *tert*-butyl substituted anilido ligands provide a convenient radical leaving group, and cleavage at the diatomic ligand is bypassed in favor of a transformation at the anilido position. It remains to be seen whether shutting down this decomposition pathway may be accomplished with anilido ligands substituted by *poorer* radical leaving groups, as in –N[*i*-Pr]Ar. Direct cyanide cleavage may still be possible with a *tris*-amido molybdenum core pending a judicious choice of the amido substituents. To my knowledge, no simple examples of a metal-mediated cyanide cleavage reaction have been reported. However, the nitrile, CO and isocyanide splitting reactions shown in Fig 1 intimate the chemical viablility of such a reaction.

4 Experimental Section

4.1 General Considerations

Unless stated otherwise, all operations were performed in a Vacuum Atmospheres dry box under an atmosphere of purified nitrogen, or using standard Schlenk techniques under an argon or dinitrogen atmosphere. Anhydrous ether and toluene were purchased from Mallinckrodt; n-pentane and n-hexane were purchased from EM Science. Ether was purified according to the procedure of Grubbs.[28] Aliphatic hydrocarbon solvents were distilled under a nitrogen atmosphere from very dark blue to purple sodium benzophenone ketyl solubilized with a small quantity of tetraglyme. Distilled solvents were transferred under vacuum into teflon-stopcocked glass vessels and stored, prior to use, in a Vacuum Atmospheres dry box. C_6D_6 was degassed and dried over activated 4 Å molecular sieves and transferred under vacuum into a storage vessel. 4 Å sieves, Celite and alumina were activated *in vacuo* overnight at a temperature above 180 °C. Mo(N[R]Ar)$_3$,[19] ferrocenium triflate,[29] LiN[Ad]Ar,[30,31] and (I)Mo(N[R]Ar)$_3$,[32] were prepared according to published procedures. ^{13}C-labeled carbon monoxide gas was purchased form Cambride Isotope Laboratory (CIL). $ClSiMe_3$ and was degassed and dried over 4Å molecular sieves prior to use. Other chemicals were purified and dried by standard procedures or were used as received. Infrared spectra were recorded on a Bio-Rad 135 Series FTIR spectrometer. UV-visible spectra were recorded on a Hewlett-Packard 8453 diode-array spectrophotometer. ^{1}H and ^{13}C NMR spectra were recorded on Varian VXR-500, Varian XL-300, or Varian Unity-300 spectrometers. ^{1}H and ^{13}C NMR chemical shifts are reported with reference to solvent resonances (residual C_6D_5H in C_6D_6, 7.15 ppm; C_6D_6, 128.0 ppm; $CHCl_3$ in $CDCl_3$, 7.24 ppm; $CDCl_3$, 77.0 ppm). ^{2}H NMR chemical shifts are reported with respect to external C_6D_6 (7.15 ppm). Solution magnetic susceptibilities were determined by ^{1}H NMR at 300 MHz using the method of Evans.[33,34] Routine coupling constants are not reported. Combustion analyses (C, H, and N) were performed by Microlytics, Southdeerfield MA. X-ray diffraction data were collected on a Siemens Platform goniometer with a Charge Coupled Device (CCD) detector. Structures were typically solved by direct methods (SHELXTL V5.0, G.M Sheldrick and Siemens Industrial Automation, Inc., 1995) unless otherwise noted. Peaks in the ^{1}H and ^{13}C NMR spectra are denoted according to Fig 11.

4.2 Electrochemical Measurements.

The electrochemical measurements[17] were performed in THF solution containing the desired compounds and 0.5 M tetra-*n*-butylammonium hexafluorophosphate, [N(*n*-Bu)$_4$][PF$_6$]. In a typical procedure 5 mg of the complex was dissolved in 0.75 mL of clean THF. To this solution was added 0.75 mL of 1.0 M THF solution of tetra-*n*-butylammonium hexafluorophosphate. A platinum disk (1.6 mm diameter, Bioanalytical systems), a platinum wire, and a silver wire were employed as the working electrode, the auxiliary, and the reference, respectively. The electrochemical response was collected with the assistance of an Eco-Chemie Autolab potentiostat (pgstat20) and the GPES 4.3 software. An IR correction drop was always employed due to the high resistance of the solutions. A typical resistance value measured with the positive feedback technique for these solutions was 975 ohms. All of the potentials are reported against the ferrocenium/ferrocene couple measured in

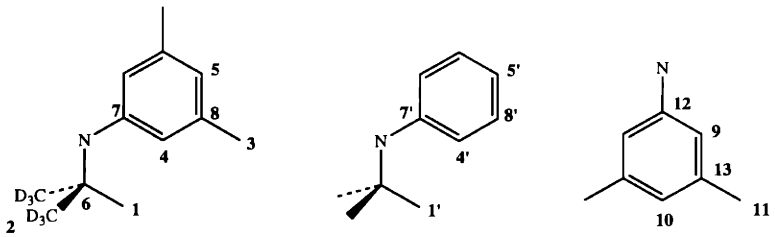

Figure 11: Labeling scheme for ^{1}H and ^{13}C NMR spectra. The positions on the adamantyl substituents have been designated generally as **Ad**.

the same solution.

4.3 Synthesis of (NC)Mo(N[R]Ar)$_3$.

A solution of 494 mg [N(n-Bu)$_4$][CN] (1.841 mmol) in 3 mL of THF was chilled to -35 °C and added via pipette to a chilled, brilliant green solution containing 1.181 g (I)Mo(N[R]Ar)$_3$ (1.534 mmol) in 20 mL of THF. The reaction mixture was allowed to warm to ambient temperature and was stirred for 2 h. At this time, 30 mL of pentane was added to precipitate the salts, and the slurry was then filtered through a sintered glass frit. The red filtrate was dried to a solid, and addition of 25 mL of OEt_2 partially dissolved the solid. The undissolved solid was collected by filtration as a first pure crop (502 mg), and storage of the ethereal filtrate afforded a second crop (284.6 mg) for an overall 77 % yield of pure (NC)Mo(N[R]Ar)$_3$. ^{2}H NMR (76 MHz, THF, 25 °C): δ = 31.0 ppm [s, $\Delta\nu_{1/2}$ = 13 Hz, C(CD$_3$)$_2$CH$_3$]. SQUID (5–300K): $\mu_{\text{eff}} = 2.81\mu_B$. μ_{eff} (300 MHz, 25 °C, C_6D_6) = $2.46\mu_B$. An FTIR spectrum did *not* show a ν_{CN} stretch. Anal. Calcd for $C_{37}H_{36}D_{18}N_4Mo$: C, 66.44; H, 8.14; N, 8.37. Found: C, 66.19; H, 8.20; N, 7.99.

4.4 Synthesis of (μ-CN){Mo(N[R]Ar)$_3$}$_2$.

Solid orange Mo(N[R]Ar)$_3$ (378 mg, 0.588 mmol) was added to a stirring red solution of (NC)Mo-(N[R]Ar)$_3$ (393.1 mg, 0.588 mmol) in 10 mL of a 4:1 OEt_2–benzene mixture at 25 °C. The solution, whose color turned to brilliant violet quickly upon mixing, was stirred for one hour, after which time the reaction volatiles were removed *in vacuo*. The resulting solid was collected on a sintered glass frit and washed thoroughly with pentane to remove a dark brown, pentane soluble impurity. The violet solid which remained was sparingly soluble in both pentane and in OEt_2. It was dried to a mass of 618 mg (80 %) and was found to be spectroscopically and analytically pure. ^{2}H NMR (46 MHz, THF, 25 °C): δ = 6.6 ppm [s, $\Delta\nu_{1/2}$ = 36 Hz, C(CD$_3$)$_2$CH$_3$], 3.3 ppm [s, $\Delta\nu_{1/2}$ = 21 Hz, C(CD$_3$)$_2$CH$_3$]. SQUID (5–300K): $\mu_{\text{eff}} = 1.61\mu_B$. UV/vis (THF): λ = 350 nm, λ = 425 nm, λ = 530 nm. FTIR (THF, KBr): 1575 cm^{-1} (overlapping with stretch for anilido ligand). Anal. Calcd for $C_{73}H_{72}D_{36}N_7Mo_2$: C, 66.84; H, 8.30; N, 7.47. Found: C, 66.53; H, 8.32; N, 7.30.

4.5 Synthesis of $(Ar[R]N)_2(ArN)Mo(\mu\text{-}NC)Mo(N[R]Ar)_3$.

Solid $(\mu\text{-}CN)\{Mo(N[R]Ar)_3\}_2$ (377 mg, 0.287 mmol) was added to a 0.40 % w/w stirring Na/Hg amalgam (9.5 mg Na in 2.38 g Hg, 0.413 mmol Na) in 5 mL of THF under N_2. Within 30 minutes the solution had turned from the intense red-purple of $(\mu\text{-}CN)\{Mo(N[R]Ar)_3\}_2$ to a deep orange. An FTIR spectrum after 45 minutes showed an intense stretch at 1584 cm^{-1} likely resulting from overlapping ν_{CC} and ν_{CC} vibrations. An aliquot of the reaction mixture was removed after 1 h and dried *in vacuo*, triturated with hexane, and extracted into C_6D_6 containing hexamethyldisiloxane as an internal standard. A ^1H NMR spectrum of this aliquot showed that $(Ar[R]N)_2(ArN)Mo(\mu\text{-}NC)Mo(N[R]Ar)_3$ had been generated in approximately 90 % yield (based on the starting material $(\mu\text{-}CN)\{Mo(N[R]Ar)_3\}_2$) by this time. Stirring was continued for an additional 2 h at 25 °C, after which time the volatiles were removed *in vacuo* and the entire reaction mixture was triturated thoroughly with hexane. The resulting residue was extracted into pentane, filtered through Celite, and dried *in vacuo*. The crude product was difficult to recrystallize from hydrocarbon solvents due to its high lypophilicity, but was obtained in > 50 % yield (215 mg) as a spectroscopically pure substance by precipitation from hexamethyldisiloxane. The orange powder obtained was then recrystallized, albeit in low yield, to afford singular orange crystals appropriate for an X-ray diffraction study. ^1H NMR (300 MHz, C_6D_6, 25 °C): Assignments for respective ligands are listed separately for each metal center: $(Ar[R]N)_2(ArN)Mo_a$: 6.93 (s, 4), 6.74 (s, 5), 6.45 (s, 10), 6.41 (s, 9), 2.23 (s, 3), 2.16 (s, 11), 1.60 (s,1). $(Ar[R]N)_3Mo_b$: 6.70 (s, 5), 6.08 (s, 4), 2.13 (s, 3), 1.62 (s, 1). ^{13}C NMR (125.66 MHz, C_6D_6, 25 °C): 153.4 (aryl), 151.20 (aryl),137.8 (aryl), 137.4 (aryl), 131.3 (aryl), 129.1 (aryl), 127.8 (aryl), 127.4 (aryl), 159.8 (aryl), 122.2 (aryl), 116.3 (aryl), 62.7 (6, Mo_b), 61.5 (6, Mo_a), 34.6 (1, Mo_b), 32.7 (1, Mo_a), 22.0 (3, Mo_b), 21.9 (3, Mo_b), 21.8 (11, Mo_b). Anal. Calcd for $C_{70}H_{69}D_{30}N_7Mo_2$: C, 66.69; H, 7.95; N, 7.78. Found: C, 65.99; H, 8.09; N, 7.48.

4.6 X-ray structure of $(Ar[R]N)_2(ArN)Mo(\mu\text{-}NC)Mo(N[R]Ar)_3$.

Deep orange crystals were grown slowly from a pentane solution at -35 °C. The crystals were quickly moved from a scintillation vial to a microscope slide containing Paratone N (an Exxon product). Under the microscope a deep orange plate was selected and mounted on a glass fiber using wax. A total of 26766 reflections were collected ($-11 \leq h \leq 10$, $-35 \leq k \leq 35$, $-22 \leq l \leq 20$) in the θ range of 1.20 to 23.26° of which 9625 were unique ($R_{int} = 0.1350$). The structure was solved by direct methods in conjunction with standard difference Fourier techniques. All non-hydrogen atoms were placed in calculated ($d_{C\text{-}H} = 0.96$ Å) positions. The largest peak and hole in the difference map were 0.912 and -1.016 e·Å^{-3}, respectively. No absorption correction was applied. The least squares refinement converged normally with residuals of R (based on F) = 0.1203, wR (based on F^2) = 0.2644, and GOF = 1.346 based upon $I > 2\sigma(I)$. Crystal data for $C_{69}H_{99}Mo_2N_7$: monoclinic, space group = $P2_1/n$, $z = 4$, $a = 10.4312(3)$ Å, $b = 32.0672(10)$ Å, $c = 20.4383(6)$ Å, $\alpha = 90°$, $\beta = 100.7510°$, $\gamma = 90°$, $V = 6716.6(3)$ Å^3, $\rho_{calc} = 1.205$ g·cm^{-3}, $F(000) = 2584$.

4.7 Synthesis of $[N(n\text{-}Bu)_4][(NC)Mo(N[Ad]Ar)_3]$.

A solution of 419 mg $[N(n\text{-}Bu)_4][CN]$ (1.560 mmol) in 15 mL of THF was added quickly to a stirring solution of 1.340 g $Mo(N[Ad]Ar)_3$ (1.560 mmol) in 20 mL of THF. The reaction mixture turned from the orange color of $Mo(N[Ad]Ar)_3$ to an intense blue instantly on mixing. Stirring was continued for 10 minutes after which time the volatiles were removed *in vacuo*, leaving a blue residue. Ten mL of pentane were added to this residue to form a slurry, and filtration left a blue, insoluble solid on a sintered glass frit. This solid was washed 2x with 5 mL of a 1:1 pentane–benzene mixture followed by thorough washing with excess pentane until washings were colorless. The blue powder was dried to a weight of 1.605 g (91 %) of $[N(n\text{-}Bu)_4][(NC)Mo(N[Ad]Ar)_3]$. FTIR: ν_{CN} = 1929 cm^{-1} (THF, CaF_2). Anal. Calcd for $C_{71}H_{108}N_5Mo$: C, 75.63; H, 9.65; N, 6.21. Found: C, 75.46; H, 9.69; N, 6.15.

4.8 $[N(n\text{-}Bu)_4][CN]$ + $Mo(N[R]Ar)_3$.

Solid white $[N(n\text{-}Bu)_4][CN]$ (181.5 mg, 0.679 mmol) was dissolved in 10 mL of THF in a scintillation vial. Crystalline $Mo(N[R]Ar)_3$ (436.7 mg, 0.679 mmol) was added slowly to the solution in small portions. The color turned to an inky blackish–blue quickly, and an intense purple color was *never* observed. *Note: A similar experiment was performed, but with a fast addition of Mo(N[R]Ar)$_3$ in one portion, and resulted instantly in a purple reaction mixture.* A crude ^2H NMR spectrum showed a signal at 6.1 ppm and several peaks between 0–2ppm. A repetitive pentane extraction process left behind 100 mg of an insoluble blue solid which was spectroscopically clean $[N(n\text{-}Bu)_4][(NC)Mo(N[R]Ar)_3]$. ^2H NMR (76 MHz, THF, 25 °C): δ = 6.1 ppm [s, $\Delta\nu_{1/2}$ = 8 Hz, $C(CD_3)_2CH_3$]. FTIR: ν_{CN} = 1941 cm^{-1} (THF, CaF_2). Elemental analysis was not obtained.

4.9 LiCl + $[N(n\text{-}Bu)_4][(NC)Mo(N[Ad]Ar)_3]$.

A slurry of 1.037 g of $Mo(N[Ad]Ar)_3$ (1.2071 mmol) was prepared in 15 mL of THF and cooled to -35 °C. While stirring this mixture, 324.1 mg $[N(n\text{-}Bu)_4][CN]$ (1.207 mmol) was added to it, as a solid, in one portion. After stirring for 45 minutes, 51.2 mg of LiCl was added to the now blue solution, effecting a color change to blue–purple. After 16 h of stirring this mixture an FTIR spectrum showing only partial Li^+ for $[N(n\text{-}Bu)_4]^+$ exchange. An additional 375 mg LiCl was added to the reaction mixture and stirring was continued for an additional 24 h. The volatiles were then removed *in vacuo*, the remaining residue was triturated thoroughly with pentane, and the solid powder which resulted was extracted with 25 mL pentane and filtered through Celite. Storage of the pentane filtrate at -35 °C afforded 618.1 mg of red-violet crystals. A ^1H NMR spectrum showed broad signals at δ = 4.45, 3.75, 1.74, 1.50, 1.40 ppm. An X-ray crystallographic study of one such crystal confirmed a solid state connectivity of $(THF)_3Li\text{-}N{=}C{=}Mo(N[Ad]Ar)_3$. A successful microanalysis rigorously consistent with this formulation was not obtained, presumably due to varying amounts of solvated THF. Anal. Calcd for $C_{67}H_{96}N_4LiMoO_3$: C, 72.60; H, 8.73; N, 5.06. Found: C, 70.56; H, 7.61; N, 5.44. The isolated species was effectively oxidized to the neutral $(NC)Mo(N[Ad]Ar)_3$ complex by AgOTf, supporting its assignment as a $[Li][(NC)Mo(N[Ad]Ar)_3]$

with a degree of THF incorporation.

4.10 Oxidation of [Li][(NC)Mo(N[Ad]Ar)$_3$] by AgOTf.

354 mg of the complex [Li][(NC)Mo(N[Ad]Ar)$_3$] (0.319 mmol when formulated as [Li(THF)$_x$][(NC)Mo-(N[Ad]Ar)$_3$]) was dissolved in 14 mL of OEt_2 to make a dark blue solution. 82 mg of solid AgOTf (0.319 mmol) was added in one portion to the solution, which quickly turned red. Silver metal plated out of solution and the volatiles were removed *in vacuo*. 15 mL of pentane were added to the crude residue and the resulting slurry was stirred and then filtered. A red solid left on the sintered glass frit dried to a mass of 210 mg (74 %) of (NC)Mo(N[Ad]Ar)$_3$. The properties of this material were analogous to that of (NC)Mo(N[Ad]Ar)$_3$ prepared below by the oxidation of [N(n-Bu)$_4$][(NC)Mo(N[Ad]Ar)$_3$] with ferrocenium triflate.

4.11 Chemical oxidation of [N(n-Bu)$_4$][(NC)Mo(N[Ad]Ar)$_3$]. Synthesis of (NC)Mo-(N[Ad]Ar)$_3$.

Solid blue [N(n-Bu)$_4$][(NC)Mo(N[Ad]Ar)$_3$] (24.2 mg, 0.0215 mmol) and orange Cp_2FeOTf (7.2 mg, 0.0215 mmol) were weighed into a 20 mL scintillation vial equipped with a magnetic stir bar. Addition of 3.5 mL of OEt_2 with concomittant stirring effected a rapid color change to red. The ν_{CN} stretch for the starting material [N(n-Bu)$_4$][(NC)Mo(N[Ad]Ar)$_3$] decayed away and no new ν_{CN} stretch could be located, as was the case for (NC)Mo(N[R]Ar)$_3$ (*vide supra*). Filtration, followed by removal of the reaction volatiles *in vacuo*, gave a reddish residue whose ^{1}H NMR spectrum (C_6D_6) showed Cp_2Fe (4.00 ppm) and broad signals for (NC)Mo(N[Ad]Ar)$_3$ as follows: δ = 13.5 ppm , 8.1, 4.1, 2.5, 1.3, -4.0, -7.8, -13.6. The solid material was recovered by drying *in vacuo*. Subsequent pentane washing of this solid effected the removal of orange ferrocene and left behind a red powder, that once dried, was analytically pure (NC)Mo(N[Ad]Ar)$_3$. Anal. Calcd for $C_{55}H_{72}N_4Mo$: C, 74.63; H, 8.20; N, 6.32. Found: C, 74.95; H, 8.38; N, 6.21.

4.12 Synthesis of (Ar[Ad]N)$_3$Mo(μ-CN)Mo(N[R]Ar)$_3$.

190.9 mg of red (NC)Mo(N[Ad]Ar)$_3$ (0.2157 mmol) was stirred in 10 mL OEt_2 followed by the addition of 138.6 mg of orange Mo(N[R]Ar)$_3$ (0.2157 mmol) at -35 °C. The reaction mixture turned to an inky violet color rapidly and was stirred for an additional 15 minutes. Some solid particulate precipitated from solution and 2 mL of THF was added to create a homogeneous solution. Filtration and storage of the solution at -35 °C for 12 h produced 175 mg (53 %) of solid burgundy (Ar[Ad]-N)$_3$Mo(μ-CN)Mo(N[R]Ar)$_3$. ^{2}H NMR (76 MHz, THF, 25 °C): δ = 6.8 ppm [s, $\Delta\nu_{1/2}$ = 60 Hz, $C(CD_3)_2CH_3$]. FTIR (THF, CaF_2): ν_{CN} = 1575 cm^{-1} (overlapping with stretch for anilido ligand). Anal. Calcd for $C_{91}H_{108}D_{18}N_7Mo_2$: C, 71.53; H, 8.31; N, 6.42. Found: C, 70.98; H, 8.29; N, 6.40.

4.13 Synthesis of $(Ar_F[R]N)_2V(\mu\text{-}NC)Mo(N[Ad]Ar)_3$.

A pre-chilled greenish brown solution of 146.4 mg of $IV(N[R]Ar_F)_2$ (0.266 mmol) in 3 mL OEt_2 was added dropwise over *approx.* 20 seconds to a pre-chilled slurry of 300 mg of $[N(n\text{-}Bu)_4][(NC)Mo(N[Ad]Ar)_3]$ (0.266 mmol) in 5 mL of a 4:1 THF–OEt_2 at -35 °C. The reaction mixture began to turn orange–brown rapidly and stirring was continued for one hour at 25 °C, after which time 5 mL pentane was added to aid in salt precipitation. Filtration through Celite, drying *in vacuo*, and thorough trituration with pentane solvent yielded a dark orange-brown powder weighing 351 mg and approximately 60 % pure by ^2H NMR spectroscopy. This powder was recrystallized from OEt_2 affording 105 mg (30 %) of a deep orange, crystalline material. ^2H NMR (76 MHz, OEt_2, 25 °C): δ = 17 ppm [s, $\Delta\nu_{1/2}$ = 600 Hz, $C(CD_3)_2CH_3$]. μ_{eff} (300 MHz, 25 °C, C_6D_6) = 1.70μ_B. FTIR: ν_{CN} (tentative) = 1615 cm^{-1} (OEt_2, KBr). Anal. Calcd for $C_{77}H_{90}D_{12}F_2MoN_6V$: C, 70.67; H, 7.86; N, 6.42. Found: C, 71.22; H, 7.53; N, 6.16.

4.14 X-ray structure of $(Ar_F[R]N)_2V(\mu\text{-}NC)Mo(N[Ad]Ar)_3$.

Deep orange crystals were grown slowly from a OEt_2 solution at -35 °C. The crystals were quickly moved from a scintillation vial to a microscope slide containing Paratone N (an Exxon product). Under the microscope a deep orange plate was selected and mounted on a glass fiber using wax. A total of 11301 reflections were collected ($-8 \leq h \leq 15$, $-18 \leq k \leq 17$, $-19 \leq l \leq 19$) in the θ range of 1.18 to 20.00° of which 6993 were unique (R_{int} = 0.0626). The structure was solved by direct methods in conjunction with standard difference Fourier techniques. A troublesome molecule of OEt_2 was present in the asymmetric unit and included during refinement (atom labels C1, C2, C3, C4, O1). This OEt_2 molecule did not refine very well but all atoms in the asymmetric were refined anisotropically. The *tert*-butyl group connected to N(4) was disordered and modeled as two postions at half occupancy. All non-hydrogen atoms were placed in calculated ($d_{C\text{-}H}$ = 0.96 Å) positions. The largest peak and hole in the difference map were 1.043 and -0.453 e·Å^{-3}, respectively. No absorption correction was applied. The least squares refinement converged normally with residuals of R (based on F) = 0.1012, wR (based on F^2) = 0.2323, and GOF = 1.109 based upon $I > 2\sigma(I)$. Crystal data for $C_{81}H_{103}F_2MoN_6V$: triclinic, space group = $P\bar{1}$,z = 2,a = 13.5574(9)Å,b = 16.3838(11)Å,c = 17.5538(12)Å,α = 92.6060(10)°, β = 99.8760(10)°, γ = 98.0680(10)°, V = 3793.7(4) Å^3, ρ_{calc} = 1.192 g·cm^{-3}, $F(000)$ = 1444.

References

[1] Cummins, C. C. *Progress Inorg. Chem.*, **1998**, *47*, 685.

[2] Schrock, R. R. *Account. Chem. Res.*, **1997**, *30*, 9.

[3] Laplaza, C. E.; Davis, W. M.; Cummins, C. C. *Angew. Chem. Int. Ed., Engl.*, **1995**, *34*, 2042.

[4] Zanetti, N. C.; Schrock, R. R.; Davis, W. M. *Angew. Chem. Int. Ed. Engl.*, **1995**, *34*, 2044.

[5] Laplaza, C. E.; Odom, A. L.; Davis, W. M.; Cummins, C. C.; Protasiewicz, J. D. *J. Am. Chem. Soc.*, **1995**, *117*, 4999.

[6] Nugent, W. A.; Mayer, J. M. *Metal-Ligand Multiple Bonds*; John Wiley and Sons: New York, 1988.

[7] Odom, A. L.; Cummins, C. C.; Protasiewicz, J. D. *J. Am. Chem. Soc.*, **1995**, *117*, 6613.

[8] Schrock, R. R.; Listemann, M. L.; Sturgeoff, L. G. *J. Am. Chem. Soc.*, **1982**, *104*, 4291.

[9] LaPointe, R. E.; Wolczanski, P. T.; Mitchell, J. F. *J. Am. Chem. Soc.*, **1986**, *108*, 6382.

[10] Neithamer, D. R.; LaPointe, R. E.; Wheeler, R. A.; Richeson, D. S.; Van Duyne, G. D.; Wolczanski, P. T. *J. Am. Chem. Soc.*, **1989**, *111*, 9056.

[11] Chisholm, M. H.; Hammond, C. E.; Johnston, V. J.; Streib, W. E.; Huffman, J. C. *J. Am. Chem. Soc.*, **1992**, *114*, 7056.

[12] Chisholm, M. H.; Heppert, J. A.; Huffman, J. C.; Streib, W. E. *J. Chem. Soc., Chem Commun.*, **1985**, 1171.

[13] Peters, J. C.; Odom, A. L.; Cummins, C. C. *J. Chem. Soc., Chem. Commun.*, **1997**, 1995.

[14] Fehlhammer, W. P.; Schröder, A.; Fuchs, J.; Würthwein, E.-U. *Angew. Chem. Int. Ed. Engl.*, **1992**, *31*, 590.

[15] Trylus, K.-H.; Schröder, A.; Brüdgam, I.; Thiel, R.; Fehlhammer, W. P. *Inorg. Chim. Acta*, **1998**, *269*, 23.

[16] Odonoghue, M. B.; Schrock, R. R. *Personal Communication*, **1998**.

[17] Baraldo, L. *Personal communication*, **1998**.

[18] Berno, P.; Gambarotta, S. *J. Chem. Soc. Chem. Commun.*, **1994**, 2419.

[19] Laplaza, C. E.; Johnson, M. J. A.; Peters, J. C.; Odom, A. L.; Kim, E.; Cummins, C. C.; George, G. N.; Pickering, I. J. *J. Am. Chem. Soc.*, **1996**, *118*, 8623.

[20] Johnson, A. R.; Davis, W. M.; Cummins, C. C.; Serron, S.; Nolan, S. P.; Musaev, D. G.; Morokuma, K. *J. Am. Chem. Soc.*, **1998**, *120*, 2071.

[21] Johnson, A. R.; Davis, W. M.; Cummins, C. C.; Serron, S.; Nolan, S. P.; Musaev, D. G.; Morokuma, K. *J. Am. Chem. Soc.*, **1998**, *120*, 2071.

[22] Dewan, J. C.; Giandomenico, C. M.; Lippard, S. J. *Inorg. Chem.*, **1981**, *20*, 4069.

[23] March, J. M. *Advanced Organic Chemistry, 4th Ed.*; John Wiley & Sons: New York, 1992, page 21.

[24] Zhang, H. H.; Filipponi, A.; Di Cicco, A.; Scott, M. J.; Holm, R. H.; Hedman, B.; Hodgson, K. O. *J. Am. Chem. Soc.*, **1997**, *119*, 2470.

[25] Fickes, M. G.; Davis, W. M.; Cummins, C. C. *J. Am. Chem. Soc.*, **1995**, *117*, 6384.

[26] Fickes, M. F. *Ph. D. Thesis in preparation*, Massachusetts Institute of Technology, **1998**.

[27] Stokes, S. L. *Ph. D. Thesis in preparation*, Massachusetts Institute of Technology, **1998**.

[28] Pangborn, A. B.; Giardello, M. A.; Grubbs, R. H.; Rosen, R. K.; Timmers, F. J. *Organometallics*, **1996**, *15*, 1518.

[29] Schrock, R. R.; Sturgeoff, L. G.; Sharp, P. R. *Inorg. Chem.*, **1983**, *22*, 2801.

[30] Johnson, A. R.; Cummins, C. C. *Inorg. Synth.*, **1997**, *In Press.*

[31] Ruppa, K. B. P.; Desmangles, N.; Gambarotta, S.; Yap, G.; Rheinghold, A. L. *Inorg. Chem.*, **1997**, *36*, 1194.

[32] Johnson, A. J. *Ph. D. Thesis. Low-Valent and Low-Coordinate Titanium and Molybdenum Complexes Supported With Bulky Amido Ligands*, Massachusetts Institute of Technology, **1998**.

[33] Evans, D. F. *J. Chem. Soc.*, **1959**, 2003.

[34] Sur, S. K. *J. Magnetic Resonance*, **1989**, *82*, 169.

Chapter 3. CO Chemistry: The Synthesis and Study of a Molecular Molybdenum Carbide Complex Featuring One Coordinate Carbon.

by Jonas C. Peters

MIT Department of Chemistry room 6-332
Massachusetts Institute of Technology

May 18, 1998

Contents

List of Figures

1 Introduction

While unravelling the reduction chemistry of cyanide as a means to install a carbido ligand on the $Mo(N[R]Ar)_3$ template, we set upon a parallel investigation in CO reduction chemistry. Rationally implemented CO deoxygenation reactions can be an effective means for the delivery of a C-atom from CO to transition metal clusters, as in the preparation of a family of $[Fe_4(C)]$ clusters achieved by Shriver and coworkers,[1] and in the preparation of a family of $[W_4(C)]$ clusters achieved by Chisholm and coworkers.[2] As introduced generally in the introductory remarks to Chapter 2, our specific goal was to implement CO as the source of a *terminal* cardide substituent. Schematically, we sought a route to the reaction shown in eqn 1.

$$\underset{\mathbf{1}}{Mo(N[R]Ar)_3} \xrightarrow{[C{\equiv}O]^-} [C{\equiv}Mo(N[R]Ar)_3]^- + \text{“ O ”} \qquad (1)$$

This chapter presents a successful reagent-based strategy whereby the O-atom of coordinated CO was removed in a stepwise fashion. Briefly summarizing, reduction of a [Mo-CO] core to an [Mo≡CH] core, followed by a subsequent deprotonation, provides a route to the anionic molybdenum carbide complex $[C{\equiv}Mo(N[R]Ar)_3]^-$. These results have appeared in a preliminary communication.[3]

2 Results and Discussion

2.1 Synthesis of $(OC)Mo(N[R]Ar)_3$.[3]

As shown in eqn 2 exposure of a chilled ethereal solution of $Mo(N[R]Ar)_3$ to gaseous carbon monoxide resulted in rapid uptake of CO to generate the monocarbonyl complex $(OC)Mo(N[R]Ar)_3$, **2**. A color change from orange to dark brown was observed and an IR spectrum of the crude product mixture, after removal of volatiles, indicated a single intense stretch at 1840 cm^{-1} in heptane solution (1797 cm^{-1} for ^{13}CO derivative) corresponding to **2**. The ν_{CO} stretching frequency of 1840 cm^{-1} is a very low energy stretch for a terminal carbonyl complex of a formally 3^+ metal center and reflects very strong backbonding by the reducing $Mo(N[R]Ar)_3$ core. A ^2H NMR spectrum of this crude solid revealed that CO uptake was fairly clean (ca. 90 % crude yield). Complex **2** has been prepared in quantities ranging from 1–15 g and has proven to be easily purified by collecting the crude solid on a sintered-glass frit and washing it thoroughly with either acetonitrile or hexamethyldisiloxane. A solution magnetic susceptibility measurement of **2** by the method of Evans[4,5] yielded a μ_{eff} value of $2.2\mu_B$, consistent with a formulation of one unpaired electron (spin only value = 1.73 μ_B). That **2** has a low spin ground state is consistent with an Extended Hückel (EH) calculation performed using the program YAEHMOP[6] on a simplified model of $(OC)Mo(N[R]Ar)_3$ as shown in Fig 1 below. An X-ray diffraction study of **2** has not been undertaken and the bond lengths and angles of model $(OC)Mo(NH_2)_3$ were crudely approximated in C_{3v} symmetry. The interaction diagram shown provides a picture of the salient Frontier Molecular Orbitals (FMO) of $(OC)Mo(N[R]Ar)_3$.

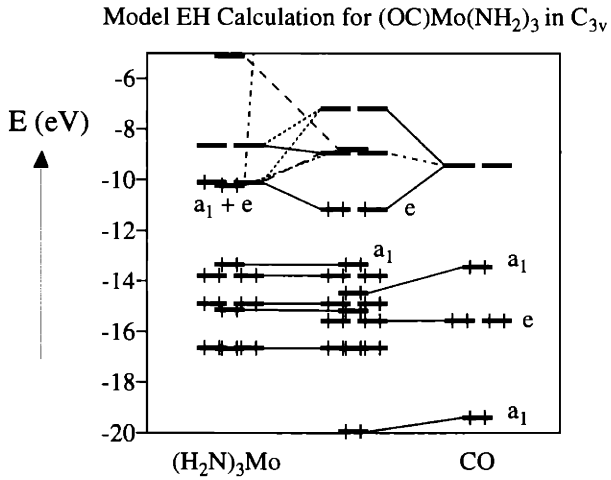

Figure 1: Extended Hückel Molecular Orbital Calculation (EHMOC) on an hypothetical C_{3v} model compound (OC)Mo(NH_2)$_3$. The diagram displays the Fragment Molecular Orbital (FMO) interaction diagram between a C≡O ligand and a Mo(NH_2)$_3$ complex, resulting in a low spin complex of molybdenum(III).

In rigorous C_{3v} symmetry the three d electrons on molybdenum occupy a degenerate e set. In the actual complex **2** this degeneracy is likely to be split by a Jahn-Teller distortion. Carbonyl complex **2** proved to be remarkably stable in comparison to its ephemeral (N_2)Mo(N[R]Ar)$_3$ analogue discussed in Chapter 1. The cyclic votammogram of **2** showed reversible waves at -0.37 V and -1.34 V (1M [N(n-Bu)$_4$][PF_6] in THF, $Cp_2Fe^{+/0}$), assigned as the one electron oxidation and reduction of **2**, respectively. Attempts to oxidize **2** synthetically with ferrocenium triflate and silver triflate did not lead to isolable products. Fortunately, the synthetic reduction of **2** was straightforward.

$$\underset{\mathbf{1}}{\text{Mo(N[R]Ar)}_3} \xrightarrow{\text{CO}} \underset{\mathbf{2}}{\text{(OC)Mo(N[R]Ar)}_3} \qquad (2)$$

2.2 Synthesis of [Na][(OC)Mo(N[R]Ar)$_3$].

Reduction of **2** by Na/Hg in THF at 25 °C resulted in a gradual color change from the dark brown of **2** to a bright orange over a period of ca. 30 minutes. Subsequent to solvent removal a ^{1}H NMR spectrum of the crude product mixture revealed that reduction had quantitatively generated a single diamagnetic product. A ^{13}C NMR spectrum showed a sharp signal at 243 ppm. The reduction product was assigned as [Na][(OC)Mo(N[R]Ar)$_3$], [Na][**3**], as shown in eqn 3. An X-ray diffraction study of a crystal obtained from a pentane–OEt_2 solution confirmed this basic formulation. A dramatic lowering of the ν_{CO} stretching frequency from 1840 cm^{-1} in neutral (OC)Mo(N[R]Ar)$_3$ to 1617 cm^{-1} for [Na][**3**] was observed (1568 cm^{-1} for ^{13}C-labeled [**3**]). The ion-pair [Na][**3**] was

soluble both in hydrocarbons and in donor solvents such as THF and OEt_2 where it yielded species of the form $[Na(THF)_x]$[**3**] and $[Na(ether)_x]$[**3**], respectively. Like $[(N_2)Mo(N[R]Ar)_3]^-$, $[(OC)Mo(N[R]Ar)_3]^-$ was isolable as a relatively solvent-free species by repeated trituration with pentane or lyophilization from frozen benzene solution. Residual solvent did persist and despite several attempts, satisfactory elemental analysis was not obtained for solvent-free [Na][**3**]. In surveying its chemistry, $[(OC)Mo(N[R]Ar)_3]^-$ was often generated cleanly *in situ*.

A structural figure derived from an X-ray study of $[Na][(OC)Mo(N[R]Ar)_3]$ is shown in Fig 2 and suggests that the crystallographically characterized species shown should be empirically formulated as $\{(OEt_2)Na(OC)Mo(N[R]Ar)_3\}_2$. This species likely reflects one point on a continuum of possible solution structures ranging from a completely solvent-free dinuclear cluster displaying a Na_2O_2 square, wherein each of the Na^+ cations is encapsulated by an aryl ring derived from an anilido ligand, to structures featuring a higher degree of solvation by donor solvent molecules.

$$\underset{\mathbf{2}}{OCMo(N[R]Ar)_3} \xrightarrow{Na/Hg} \underset{[Na][\mathbf{3}]}{Na^+[^-O\text{–}C{\equiv}Mo(N[R]Ar)_3]} \qquad (3)$$

2.3 Synthesis of $(Ph[t\text{-}Bu]N)_3Ti(\mu\text{-}OC)Mo(N[R]Ar)_3$.

Similar to the synthesis of $(Ph[t\text{-}Bu]N)_3Ti(\mu\text{-}N_2)Mo(N[R]Ar)_3$ from $(N_2)Mo(N[R]Ar)_3$ and d^1 reductant $Ti(N[t\text{-}Bu]Ph)_3$,[7] which was discussed in chapter 1, one electron reduction of $(OC)Mo(N[R]Ar)_3$ by $Ti(N[t\text{-}Bu]Ph)_3$ was effected by simple mixing of ethereal solutions of $(OC)Mo(N[R]Ar)_3$ and $Ti(N[t\text{-}Bu]Ph)_3$ as shown in eqn 4. A color change occurred instantly and $(Ph[t\text{-}Bu]N)_3Ti(\mu\text{-}OC)Mo(N[R]Ar)_3$, **4**, was isolated by crystallization from OEt_2 in 88.5 % yield as an orange crystalline solid. The diamagnetic complex exhibited a ^{13}C NMR signal for the Mo-*C*-O-Ti carbon at 247.5 ppm and showed a distinct set of resonances for the –N[*t*-Bu]Ph and –N[R]Ar ligands, respectively. The general features of the ^1H NMR spectrum of **4** resemble those of $(Ph[t\text{-}Bu]N)_3Ti(\mu\text{-}N_2)Mo(N[R]Ar)_3$. A ν_{CO} stretch was not located despite the preparation of both ^{12}C and ^{13}C-labeled derivatives and plotting the difference of their respective IR spectra. Complex **4** may be drawn with a single titanium-oxygen bond and a molybdenum-carbon triple bond. This resonance form suggests d^0 titanium(IV) and d^0 molybdenum(VI) centers and a formal four electron reduction of carbon monoxide gas.

$$Ti(N[t\text{-}Bu]Ph)_3 + \underset{\mathbf{2}}{(OC)Mo(N[R]Ar)_3} \longrightarrow \underset{\mathbf{4}}{(Ar[R]N)_3Ti\text{–}O\text{–}C{\equiv}Mo(N[R]Ar)_3} \qquad (4)$$

2.4 Silylation of $[(OC)Mo(N[R]Ar)_3]^-$.

Like **4**, diamagnetic $[(OC)Mo(N[R]Ar)_3]^-$ may be formulated with a molybdenum-carbon triple bond as in $[^-O\text{-}C{\equiv}Mo(N[R]Ar)_3]$. Its Mo-C bond length of 1.776(6)Å suggests strong multiple

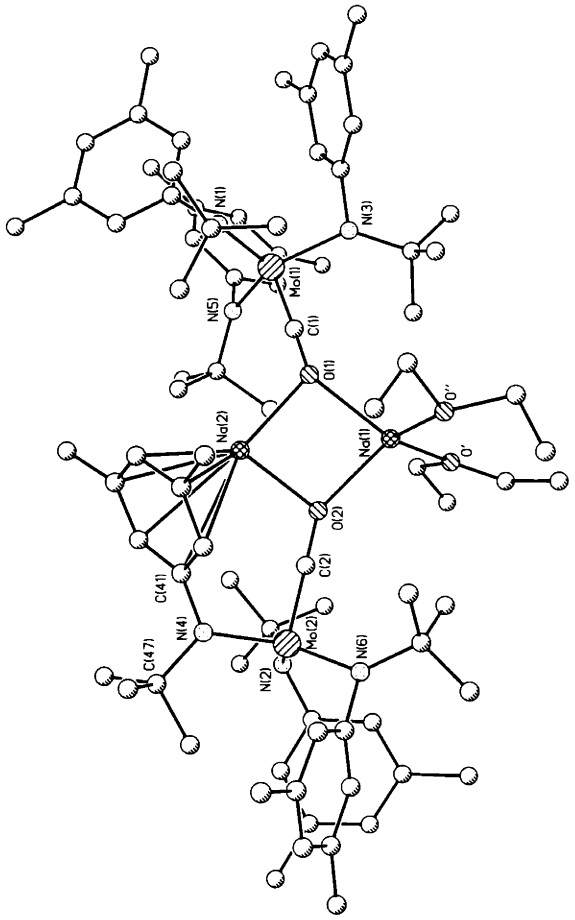

Figure 2: PLUTO representation of $[Na(OEt_2)][(OC)Mo(N[R]Ar)_3]$, **3**, from an X-ray study. A discrete and disordered molecule of OEt_2 was present in the asymmetric unit and has been omited in the above figure. Selected bond distances (Å) and angles (°): Mo(1)-C(1), 1.777(6); Mo(2)-C(2), 1.777(6); O(1)-C(1), 1.258(7); O(2)-C(2), 1.253(8); Na(1)-O(1), 2.282(5); Na(1)-O(2), 2.244(5); Na(2)-O(1), 2.277(5); Na(2)-O(2), 2.277(5); Mo(1)-N(1), 2.000(5); Mo(1)-N(3), 1.998(5); Mo(1)-N(5), 2.007(5); Mo(2)-N(2), 2.020(5); Mo(2)-N(4), 2.010(5); Mo(2)-N(6),1.990(5); C(1)-Mo(1)-N(1), 98.9(2); C(1)-Mo(1)-N(3), 100.6(2); C(1)-Mo(1)-N(5), 98.5(2); C(2)-Mo(2)-N(2), 101.7(2); C(2)-Mo(2)-N(4), 95.9(2); C(2)-Mo(2)-N(6), 97.8(2); N(1)-Mo(1)-N(3), 116.7(2); N(5)-Mo(1)-N(3), 117.3(2); N(1)-Mo(1)-N(5), 118.3(2); N(6)-Mo(2)-N(2), 119.6(2); N(6)-Mo(2)-N(4), 120.2(2); N(4)-Mo(2)-N(2), 113.9(2); Na(2)-O(1)-Na(1), 94.2(2); Na(2)-O(2)-Na(1), 96.6(2); O(2)-Na(1)-O(1), 83.5(2); O(2)-Na(1)-Na(2), 41.49(13); O(2)-Na(2)-Na(1), 41.89(13).

bonding and is consistent with this resonance contributor. This formulation for [**3**] is reminiscent of an alkoxide anion and it was our hope that the oxygen atom of [**3**] would exhibit nucleophilic character. Treatment of an ethereal solution of [Na][**3**] with $ClSiMe_3$ rapidly resulted in salt elimination and formation of Me_3Si-O-C≡Mo(N[R]Ar)$_3$, **5**, shown eqn 5. A ^1H NMR spectrum of the crude product showed that the reaction was virtually quantitative, with a new signal for the –Si*Me*$_3$ group resonating at 0.35 ppm. Having established that [**3**] could behave as a nucleophile, it next became necessary to choose an appropriate electrophile such that the O-atom of [**3**] would be incorporated into a convenient leaving group.

$$\underset{[Na][\mathbf{3}]}{[Na][(OC)Mo(N[R]Ar)_3]} + ClSiMe_3 \xrightarrow{\text{- NaCl}} \underset{\mathbf{5}}{Me_3Si\text{-}O\text{-}C{\equiv}Mo(N[R]Ar)_3} \quad (5)$$

2.5 Synthesis of ^{t}BuC(O)-O-C≡Mo(N[R]Ar)$_3$.[3]

By analogy to the facile oxidative decarboxylation of carboxylic acids possessing viable radical leaving groups[8,9] we chose pivaloyl chloride, ClC(O)-*t*-Bu, as a suitable electrophile. Fig 3 attempts to illustrate our motivation for adopting this strategy. Funtionalization of nucleophilic [**3**] with ClC(O)-*t*-Bu promised to afford a pivalato carbyne species well poised for fragmentation. We hoped that upon subsequent reduction, the resulting radical anion, [^{t}BuC(O)-O-C≡Mo(N[R]-Ar)$_3$]$^{\cdot -}$, would undergo a facile loss of CO_2 and *tert*-butyl radical, thereby delivering the carbide substituent to Mo(N[R]Ar)$_3$. Ideally, this strategy might afford the target species [C≡Mo(N[R]-Ar)$_3$]$^-$ and easily removed gaseous byproducts CO_2, isobutylene, and isobutane.

Treatment of a chilled OEt_2 solution of [**3**] with stoichiometric pivaloyl lchloride resulted in the relatively clean generation of the desired product ^{t}BuC(O)-O-C≡Mo(N[R]Ar)$_3$, **6**, as shown in eqn 6. The reaction was monitored by IR spectroscopy and was found to proceed to completion over a period of ca. 15 h when stirred at 25 °C. The pivalato functionality of **6** exhibited a signature carboxyl stretch at 1771 cm^{-1} and a new ^1H NMR signal for the *tert*-butyl group at 1.22 ppm. The ^{13}C NMR signal for the carbyne carbon atom of **6** resonates at 217 ppm. Chilling of the solution prior to addition of pivaloyl chloride was found to minimize undesirable formation of neutral carbonyl **2** via redox chemistry. Complex **6** has been prepared on scales ranging from 1–5 g in yields greater than 80 %. An X-ray diffraction study confirmed the proposed connectivity for **6** (Fig 4).

$$\underset{[Na][\mathbf{3}]}{[Na^+][^-O\text{–}C{\equiv}Mo(N[R]Ar)_3]} + {}^tBuC(O)Cl \xrightarrow{-\ NaCl} \underset{\mathbf{6}}{{}^tBuC(O)O\text{–}C{\equiv}Mo(N[R]Ar)_3} \quad (6)$$

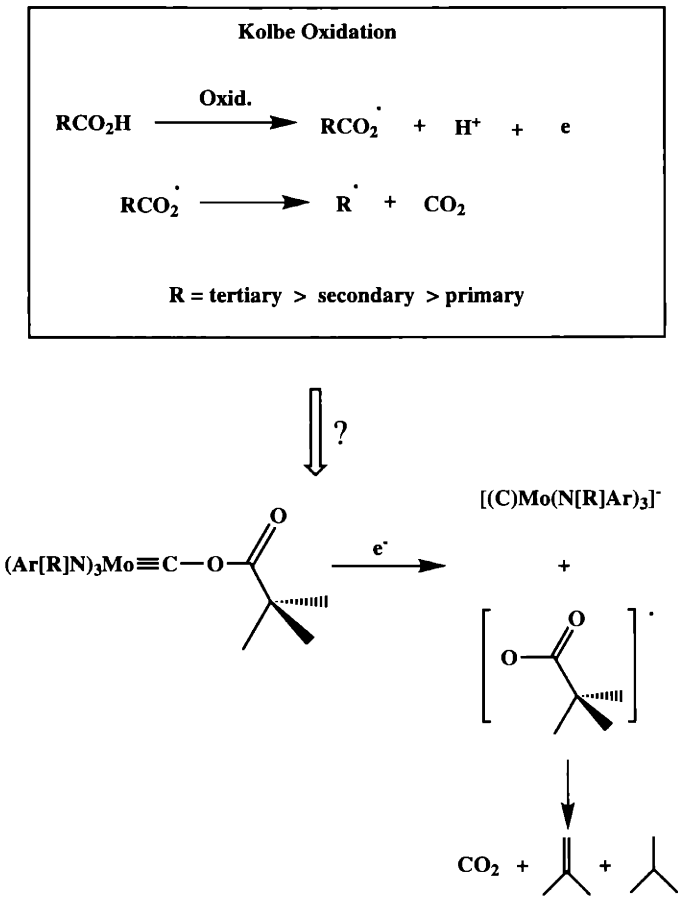

Figure 3: Potential C-O bond cleavage via a facile decarboxylation reaction.

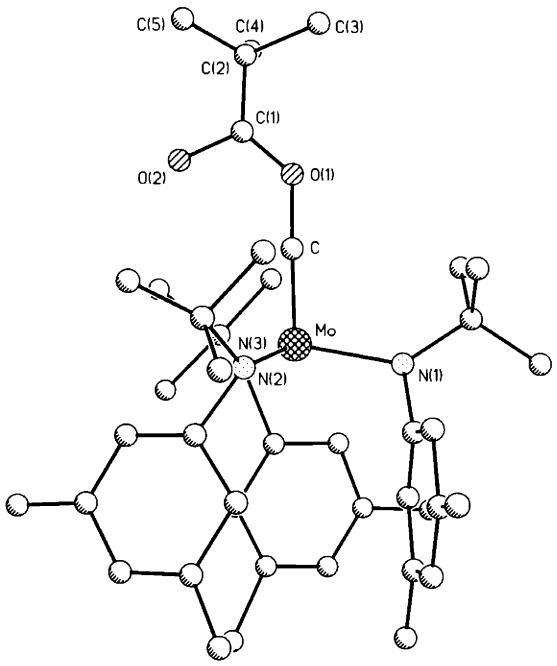

Figure 4: PLUTO drawing of ^{t}BuC(O)-O-C≡Mo(N[R]Ar)$_3$, **6**, from an X-ray study.

2.6 Reaction of ^{t}BuC(O)-O-C≡Mo(N[R]Ar)$_3$ with Na in THF.

Removal of the pivalato functionality was achieved by reaction of **6** with solid sodium metal in THF. A color change from beige to orange was observed when THF solutions of **6** were stirred vigorously at 25 °C over metallic sodium for several hours. Monitoring of a small scale probe reaction (< 100 mg) by IR spectroscopy showed a decay of the intense band at 1771 cm^{-1} of **6** and formation of a band at 1617 cm^{-1} corresponding to the carbonyl anion [(OC)Mo(N[R]-Ar)$_3$]$^-$. After 2 h, the starting complex **6** had been completely consumed and inspection by ^{1}H and ^{13}C NMR spectroscopies indicated that *three* products had formed. Exhaustive repetition of this experiment confirmed these products to be the undesirable [Na][(OC)Mo(N[R]Ar)$_3$], [Na][**3**]; a new methylidyne species HC≡Mo(N[R]Ar)$_3$, **7**; and a third species which we cautiously formulated as [Na][C≡Mo(N[R]Ar)$_3$], [Na][**8**]. A ^{13}C NMR spectrum of one such crude reaction mixture, shown in Fig 5 below, shows ^{13}C NMR signals at ca. 243.5, 287.5, and ca. 475 ppm, respectively, for these three species. A ^{1}H NMR spectrum of this same residue did not show a resonance corresponding to the *tert*-butyl signal of the pivalato functionality of the starting material. The spectrum also revealed that [Na][**8**] represented ca. 50 % of the product mixture, while **7** and [Na][**3**] were each present in the amount of ca. 25 %. Despite much effort, direct separation of this mixture was not fruitful. Treatment of the crude product mixture with excess ClSiMe$_3$ resulted in silylation of the two *anionic* products [**8**] and [**3**], affording a mixture which was identified as unreacted HC≡Mo(N-[R]Ar)$_3$, newly generated Me$_3$Si-C≡Mo(N[R]Ar)$_3$, and previously characterized Me$_3$Si-O-C≡Mo(N-[R]Ar)$_3$. This mixture was examined by ^{13}C and ^{1}H NMR spectroscopies, but attempts to separate the mixture were not successful. However, as shall be described below, Me$_3$Si-C≡Mo(N[R]Ar)$_3$ was

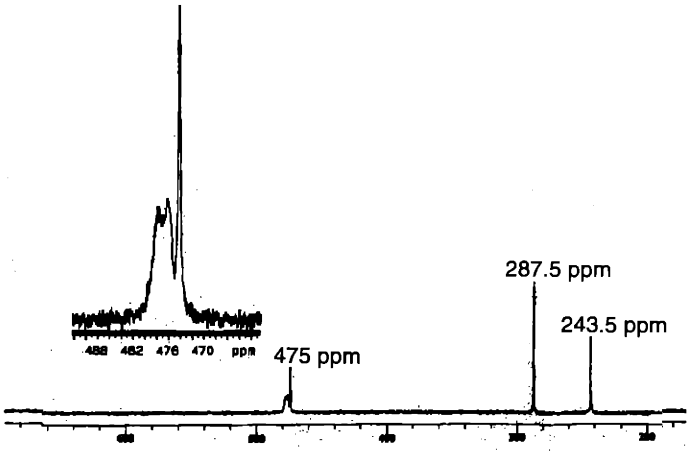

Figure 5: ^{13}C NMR spectrum of crude product mixture from the reaction of ^{t}BuC(O)-O-C≡Mo-(N[R]Ar)$_3$, **6**, with Na(s) in THF after 70 minutes of vigorous stirring at 25 °C. See main text for discussion.

later generated and spectroscopically identified from the direct reaction of $ClSiMe_3$ and cleanly isolated [K][C≡Mo(N[R]Ar)$_3$]. Hence, the generation of Me_3Si-C≡Mo(N[R]Ar)$_3$ by treatment of the crude product mixture resulting from ^{t}BuC(O)-O-C≡Mo(N[R]Ar)$_3$ reduction with $ClSiMe_3$ has been *spectroscopically* confirmed by its independent generation. An independent attempt was made to examine the volatile products of ^{t}BuC(O)-O-C≡Mo(N[R]Ar)$_3$ reduction reaction by ^{13}C NMR spectroscopy. In two independent experiments, the volatile products of small scale reactions performed in THF were vacuum distilled into NMR tubes that were subsequently flame sealed. ^{13}C NMR spectra of these samples showed only resonances corresponding to the THF solvent.

We had anticipated the possibility of isobutylene and isobutane byproducts as a result of *tert*-butyl radical generation. If generated, it is plausible that *tert*-butyl radicals would react faster with the THF solvent than with each other. Definitive conclusions regarding the mechanism leading to the three species formed by Na reduction of ^{t}BuC(O)-O-C≡Mo(N[R]Ar)$_3$ cannot be made. It is likely that more than one mechanistic pathway is operative. In fact, the generation of [Na][(OC)Mo(N[R]Ar)$_3$] may occur by decarbonylation and *tert*-butyl radical loss rather than the originally envisioned decarboxylation. Such processes have been documented in the oxidation of pivaldehyde.[10] Additionally, metallic sodium is known to facilitate C-O bond cleavage in certain ethers such as benzyl methyl ether,[11] and removal of the pivalate anion as [Na][OC(O)-*t*-Bu] may also be operative. A general review on radical deoxygenation leading to C-O cleavage in organic substrates has appeared.[12]

2.7 Synthesis of HC≡Mo(N[R]Ar)$_3$.[3]

The list of observations detailed above may be summarized quite simply. Stirring ^{t}BuC(O)-O-C≡Mo(N[R]Ar)$_3$, **6**, over metallic sodium in THF effects a reaction in which C-O bond rupture does occur, albeit not quantitatively. Because the metallated carbide complex, [Na][**8**], was spectroscopically identified but not isolable from the crude product mixture, we turned to an alternate strategy for a cleaner synthesis of the metallated carbide species. Fortunately, addition of acetonitrile to a crude product mixture of [Na][**8**], methylidyne **7**, and [Na][**3**] effected conversion of [**8**] to **7** with concomittant precipitation of hydrophobic **7** from the polar solvent. Filtration afforded relatively pure HC≡Mo(N[R]Ar)$_3$ as a beige solid in ca. 50 % yield and a deep orange filtrate containing the undesirable [Na][**3**] side product. **7** has been isolated cleanly on scales ranging from 0.2–2.8 g reproducibly by this methodology, which is summarized in Fig 6. The methylidyne proton Mo≡C*H* showed a ^{1}H NMR signal at 5.66 ppm and a J_{CH} of 157 Hz. A gate-decoupled ^{13}C NMR spectrum of **7** showed a doublet at 287.5 ppm with a J_{CH} consistent with the ^{1}H NMR spectrum. An effort was made to identify the Mo≡*C*H stretch of **7** by IR spectroscopy. Fig 7 shows an overlay of pure ^{12}C and ^{13}-labeled derivatives. As is clear from the spectra shown, no assignment for this stretch can be made. Recently, Jane Brock obtained a crystal structure of HC≡Mo(N[R]Ar)$_3$ and determined the Mo-C bond length to be 1.699(5)Å, consistent with a strong metal-carbon triple bond.[13] Alternate strategies leading to highly related tungsten and molybdenum(VI) methylidyne complexes have recently been reported.[14–16] While they remain relatively rare species, other methylidynes have been prepared.[17–21]

2.8 Reaction of HC≡Mo(N[R]Ar)$_3$ with *tert*-butyllithium.

With methylidyne complex **7** cleanly in hand, we were in a position to test the viability of deprotonation as a cleaner route to the target carbide complex. To our gratification, reaction of **7** with *tert*-butyllithium in C_6D_6 solution resulted in the decay of the peak for **7** at 287.5 ppm (^{13}C NMR) and the generation of a single new peak downfield at 470.1 ppm. This value agreed well with that mentioned above (ca. 475 ppm) for the tentatively assigned [Na][C≡Mo(N[R]Ar)$_3$]. A ^{1}H NMR spectrum of this reaction solution showed a single set of sharp anilido ligand resonances and a doublet indicative of the presence of isobutane (0.85 ppm). The reaction scale was increased and solvent-free, pentane soluble [Li][C≡Mo(N[R]Ar)$_3$], [Li][**8**], was isolated in 50 % yield by crystallization from pentane. To my knowledge, examples of transition metal carbyne complexes in which an alkali metal serves as the functional group at the carbyne carbon, as in [Li][**8**], were previously unknown. This complex bears an isolobal resemblance to simple species such as LiC≡N and LiC≡CH.

2.9 Synthesis of [K][C≡Mo(N[R]Ar)$_3$].[3]

We wondered whether the [C≡Mo(N[R]Ar)$_3$]$^-$ species would yield a stable ion-pair if we replaced the Li$^+$ cation with a K$^+$ cation. To address this question, we adopted a similar methodology using benzylpotassium[22] as the base of choice. It was found that addition of benzylpotassium to a chilled

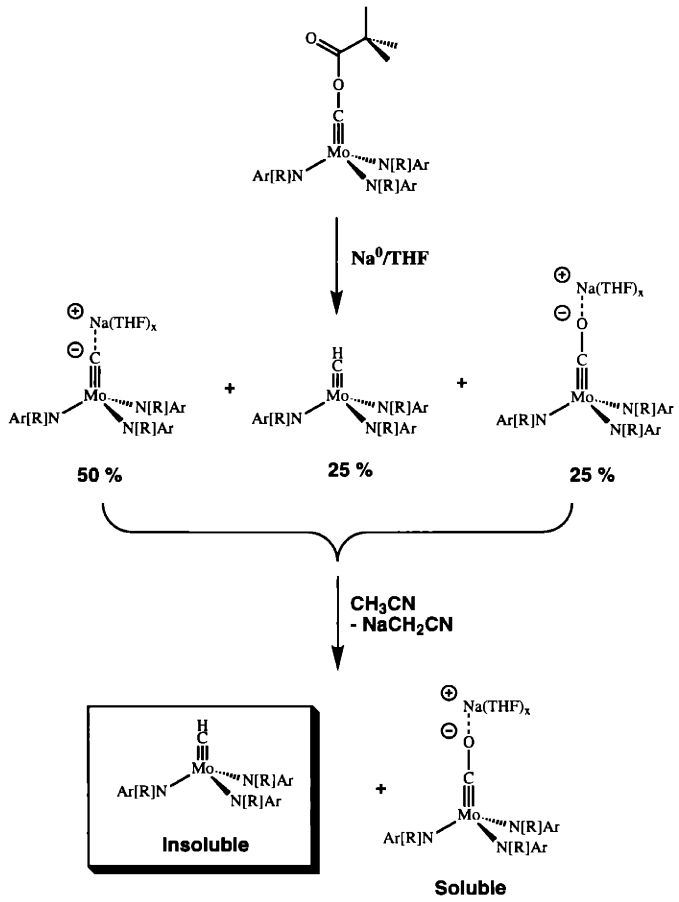

Figure 6: Scheme depicting Synthesis of HC≡Mo(N[R]Ar)$_3$.

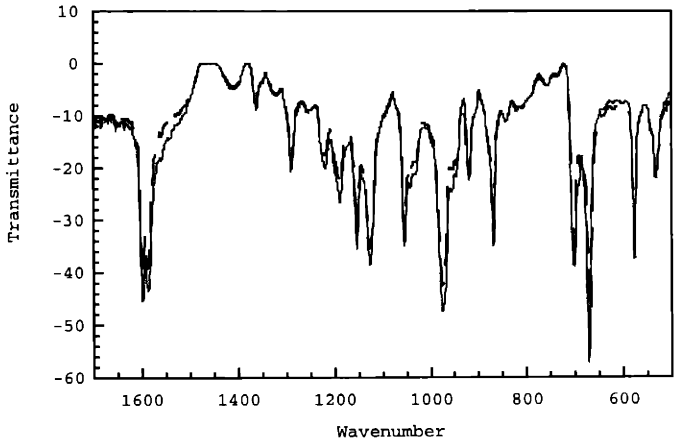

Figure 7: Overlay of the IR spectra of H^{12}C≡Mo(N[R]Ar)$_3$ and H^{13}C≡Mo(N[R]Ar)$_3$. A ν(Mo≡CH) stretch is not assignable.

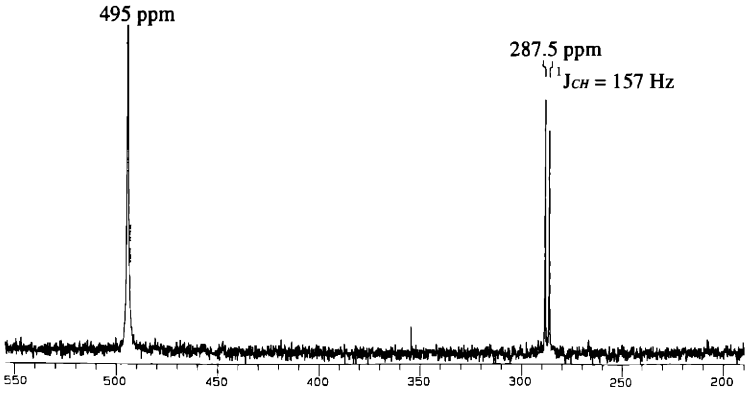

Figure 8: ^{13}C NMR (gate-decoupled in C_6D_6) spectrum of a crude product mixture of benzylpotassium deprotonation of HC≡Mo(N[R]Ar)$_3$, **7**, showing remaining **7** at 287.5 ppm and [K][**8**] at 495 ppm.

THF solution of **7** resulted, upon warming of the solution to ambient temperature, in the formation of [K][C≡Mo(N[R]Ar)$_3$], [K][**8**]. The reaction was relatively clean, and [K][**8**] has been obtained in 69 % yield by recrystallization from pentane–THF solution. The only side-product in this reaction was HC≡Mo(N[R]Ar)$_3$, **7**. This is likely due to some degree of reformation of **7** from [K][**8**] during work-up. Toluene, a byproduct of the deprotonation reaction, has been observed to react with cleanly isolated [K][C≡Mo(N[R]Ar)$_3$] to form HC≡Mo(N[R]Ar)$_3$ (*vide infra*). A sample ^{13}C NMR spectrum of a crude product mixture resulting from stoichiometric addition of benzylpotassium to **7** is shown in Fig 8. The spectrum displayed shows a sharp resonance at 495 ppm for [K][**8**] in C_6D_6. Additional benzylpotassium was typically added to such a crude product in order to effect a more complete deprotonation and an improved yield of [K][**8**].

In THF solution, [K][**8**] likely exists as a THF solvate, [K(THF)$_x$][C≡Mo(N[R]Ar)$_3$], but the rigorously solvent-free derivative [K][**8**] was easily obtained by dissolution of [K(THF)$_x$][C≡Mo(N[R]Ar)$_3$] in pentane followed by thorough drying *in vacuo*. Solvent-free [K][**8**] is insoluble in pentane but readily dissolves in ether, benzene, and THF. A ^1H NMR spectrum of [K][**8**] in THF-d_8 showed one set of anilido ligand resonances with a broad resonance for the *ortho*-protons of the aryl rings and a broad resonance for the *tert*-butyl group (see Fig 11). Broadening of the proton signals at these positions on the ^1H NMR time scale has been typical of ion-pair complexes bearing bulky –N[R]Ar ligands. An X-ray diffraction study of [K][**8**] revealed that intramolecular K^+–arene interactions[23] stabilize the solvent-free derivative. [K][**8**] exists in the solid state as a dimer with a central K_2C_2 square array situated about a crystallographic inversion center. A structural figure of [K][**8**] is shown in Fig 9. Because [K][**8**] was rather stable and was easily obtained in its solvent-free form it proved a convenient precursor to subsequent reaction chemistry.

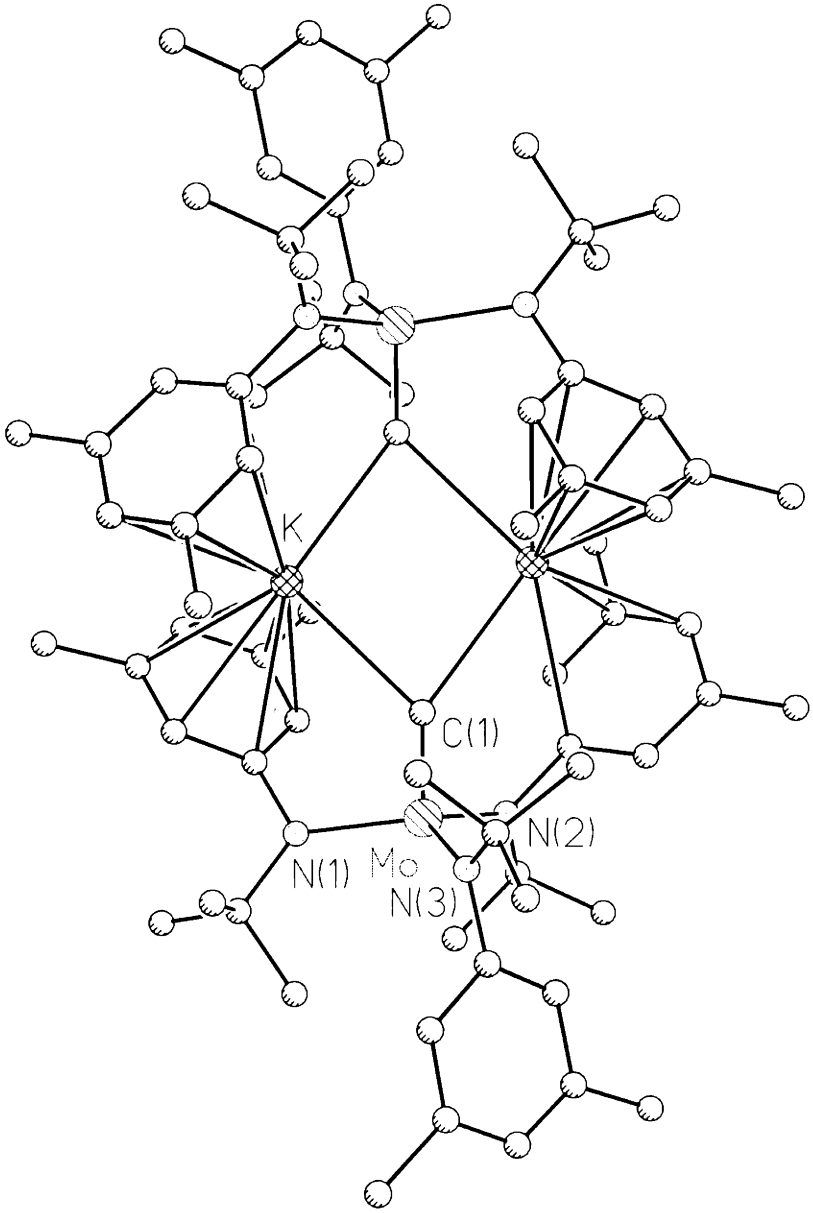

Figure 9: PLUTO drawing of [K][C≡Mo(N[R]Ar)$_3$], [K][**8**], derived from X-ray coordinates. Selected bond distances (Å) and angles (°):Mo-C(1), 1.68(3); Mo-N(1), 2.080(14); Mo-N(2), 2.02(2); Mo-N(3), 2.01(2); K-C(1), 2.94(2); C(1)-Mo-N(3), 100.3(13); C(1)-Mo-N(2), 98.0(10); C(1)-Mo-N(1), 99.6(8); N(2)-Mo-N(1), 115.8(9); N(3)-Mo-N(1), 119.5(5); N(3)-Mo-N(2), 117.0(6).

2.10 Isolation and Characterization of the terminal carbide complexes [K(2.2.2-crypt)][C≡Mo(N[R]Ar)$_3$] and [K(benzo-15-crown-5)$_2$][C≡Mo(N[R]Ar)$_3$].[3]

The potassium cation of [K][**8**] was readily sequestered by an appropriate cryptand or crown ether. Treatment of a THF solution of [K][**8**] with 1 eq of 2.2.2-crypt and subsequent work-up lead to the isolation of the discrete salt complex [K(2.2.2-crypt)][**8**]. [K(2.2.2-crypt)][**8**] was insoluble in pentane, benzene, and OEt_2 but was solubilized by tetrahydrofuran. Pure samples of [K(2.2.2-crypt)][**8**] were obtained in good yield by crystallization from pentane–THF. In stark contrast to the ^{1}H NMR spectrum of solvent-free [K][**8**], the anilido ligand resonaces of [K(2.2.2-crypt)][**8**] were sharp and showed features grossly similar to the isoelectronic terminal nitride complex N≡Mo(N[R]Ar)$_3$, as shown in Fig 11. Signals confirming the presence of K^+(2.2.2-crypt) were also apparent. Curiously, ^{13}C NMR spectra of [K(2.2.2-crypt)][C≡Mo(N[R]Ar)$_3$] exhibited a broad resonance centered at ca. 483 ppm. It was later found that this broadness was due to a small impurity of **7** that resulted in a fast exchange process between [K(2.2.2-crypt)][**8**] and HC≡Mo(N[R]Ar)$_3$ (eqn 7).

$$[^{-}C{\equiv}Mo(N[R]Ar)_3] \;+\; HC{\equiv}Mo(N[R]Ar)_3 \;\underset{\longleftarrow}{\overset{THF}{\longrightarrow}}\; HC{\equiv}Mo(N[R]Ar)_3 \;+\; [^{-}C{\equiv}Mo(N[R]Ar)_3] \qquad (7)$$

This was confirmed by the addition of benzylpotassium to "wet" THF solutions containing [K(2.2.2-crypt)][**8**] and **7**. The ^{13}C NMR signal for the carbide carbon of [K(2.2.2-crypt)][**8**] sharpened dramatically and shifted to 501.8 ppm as shown in Fig 12. If the THF solvent employed to handle [K(2.2.2-crypt)][**8**] was rigorously dried by passage through an activated alumina column, impurities of **7** were minimized and relatively sharp spectra were obtained. An X-ray diffraction study of a single crystal of [K(2.2.2-crypt)][**8**] was undertaken, but was hampered by the presence of four distinct molecules of [K(2.2.2-crypt)][**8**] present in the asymmetric unit in addition to positional disorder in the cryptands of the cationic K^+(2.2.2-crypt) units. We opted to use benzo-15-crown-5 in place of 2.2.2-cryptand in order to sequester the potassium cations after a search of the Cambridge Structural Database (CSD) revealed many K^+ containing structures featuring a potassium cation sandwiched by a pair of benzo-15-crown-5 ligands. Obtainment of the discrete salt [K(benzo-15-crown-5)$_2$][**8**] proceeded analogously to that of [K(2.2.2-crypt)][**8**]. The X-ray diffraction study of [K(benzo-15-crown-5)$_2$][**8**], thermal ellipsoid representations of which are shown in figures 13 and 14, confirmed that [K(benzo-15-crown-5)$_2$][**8**] indeed exists in the solid state as a discrete salt with no potassium-carbon interactions. Fig 10 summarizes the syntheses of [Li][**8**], [K][**8**], [K(2.2.2-crypt)][**8**], and [K(benzo-15-crown-5)$_2$][**8**].

The gross structural features of the anionic unit of [K(benzo-15-crown-5)$_2$][**8**], [C≡Mo(N[R]-Ar)$_3$]$^-$, are related to the isoelectronic derivatives N≡Mo(N[^{t}Bu]Ph)$_3$ and P≡Mo(N[R]Ar)$_3$, both of which have been structurally characterized.[24,25] The three –N[R]Ar ligands adopt the typical propeller motif with the aryl rings π-stacked on one side of the molecule and the "upward" *tert*-butyl groups forming a pocket containing the Mo≡C linkage. A molybdenum-carbon bond length of 1.713(9) angstroms for Mo≡C$^-$ suggests strong multiple bonding at the molybdenum-carbido linkage. This bond length is not statistically different from that found for HC≡Mo(N[R]Ar)$_3$, **7**.

Fig 15 describes the bonding in [C≡Mo(N[R]Ar)$_3$]$^-$ schematically by showing a simple frag-

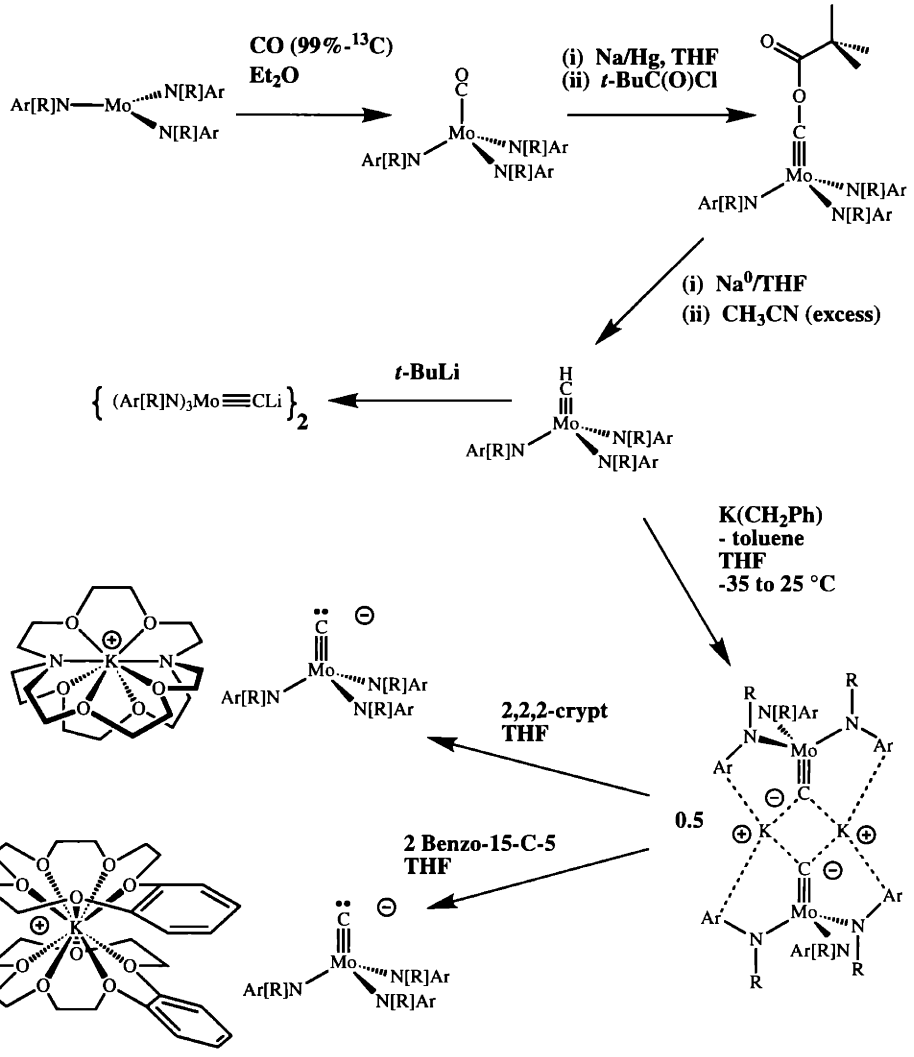

Figure 10: Synthesis of a Molecular Molybdenum Carbide Complex.

ment molecular orbital (FMO) diagram in which the model three-coordinate complex $Mo(NH_2)_3$ in idealized C_3 symmetry is allowed to interact with an anionic C^- ligand along the z axis.[6] A diamagnetic singlet ground state results in which three rigorously bonding orbitals comprise the frontier set. The highest occupied molecular orbital (HOMO) is of a symmetry and is composed of molybdenum d_{z^2} and carbon p_z character, i.e. a sigma bond along the z axis which is occupied by two electrons. Two degenerate orbitals lie just below the HOMO and are a degenerate e set composed of molybdenum d_{xz},d_{yz} and carbon p_x,p_y character, making up the π bonding manifold. A fourth a interaction is symmetry allowed but the carbon-based 2s orbital is at low energy and is best regarded as a non-bonding lone pair buried well beneath the valence electrons of the model $[CMo(NH_2)_3]^-$ complex. This simple EH calculation has been performed employing the actual anilido ligands –N[R]Ar with crystallographically obtained coordinates for the $[C{\equiv}Mo(N[R]Ar)_3]$ fragment and provides an analogous orbital picture. Hence, the $[C{\equiv}Mo(N[R]Ar)_3]^-$ is comparable to $N{\equiv}Mo(N[R]Ar)_3$ and $P{\equiv}Mo(N[R]Ar)_3$, both structurally and electronically. Worthy of note are the signature downfield-shifted NMR signals in the ^{15}N NMR spectrum of $N{\equiv}Mo(N[R]Ar)_3$, the ^{31}P NMR spectrum of $P{\equiv}Mo(N[R]Ar)_3$, and the ^{13}C NMR spectrum of $[C{\equiv}Mo(N[R]Ar)_3]$. These downfield shifts presumably result from a large z-component in the anisotropic chemical shift tensor. A formal discussion has appeared for the terminal phosphide $P{\equiv}Mo(N[R]Ar)_3$ and some related species.[26] Notably, Casey and coworkers have reported several complexes exhibiting dramatically downfield ^{13}C NMR signals.[27,28]

2.11 Gauging the Acidity of $HC{\equiv}Mo(N[R]Ar)_3$.

The results discussed above yield a rather wide margin for the acidity of $HC{\equiv}Mo(N[R]Ar)_3$ **7**, or alternatively, the basicity of $[^-C{\equiv}Mo(N[R]Ar)_3]$. Qualitatively, acetonitrile was a strong enough acid to protonate [Na][**8**] and benzylpotassium was a strong enough base to deprotonate **7**. It was also found that phenylacetylene quantitatively protonated [K][**8**] to form **7**. While very qualitative, these crude observations led to the successful isolation of both **7** and [K][**8**] in their pure and chemically useful forms. We attempted to narrow the range in our estimate of the acidity of **7** by treating [K][**8**] with a number of acids in THF solution and, alternatively, treating **7** with the conjugate base of these acids. Problematic in this study was the propensity of [K][**8**] to convert to **7** over time in solution at 25 °C. For example, although benzylpotassium is a strong enough base to deprotonate **7** in THF (*vide supra*), the conjugate acid of benzylpotassium, toluene, reacted with [K][**8**] slowly, in the presence of THF, to quantitatively convert [K][**8**] to **7**. A solution of [K][**8**] in THF alone was stable at 25 °C for a 16 h period. It was also found that [K][**8**] was partially converted to **7** at 50 °C over a period of 72 h in the presence of excess i-Pr_2NH. However, no reaction was observed at 25 °C over a 25 minute period. These results may reflect a propensity for redox chemistry by [K][**8**], leading to the formation of **7** via radical pathways. Hence, experiments attempting to protonate [K][**8**] by a potential acid in THF must be scrutinized for their potential to undergo both acid-base and redox chemistry. More telling, if only qualitatively, is the case in which a strong base generates detectable amounts of $[C{\equiv}Mo(N[R]Ar)_3]^-$, easily observed by both ^{13}C and ^1H NMR spectroscopy. It was found that a conjugate base of triphenylmethane, Ph_3CK, reacted with **7** to generate a detectable quantity of [K][**8**]. Spectra have been obtained showing that $[K][C{\equiv}Mo(N[R]Ar)_3]$, $HC{\equiv}Mo(N[R]Ar)_3$, and Ph_3CH, are all present in appreciable quantities in THF solution at 25 °C when *insitu* generated Ph_3CK is added to pure $HC{\equiv}Mo(N[R]$-

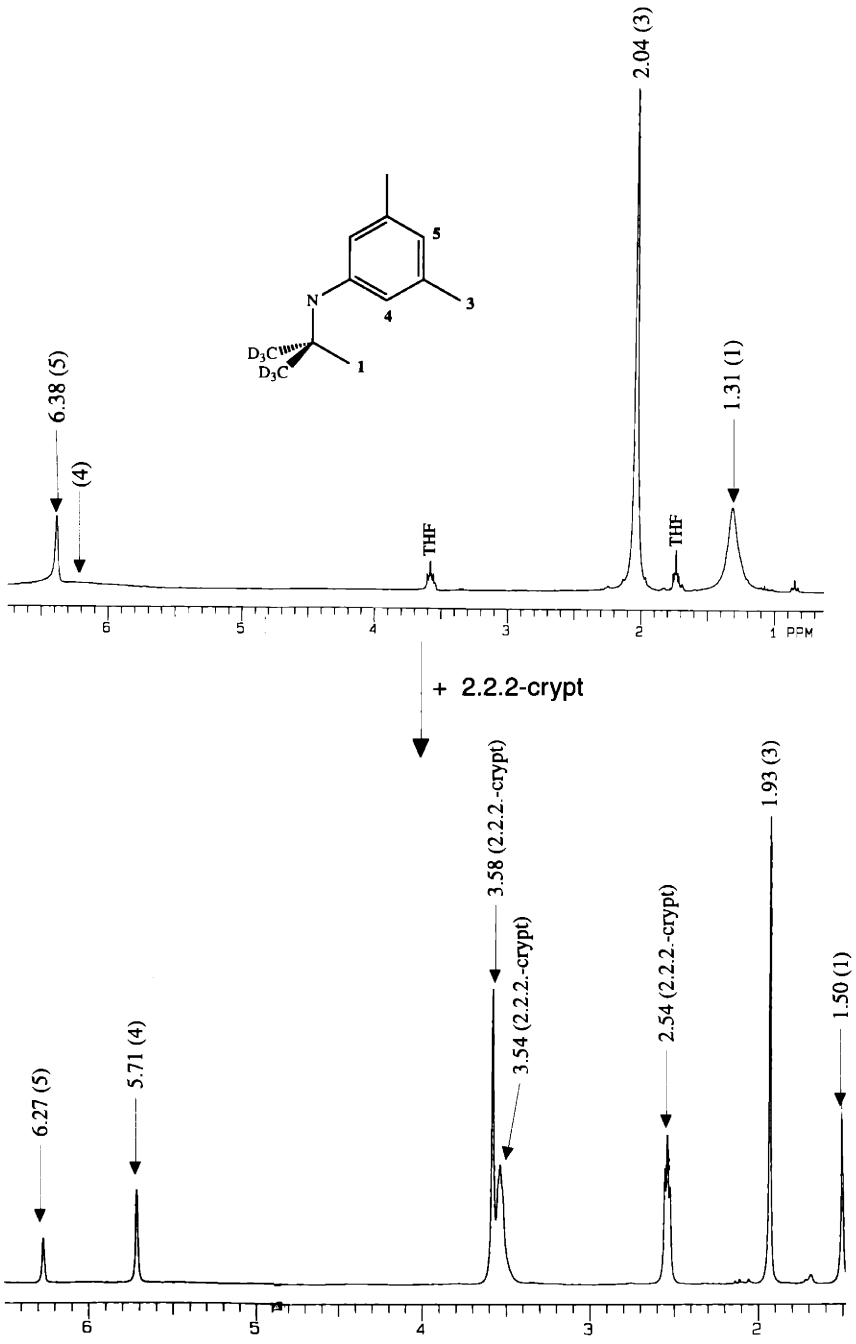

Figure 11: Top: ^{1}H NMR spectrum taken in THF-d_8 showing [K][**8**]. Bottom: ^{1}H NMR spectrum of [K(2.2.2-crypt)][**8**] in THF-d_8 taken after addition of stoichiometric 2.2.2-cryptand to a THF solution of [K][C≡Mo(N[R]Ar)$_3$].

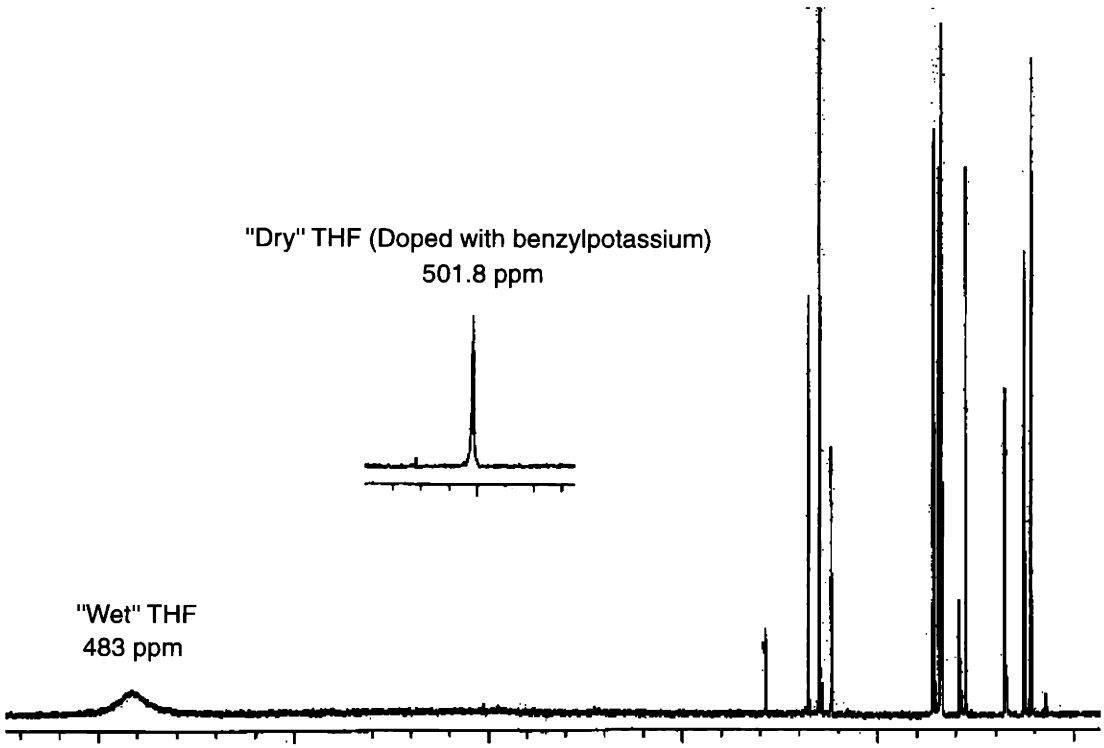

Figure 12: ^{13}C NMR spectra of [K(2.2.2-crypt)][**8**] in "wet" THF-d_8, showing a broad signal indicative of a small HC≡Mo(N[R]Ar)$_3$ impurity, and an inset spectrum showing a much sharper signal in the presence of added benzylpotassium (ca. 5 mol%). Reasonably sharp signals were also obtained by passing the THF solvent through activated alumina prior to dissolution of [K(2.2.2-crypt)][**8**].

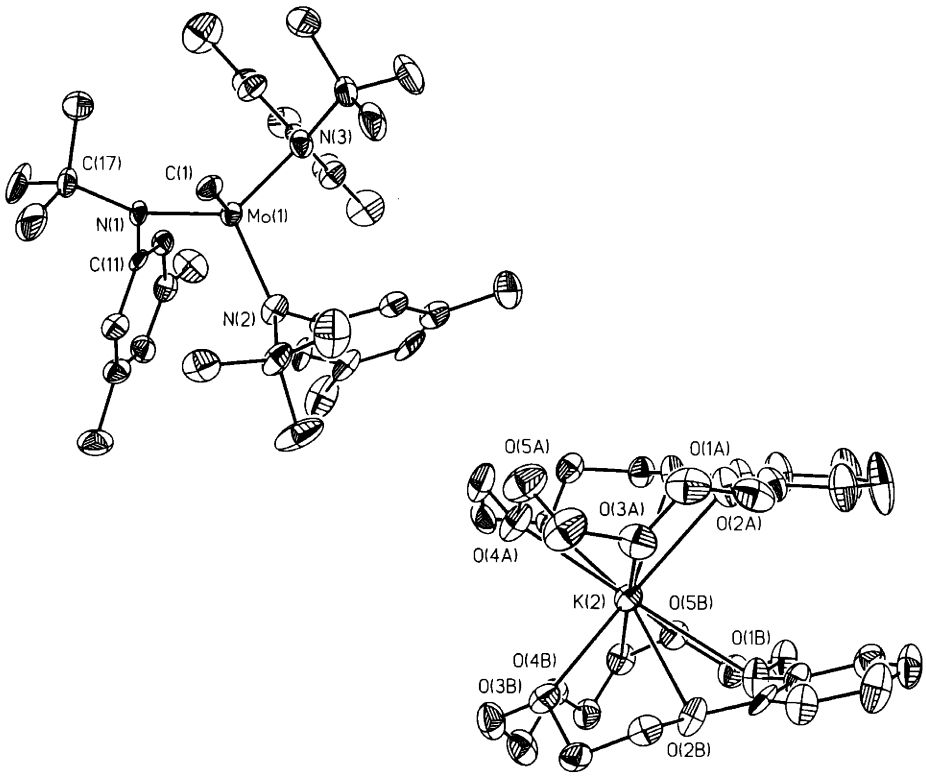

Figure 13: Thermal ellipsoid representation of [K(benzo-15-crown-5)$_2$][C≡Mo(N[R]Ar)$_3$], [K(benzo-15-crown-5)$_2$][**8**], from an X-ray study. Ellipsoids are at the 35 % probability level.

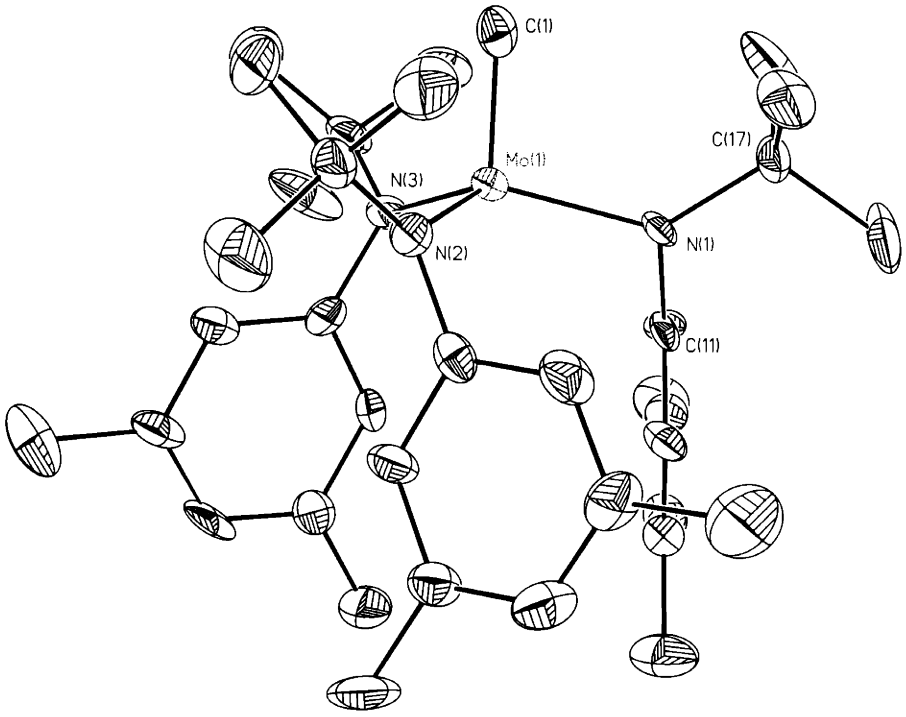

Figure 14: Thermal ellipsoid representation of anionic fragment of $[K(benzo\text{-}15\text{-}crown\text{-}5)_2][C{\equiv}Mo(N[R]Ar)_3]$, **8**, from an X-ray study. Ellipsoids are at the 35 % probability level. Selected bond distances (Å) and angles (°): Mo(1)-C(1), 1.713(9); Mo(1)-N(1), 2.008(6); Mo(1)-N(2), 2.010(7); Mo(1)-N(3), 2.013(6); C(1)-Mo(1)-N(1), 102.7(3); C(1)-Mo(1)-N(2), 103.9(3); C(1)-Mo(1)-N(3), 103.8(3); N(1)-Mo(1)-N(2), 114.7(3); N(1)-Mo(1)-N(3), 116.9(3); N(2)-Mo(1)-N(3), 112.6(3).

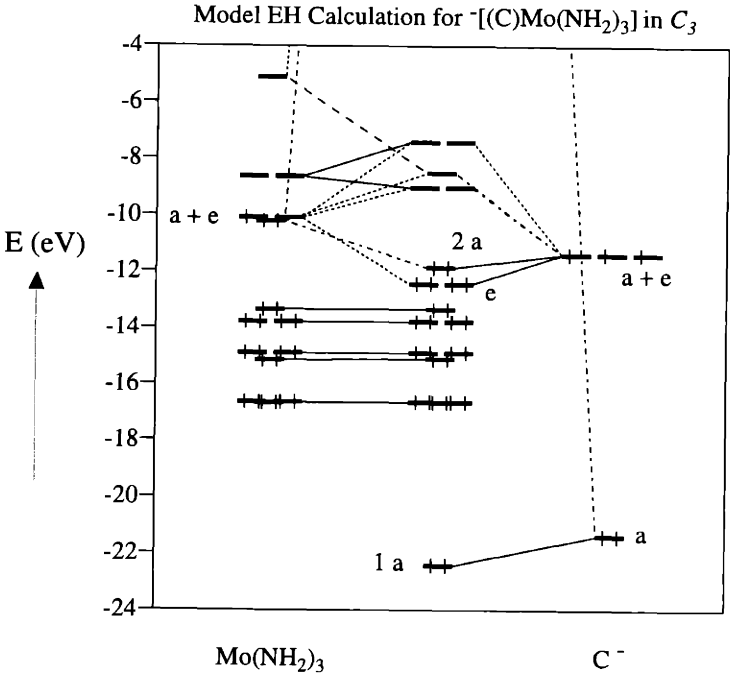

Figure 15: Extended Hückel Molecular Orbital Calculation (EHMOC) on an idealized C_3 model compound $^{-}$[(C)Mo(NH$_2$)$_3$]. The Fragment Molecular Orbital (FMO) diagram displays the interaction between a C$^-$ carbido ligand and a Mo(NH$_2$)$_3$ complex.[6]

$Ar)_3$. Correspondingly, a mixture of **7** and [K][**8**] was observed to result when [K][**8**] was treated with a stoichiometric amount of Ph_3CH. These results suggest that the acidity of Ph_3CH (with a pK_a of approximately 31.5 relative to water) is very similar to the acidity of **7** in THF.[29] Toluene is approximately 10 pK_a units *less* acidic than triphenylmethane. Toluene should not be able to directly protonate [K][**8**] in THF. As discussed above, benzylpotassium is able to deprotonate $HC{\equiv}Mo(N[R]Ar)_3$ quickly. That this reaction is not quantitative likely reflects the regeneration of $HC{\equiv}Mo(N[R]Ar)_3$ by some alternate, but not well understood, pathway.

2.12 Chemical Reactivity of $[C{\equiv}Mo(N[R]Ar)_3]^-$.

The isolation of synthetically viable quantities of anionic [**8**] provides the opportunity, in principle, to rationally prepare organometallic complexes beginning from the simple terminal carbido substituent. The anionic nature of [**8**] suggests that electrophilic substrates are viable reaction candidates. That this should be the case has already been demonstrated by the ready silylation of [**8**] during our early attempts to identify [Na][**8**] in solution (*vide supra*).

Relatively clean chemistry resulted when [K][**8**] was treated with PCl_3 as shown in eqn 8, respectively. The complexe $Cl_2PC{\equiv}Mo(N[R]Ar)_3$, **9**, was selected as a potential precursor for the preparation of complexes exhibiting phosphorus-to-carbon multiple bonding upon further reduction chemistry.

$$\underset{[K][\mathbf{8}]}{[K][C{\equiv}Mo(N[R]Ar)_3]} + PCl_3 \xrightarrow{OEt_2} \underset{\mathbf{9}}{Cl_2PC{\equiv}Mo(N[R]Ar)_3} \quad (8)$$

Disubstitution on PCl_3 by [K][**8**] was not problematic in the preparation of **9**. This was evident by examination of the ^{31}P NMR spectrum of a crude product mixture in which PCl_3 was treated with [K][**8**] containing a 50 % enrichment of ^{13}C-labeled $Mo{\equiv}C$. The spectrum showed a singlet centered between a doublet (J_{CP} = 144 Hz) in a 1:1 ratio, consistent with a mono-substituted product. Yellow **9** reacted with a second equivalent of [K][**8**] to generate the disubstituted monohalophosphine $ClP(C{\equiv}Mo(N[R]Ar)_3)_2$, **10**, albeit not very cleanly. Purification of this complex was complicated by the formation of $HC{\equiv}Mo(N[R]Ar)_3$ as a side product that was difficult to remove. Because complex **9** is sterically encumbered, undesirable redox chemistry probably competes with nucleophilic attack. However, spectroscopic analysis (^1H, ^{13}C, ^{31}P, NMR) definitively confirmed that $ClP(C{\equiv}Mo(N[R]Ar)_3)_2$ was the major species produced, as shown in eqn 9. The complex $ClP(C{\equiv}Mo(N[R]Ar)_3)_2$ gave rise to a carbide-carbon ^{13}C NMR signal at 301.4 ppm with a $^1J_{CP}$ coupling constant of = 149 Hz, similar to that found in $Cl_2PC{\equiv}Mo(N[R]Ar)_3$. Its ^{31}P NMR signal was found at 129.7 ppm. The ^1H NMR spectrum of $ClP(C{\equiv}Mo(N[R]Ar)_3)_2$ showed signals significantly broader than those observed for $Cl_2PC{\equiv}Mo(N[R]Ar)_3$, reflecting the enhanced steric crowding about phosphorus in $ClP(C{\equiv}Mo(N[R]Ar)_3)_2$.

$$\underset{[K][\mathbf{8}]}{[K][C{\equiv}Mo(N[R]Ar)_3]} + \underset{\mathbf{9}}{Cl_2PC{\equiv}Mo(N[R]Ar)_3} \xrightarrow{OEt_2} \underset{\mathbf{10}}{ClP(C{\equiv}Mo(N[R]Ar)_3)_2} \quad (9)$$

The chlorine atoms of **9** were replaced with hydrogen atoms by treatment of **9** with two equivalents of Schwartz's reagent,[30] $Cp_2Zr(H)(Cl)$, in benzene (eqn 10). Hydrocarbon insoluble Cp_2ZrCl_2 was easily removed by extraction of the novel phosphine $H_2PC{\equiv}Mo(N[R]Ar)_3$, **11**, into pentane. Spectroscopic analysis (^1H, ^{13}C, ^{31}P, NMR) suggested the relatively clean isolation of **11**. Intense blue-purple impurities typically discolored the product (off-white being its presumed true color).

$$2\ Cp_2Zr(H)(Cl) + \underset{\mathbf{9}}{Cl_2PC{\equiv}Mo(N[R]Ar)_3} \xrightarrow{-\ 2\ Cp_2ZrCl_2} \underset{\mathbf{11}}{H_2PC{\equiv}Mo(N[R]Ar)_3} \quad (10)$$

Phosphorus containing complexes **9**, **10**, and **11** were investigated as potential precursors to complexes bearing either neutral or anionic " C≡P " ligands, as in the hypothetical species $(P{\equiv}C\text{-}Mo(N[R]Ar)_3$ and $[P{=}C{=}Mo(N[R]Ar)_3]^-$. Having prepared the isoelectronic fragments $(NC)Mo(N[R]Ar)_3$ and $[(NC)Mo(N[Ad]Ar)_3]^-$, coordination of C≡P was deemed a worthwhile goal. To date efforts in this vein have not been successful. An alternative strategy has been investigated by the reaction of [K][**8**] with white phosphorus in toluene. A major reddish product was formed but despite a good deal of effort to isolate and fully characterize this species, its chemical nature remains unclear. Transition metal carbyne complexes functionalized by phosphorus, as in $Mo{\equiv}C\text{-}PR_2$, appear to be rare species. Somewhat related phosphoniocarbyne complexes of tungsten have been structurally characterized.[31,32] The complex $Ph_3P\text{-}C{\equiv}W(CO)(Cl)_2(PMePh_2)_2$ was structurally characterized by Hillhouse and coworkers.[33]

Noteworthy of the chemical reactivity of $[K][C{\equiv}Mo(N[R]Ar)_3]$ is the ease with which $HC{\equiv}Mo(N[R]Ar)_3$ is generated as a significant and undesirable byproduct. This point first became clear when a cold ethereal slurry of $[K][C{\equiv}Mo(N[R]Ar)_3]$ was treated with a small excess of $ClSiMe_3$. The silylated carbyne, $Me_3Si\text{-}C{\equiv}Mo(N[R]Ar)_3$, was generated and exhibited ^1H NMR signal for the $-Si\mathit{Me}_3$ at 0.54 ppm which was much broader than the related complex $Me_3Si\text{-}O\text{-}C{\equiv}Mo(N[R]Ar)_3$. Removal of the O-atom brings the $-SiMe_3$ group closer to the metal center and results in hindered rotation on the ^1H NMR time scale. The carbyne carbon signal was found at 345.6 ppm by ^{13}C NMR. Spectroscopic analyis of the crude product mixture showed that $Me_3Si\text{-}C{\equiv}Mo(N[R]Ar)_3$ and $HC{\equiv}Mo(N[R]Ar)_3$ had been generated in approximately a 3:2 ratio. The similar solubility properties of the two species impeded their separation.

Having deoxygenated $[(OC)Mo(N[R]Ar)_3]^-$, [**3**], en route to the isolation of $[C{\equiv}Mo(N[R]Ar)_3]^-$, we sought to install the heavier chalcogenides S, Se, and Te upon the carbide template. Elemental S, Se, and Te reacted readily with [K][**8**] in OEt_2 to ultimately afford anionic thiocarbonyl,[34] selenocarbonyl,[35,36] and tellurocarbonyl complexes,[35] respectively. Isolation of the yellow selenocarbonyl $[Se\text{-}C{\equiv}Mo(N[R]Ar)_3]^-$, [**12**], and $[Te\text{-}C{\equiv}Mo(N[R]Ar)_3]^-$, [**13**], was straightforward (eqns 11 and 12). Although methylidyne impurities are generated upon addition of excess Se and Te to cold ethereal solutions of $[K][C{\equiv}Mo(N[R]Ar)_3]$, the hydrocarbon insolubility of [K][**12**] and [K][**13**] renders

them easily purified by pentane washing. The carbide-carbon of [K][**12**] exhibits a ^{13}C NMR signal at 271.9 ppm and that for [K][**13**] resonates at 252.6 ppm. The discrete salt [K(benzo-15-crown-5)$_2$][Se-C≡Mo(N[R]Ar)$_3$] was prepared by simple addition of 2 eq of benzo-15-crown-5 to a solution of [K][**12**]. Crystals of this complex were readily obtained and a thermal ellipsoid representation is shown in Fig 16. The structure simply shows a linear selenocarbonyl entity resting upon on the z-axis of an approximately C_3 molybdenum fragment. The Mo-C bond length of 1.750(12)Å compares well with [(OC)Mo(N[R]Ar)$_3$]$^-$ and with Johnson's bent μ-CS complex (Ar[R]N)$_3$Mo≡C-S-Mo(N[R]Ar)$_3$ (1.777(6)Å and 1.751(12)Å, respectively). [37] The clean isolation of [S-C≡Mo(N-[R]Ar)$_3$]$^-$, [**14**], was more problematic. Elemental sulfur reacted readily with [K][**8**] to form the orange, highly pentane soluble bridged disulfide complex (Ar[R]N)$_3$Mo≡C-S-S-C≡Mo(N[R]Ar)$_3$, **15**, with a carbide-carbon signal at 253.8 ppm. The yellow ion-pair [Na][S-C≡Mo(N[R]Ar)$_3$] was cleanly obtained from *in situ* generated **15** followed by reduction with Na/Hg. [Na][S-C≡Mo(N-[R]Ar)$_3$] showed a ^{13}C NMR signal at 292.4 ppm and was converted to the discrete salt complex [Na(12-crown-4)$_2$][**14**] upon addition of 2 eq of 12-crown-4. Ethylene sulfide was a potential candidate for the direct preparation of [K][S-C≡Mo(N[R]Ar)$_3$] by reaction with [K][**8**]. However, mixing of these species resulted in nucleophilic ring-opening and generation of [K][S-CH$_2$CH$_2$C≡Mo(N[R]-Ar)$_3$], [K][**16**], which was easily isolated as the discrete salt complex [K(benzo-15-crown-5)$_2$][**16**] by addition of 2 eq of benzo-15-crown-5. The carbide carbon ^{13}C NMR signal was located at 304.0 ppm for the ion-pair [K][**16**].

$$\underset{[K][\mathbf{8}]}{[K][C{\equiv}Mo(N[R]Ar)_3]} \xrightarrow{\text{xs Se}} \underset{[K][\mathbf{12}]}{[K][Se\text{-}C{\equiv}Mo(N[R]Ar)_3]} \tag{11}$$

$$\underset{[K][\mathbf{8}]}{[K][C{\equiv}Mo(N[R]Ar)_3]} \xrightarrow{\text{xs Te}} \underset{[K][\mathbf{13}]}{[K][Te\text{-}C{\equiv}Mo(N[R]Ar)_3]} \tag{12}$$

$$\underset{[K][\mathbf{8}]}{[K][C{\equiv}Mo(N[R]Ar)_3]} \xrightarrow{\text{xs } S_8} \underset{\mathbf{15}}{1/2\ (Ar[R]N)_3Mo{\equiv}C\text{-}S\text{-}S\text{-}C{\equiv}Mo(N[R]Ar)_3} \tag{13}$$

$$\underset{\mathbf{15}}{(Ar[R]N)_3Mo{\equiv}C\text{-}S\text{-}S\text{-}C{\equiv}Mo(N[R]Ar)_3} \xrightarrow{\text{xs Na/Hg}} \underset{[Na][\mathbf{14}]}{[Na][S\text{-}C{\equiv}Mo(N[R]Ar)_3]} \tag{14}$$

$$\underset{[K][\mathbf{8}]}{[K][C{\equiv}Mo(N[R]Ar)_3]} \xrightarrow{\text{ethylene sulfide}} \underset{[K][\mathbf{16}]}{[K][S\text{-}CH_2CH_2C{\equiv}Mo(N[R]Ar)_3]} \tag{15}$$

The above reactions suggest that [C≡Mo(N[R]Ar)$_3$]$^-$ is readily functionalized in a predictable fashion. However, [C≡Mo(N[R]Ar)$_3$]$^-$ also shows a tendency to be readily oxidized. Hence, HC≡Mo(N[R]Ar)$_3$ is frequently generated as a reaction byproduct, as in the reaction of [K][C≡Mo-(N[R]Ar)$_3$] with ClSiMe$_3$. An attempt was made to use [C≡Mo(N[R]Ar)$_3$]$^-$ as an *inner-sphere*

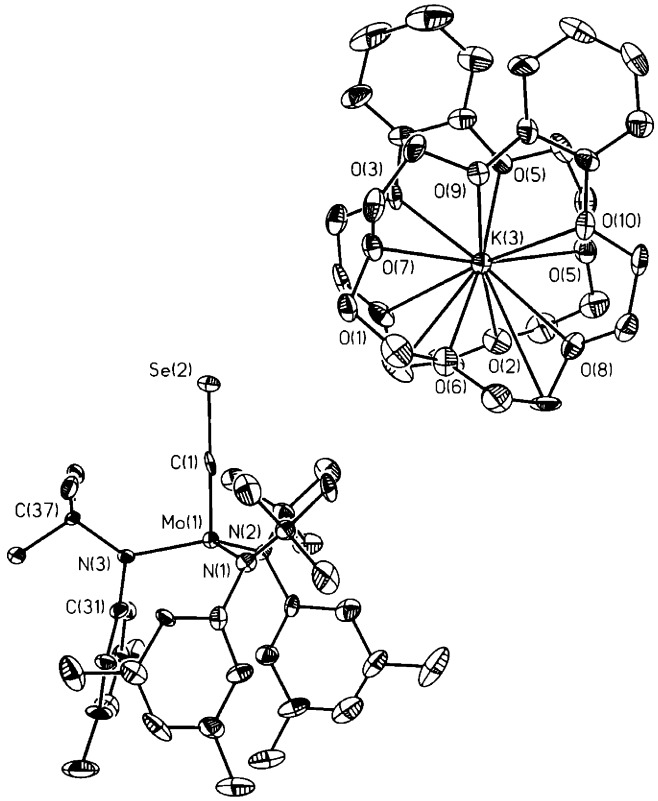

Figure 16: Thermal ellipsoid representation of [K(benzo-15-crown-5)$_2$][Se-C≡Mo(N[R]Ar)$_3$], [K(benzo-15-crown-5)$_2$][**12**], from an X-ray study. Ellipsoids are at the 35 % probability level. Selected bond distances (Å) and angles (°): Mo(1)-C(1), 1.750(12); Se(2)-C(1), 1.835(12); Mo(1)-N(1), 1.989(9); Mo(1)-N(2), 1.990(9); Mo(1)-N(3), 1.996(9); C(1)-Mo(1)-N(1), 101.5(5); C(1)-Mo(1)-N(2), 101.3(4); C(1)-Mo(1)-N(3), 100.9(4); N(1)-Mo(1)-N(2), 114.3(4); N(1)-Mo(1)-N(3), 118.7(4); N(2)-Mo(1)-N(3), 115.9(4).

reductant to generate an N-C bond. The chemistry presented in Chapter 1 established that neutral $(N_2)Mo(N[R]Ar)_3$ may be captured by a suitable one electron reductant. Hence, $[K][C{\equiv}Mo(N[R]Ar)_3]$ was stirred under N_2 in the presence of $Mo(N[R]Ar)_3$ in an effort to exploit these principles to synthesize $(Ar[R]N)_3Mo{\equiv}C\text{-}N{=}N\text{-}Mo(N[R]Ar)_3$. Not surprisingly, chemistry suggestive of an *outer-sphere* redox event was observed and the products, as characterized by IR, ^1H NMR, and ^{13}C NMR spectroscopies, were $[K][(N_2)Mo(N[R]Ar)_3]$ and $HC{\equiv}Mo(N[R]Ar)_3$ (eqn 16).

$$[K][\mathbf{8}] \quad + \quad \underset{\mathbf{1}}{Mo(N[R]Ar)_3} \quad \xrightarrow{N_2} \quad \underset{\mathbf{7}}{HC{\equiv}Mo(N[R]Ar)_3} \quad + \quad [K][(N_2)Mo(N[R]Ar)_3] \tag{16}$$

3 Conclusions

Chapters 1, 2, and 3 presented chemistry regarding the reduction and functionalization of N_2, CN^-, and CO, respectively. The latter two chapters have been intimately threaded by their objective in using CN^- and CO as viable synthons for the installation of a terminal carbido substituent upon the $Mo(N[R]Ar)_3$ template. While our efforts were not fully realized in the case of the cyanide synthon, this chapter shows a successful strategy by which CO serves as the source of a terminal carbide substituent. The following conclusions may be drawn:

- (i) $(OC)Mo(N[R]Ar)_3$ can be reduced in a stepwise fashion to $HC{\equiv}Mo(N[R]Ar)_3$, formally a four electron reduction of carbon monoxide. The d^3 $Mo(N[R]Ar)_3$ template provided three of the necessary electrons and sodium metal provided the fourth electron.
- (ii) A key component in the CO reduction chemistry was to find a synthetically viable deoxygenation strategy. This was accomplished by the conversion of $(OC)Mo(N[R]Ar)_3$ to $^tBuC(O)\text{-}O\text{-}C{\equiv}Mo(N[R]Ar)_3$ followed by a fragmentation reaction under rather forcing conditions. $[Na][C{\equiv}Mo(N[R]Ar)_3]$ was a major product of this fragmentation reaction. ^{13}C NMR spectroscopy proved an invaluable tool in the identification of $[Na][C{\equiv}Mo(N[R]Ar)_3]$, making ^{13}CO an elegant carbide synthon.
- (iii) $HC{\equiv}Mo(N[R]Ar)_3$ was isolated in pure form from $^tBuC(O)\text{-}O\text{-}C{\equiv}Mo(N[R]Ar)_3$ and was readily deprotonated by *tert*-butyllithium and benzylpotassium to generate $[Li][C{\equiv}Mo(N[R]Ar)_3]$ and $[K][C{\equiv}Mo(N[R]Ar)_3]$, respectively. The K^+ cation of $[K][C{\equiv}Mo(N[R]Ar)_3]$ was readily sequestered by a cryptand or two crown ether molecules. The isolation and complete characterization of $[K(2.2.2\text{-crypt})][C{\equiv}Mo(N[R]Ar)_3]$ and $[K(benzo\text{-}15\text{-}crown\text{-}5)_2][C{\equiv}Mo(N[R]Ar)_3]$ unambiguously establishes that the $Mo(N[R]Ar)_3$ template will support a one coordinate carbon atom.
- (iv) Terminal carbide complexes feature ^{13}C NMR signals which are dramatically downfield shifted. The metallated carbides $[Li][C{\equiv}Mo(N[R]Ar)_3]$, $[Na][C{\equiv}Mo(N[R]Ar)_3]$, and $[K][C{\equiv}Mo(N[R]Ar)_3]$, as well as the rigorously terminal carbide complexes $[K(2.2.2\text{-crypt})][C{\equiv}Mo(N[R]Ar)_3]$ and $[K(benzo\text{-}15\text{-}crown\text{-}5)_2][C{\equiv}Mo(N[R]Ar)_3]$, exhibit carbido-carbon ^{13}C NMR

signals ranging from ca. 475 to 500 ppm. These downfield shifts for the sp^3 carbido-carbon atom differ markedly from those typically observed in metallated organic analogues, as in lithiated phenlyacetylene PhC≡CLi (δ = 145.5 ppm).[38]

- (v) The complex [K(2.2.2-crypt)][C≡Mo(N[R]Ar)$_3$] undergoes a fast proton-exchange phenomenon with its protonated analogue HC≡Mo(N[R]Ar)$_3$. HC≡Mo(N[R]Ar)$_3$ should be regarded as a very weak acid whose acidity compares well with that of triphenylmethane in THF. An estimated pK_a for triphenylmethane in water is 31.5.[29]

- (vi) Exploratory reactions suggest that the [C≡Mo(N[R]Ar)$_3$]$^-$ provides a convenient starting point for the rational synthesis of novel organometallics. The Mo≡C core has been delivered to C, Si, P, S, Se, and Te.

Delivery of the Mo≡C core to new metal centers is an avenue which remains to be explored. In particular, [C≡Mo(N[R]Ar)$_3$]$^-$ may serve as a C-atom or C$^-$ transfer reagent — should an appropriate acceptor complex be defined. To my knowledge, no simple C-atom transfer reactions have been elucidated.

In closing, under the guidance and imagination of Professor "Kit" Cummins, our research group has elucidated new transformations by which low coordinate transition metal complexes may be delivered to single atoms derived from small molecule sources. This chapter contributes to that effort and adds the one-coordinate carbide ligand to the list of metal to ligand multiple bonds.

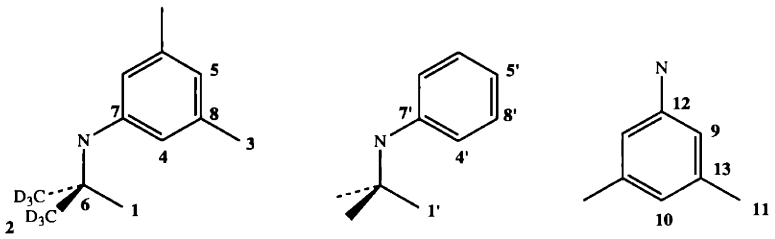

Figure 17: Labeling scheme for ^{1}H and ^{13}C NMR spectra. The positions on the adamantyl substituents have been designated generally as **Ad**.

4 Experimental Section

4.1 General Considerations

Unless stated otherwise, all operations were performed in a Vacuum Atmospheres dry box under an atmosphere of purified nitrogen, or using standard Schlenk techniques under an argon or dinitrogen atmosphere. Anhydrous ether and toluene were purchased from Mallinckrodt; *n*-pentane and *n*-hexane were purchased from EM Science. Ether was purified according to the procedure of Grubbs.[39] Aliphatic hydrocarbon solvents were distilled under a nitrogen atmosphere from very dark blue to purple sodium benzophenone ketyl solubilized with a small quantity of tetraglyme. Distilled solvents were transferred under vacuum into teflon-stopcocked glass vessels and stored, prior to use, in a Vacuum Atmospheres dry box. C_6D_6 was degassed and dried over activated 4 Å molecular sieves and transferred under vacuum into a storage vessel. 4 Å sieves, Celite and alumina were activated *in vacuo* overnight at a temperature above 180 °C. $Mo(N[R]Ar)_3$,[24] and $Ti(N[R]Ar)_3$,[7] were prepared according to published procedures. ^{13}C-labeled carbon monoxide gas was purchased form Cambridge Isotope Laboratories (CIL). $ClSiMe_3$ was degassed and dried over 4Å molecular sieves prior to use. *i*-Pr_2NH and phenylacetylene were dried over 3Åmolecular sieves. Triphenylmethane was dissolved in THF and then passed through a short column of activated alumina prior to use. Other chemicals were purified and dried by standard procedures or were used as received. Infrared spectra were recorded on a Bio-Rad 135 Series FTIR spectrometer. UV-visible spectra were recorded on a Hewlett-Packard 8453 diode-array spectrophotometer. ^{1}H and ^{13}C NMR spectra were recorded on Varian VXR-500, Varian XL-300, or Varian Unity-300 spectrometers. ^{1}H and ^{13}C NMR chemical shifts are reported with reference to solvent resonances (residual C_6D_5H in C_6D_6, 7.15 ppm; C_6D_6, 128.0 ppm; $CHCl_3$ in $CDCl_3$, 7.24 ppm; $CDCl_3$, 77.0 ppm). ^{2}H NMR chemical shifts are reported with respect to external C_6D_6 (7.15 ppm). Solution magnetic susceptibilities were determined by ^{1}H NMR at 300 MHz using the method of Evans.[4,5] Routine coupling constants are not reported. Combustion analyses (C, H, and N) were performed by Microlytics, Southdeerfield MA. X-ray diffraction data were collected on a Siemens Platform goniometer with a Charge Coupled Device (CCD) detector. Structures were typically solved by direct methods (SHELXTL V5.0, G.M Sheldrick and Siemens Industrial Automation, Inc., 1995) unless otherwise noted. Peaks in the ^{1}H and ^{13}C NMR spectra are denoted according to Fig 17.

4.2 Synthesis of (OC)Mo(N[R]Ar)$_3$.

A 250 mL round-bottomed Schlenk flask was charged with a stir bar and Mo(N[R]Ar)$_3$ (2.736g, 4.256 mmol). 60 mL of THF was added to this solid and stirring resulted in a deep orange solution. The flask was evacuated and cooled to -78 °C and then exposed to 500 torr of ^{13}CO gas (2 molar equivalents in total). The reaction vessel was allowed to warm gradually to 22 °C during which time the solution turned a dark brown. After 30 minutes the volatiles were removed, yielding a dark brown solid. A ^{2}H NMR spectrum of this crude material showed no remaining Mo(N[R]Ar)$_3$, and an integrated yield of 90 % of the desired (OC)Mo(N[R]Ar)$_3$. 15 mL of hexamethyldisiloxane was added to the crude solid and the mixture was stirred vigorously. The undissolved material was collected on a sintered glass frit, washed with three 5 mL portions of hexamethyldisiloxane (until the washings were nearly colorless), and recrystallized from OEt_2 yielding 2.41 g (84 %) of a lusterous black solid. This solid was spectroscopically pure. ^{2}H NMR (46 MHz, pentane, 25 °C): δ = 8.0 ppm (s, $\Delta\nu_{1/2}$ = 14 Hz, C(CD$_3$)$_2$CH$_3$). μ_{eff} (300 MHz, 25 °C, C_6D_6): 2.2μ_B. FTIR (heptane, KBr) ν_{CO} = 1797 cm^{-1} (^{13}C≡O), ν_{CO} = 1840 cm^{-1} (^{12}C≡O), in heptane. Anal. Calcd for $C_{37}H_{36}D_{18}N_3OMo$: C, 66.24; H, 8.11; N, 6.26. Found: C, 65.85; H, 8.44; N, 6.19.

4.3 Synthesis of (Ph-[*t*-Bu]N)$_3$Ti(μ-CO)Mo(N[R]Ar)$_3$.

An emerald green solution consisting of 174.6 mg of Ti(N[*t*-Bu]Ph)$_3$ (0.3545 mmol) in 4 mL of OEt_2 chilled to -35 °C was added to a 20 mL scintillation vial containing a chilled and stirring brown solution of Mo(CO)(N[R]Ar)$_3$ in 4 mL OEt_2. An instant color change to bright orange occurred and the solution was allowed to warm to 25 °C after which time it was filtered through celite and pumped dry to a solid orange powder. A ^{1}H NMR spectrum of this crude powder showed a clean transformation to one diamagnetic product displaying resonances for each ligand set in a 1:1 ratio, the amides on Ti being distinguishable from those on Mo. The crude product was extracted into 4 mL OEt_2 and recrystallized at -35 °C to afford 365 mg of a bright orange, semi-crystalline compound (88.5 %) which was analytically pure. ^{1}H NMR (300 MHz, C_6D_6, 45 C): δ = 7.15 (m, 8' and 5'), 6.73 (s, 5), 6.40 (br s, 4), 5.75 (br s, 4'), 2.13 (s, 3), 1.28 (s, 1), 1.26 (s, 1'). ^{13}C NMR (125.66 MHz, $CHCl_3$, 25 °C). δ = 247.5 (Mo≡*C*-O-Ti), 152.73 (aryl), 150.43 (aryl), 136.11 (aryl), 132.47 (aryl), 130.02 (aryl), 127.30 (aryl), 125.02 (aryl), 62.95 (6 or 6'), 61.27 (6 or 6'), 33.06 (2), 30.59 (1'), 21.66 (3) Anal. Calcd for $C_{67}H_{78}D_{18}N_6MoOTi$: C, 69.17; H, 8.32; N, 7.22. Found: C, 68.88; H, 8.20; N, 7.03. Assignment of the carbon atom ligated to Mo in the ^{13}C NMR spectrum noted above was confirmed by the preparation of a sample using enriched ^{13}CO. A ν_{CO} stretch was not observable by infrared spectroscopy (heptane, KBr) despite inspection of a difference spectrum of both ^{13}C-labeled and ^{12}C-labeled samples.

4.4 Synthesis of [Na][(OC)Mo(N[R]Ar)$_3$].

220 mg of sodium metal (9.57 mmol) were cut into small pieces and placed in a 20 mL scintillation vial with 5 of mL OEt_2. 510 mg of (OC)Mo(N[R]Ar)$_3$ (0.7602 mmol) dissolved in 10 mL of THF were added directly to the sodium containing mixture. Stirring was continued at 25 °C for 1.5 h,

during which time the color turned from the deep brown of (OC)Mo(N[R]Ar)$_3$ to yellow-orange. An FTIR spectrum at this time showed that (OC)Mo(N[R]Ar)$_3$ had been completely consumed. The solution was filtered through Celite, dried *in vacuo*, triturated thoroughly with hexane and then washed on a sintered-glass frit with hexamethyldisiloxane to afford 400 mg (76 %) of the solvent-free [Na][(OC)Mo(N[R]Ar)$_3$] as a yellow powder. Microanalysis on solvent-free [Na][(OC)Mo(N[R]Ar)$_3$] was attempted on a powder obtained by lyophilization from frozen benzene solution. Despite several attempts the samples always analyzed low in carbon. Spectroscopically pure samples were readily obtained. ^{1}H NMR (300 MHz, C_6D_6, 25 °C): δ = 6.83 ppm (s, 4), 6.09 (s, 6), 2.22 (s, 3), 1.41 (s, 1): ^{13}C NMR (125.66 MHz, C_6D_6, 25 °C): δ = 243.5 ppm (Mo*C*ONa), 158 (br aryl), 137.2 (aryl), 130.3 (aryl), 124.6 (aryl), 60.0 (6), 33.8 (1, 2), 21.9 (3): FTIR: ν_{CO} (THF, KBr) = 1617 cm^{-1} (for the ^{12}CO derivative. The ^{13}CO exhibits a stretch at 1568 cm^{-1}) Anal. Calcd for $C_{37}H_{36}D_{18}MoN_3NaO$: C, 64.05; H, 7.84; N, 6.06. Found: C, 62.92; H, 8.05; N, 5.63.

4.5 X-ray structure of [Na(OEt$_2$)][(OC)Mo(N[R]Ar)$_3$].

Yellow crystals were grown slowly from an pentane–OEt$_2$ solution at -35 °C. The crystals were quickly moved from a scintillation vial to a microscope slide containing Paratone N (an Exxon product). Under the microscope a yellow plate was selected and mounted on a glass fiber using wax. A total of 18028 reflections were collected ($-12 \leq h \leq 12$, $-21 \leq k \leq 20$, $-15 \leq l \leq 24$) in the θ range of 1.11 to 23.26° of which 12340 were unique ($R_{int} = 0.0319$). The structure was solved by direct methods in conjunction with standard difference Fourier techniques. All non-hydrogen atoms were placed in calculated ($d_{C\text{-}H}$ = 0.96 Å) positions. The largest peak and hole in the difference map were 3.365 and -0.662 e·Å^{-3}, respectively. A semi-empirical absorption correction was applied based on pseudo-ψ-scans with maximum and minimum transmission equal to 0.5520 and 0.4806, respectively. The least squares refinement converged normally with residuals of R (based on F) = 0.0703, wR (based on F^2) = 0.1872, and GOF = 1.184 based upon $I > 2\sigma(I)$. Final refinement included a disordered molecule of OEt$_2$ present in the assymetric unit assigned with the atom labels O(1S),C(2S),C(2S),C(3S),C(2SA),C(2SB),C(3SA). C(2S), C(2S) and C(2SA), C(2SB) were refined at half occupancy. Crystal data for $C_{42}H_{56.50}MoN_3NaO_{2.25}$: triclinic, space group = $P\bar{1}$,z = 4,a = 10.8566(12)Å,b = 19.235(5)Å,c = 22.453(5)Å,α = 79.07(2)°, β = 89.17(2)°, γ = 75.831(12)°, V = 4461(2) Å^3, ρ_{calc} = 1.129 g·cm^{-3}, $F(000)$ = 1602.

Note: The following complexes were prepared from samples containing approximately a 50 % ^{13}C-enrichment at the carbyne-carbon position.

4.6 Synthesis of Me$_3$Si-O-C≡Mo(N[R]Ar)$_3$.

Separate solutions containing 68 mg of [Na][(OC)Mo(N[R]Ar)$_3$] (0.0979 mmol) in 2 mL OEt$_2$ and 19 mg chlorotrimethylsilane (0.175 mmol) in 2 mL OEt$_2$ were pre-chilled to -35 °C. The solutions were mixed and allowed to stir for 2 h at 25 °C during which time a white flocculent precipitated. The yellow mixture was filtered through Celite and the volatiles were removed *in vacuo* to afford a crude residue which showed near quantitative silylation by ^{1}H NMR spectroscopy. Recrystallization from pentane afforded 51 mg (70 %) of crystalline Me$_3$Si-O-C≡Mo(N[R]Ar)$_3$. ^{1}H NMR (300 MHz,

C_6D_6, 25 °C): δ = 6.67 ppm (s, 5), 6.13 (s, 4), 2.13 (s, 3), 1.46 (s, 1), 0.35 (s, SiMe_3): ^{13}C NMR (125.66 MHz, C_6D_6, 25 °C): δ = 218.8 ppm (MoCOSiMe$_3$),152.0 (aryl), 137.2 (aryl), 131.2 (aryl), 127.6 (aryl), 61.1 (6), 34.3 (1, 2), 22.0 (3), 1.87 (SiMe_3): Anal. Calcd for $C_{40}H_{45}D_{18}MoN_3OSi$: C, 64.57; H, 8.53; N, 5.65. Found: C, 66.36; H, 8.65; N, 5.67.

4.7 Synthesis of ^{t}BuC(O)-O-C≡Mo(N[R]Ar)$_3$.

A 1 % sodium amalgam (852 mg Na in 85 g Hg) was prepared in a 250 mL round-bottom flask. THF (100 mL) was added and the mixture was stirred vigorously. Solid black (OC)Mo(N[R]Ar)$_3$ (4.346 g, 6.47 mmol) was added in one portion at 25 °C. After 2 h the reaction mixture turned a bright orange color and was filtered through celite and dried *in vacuo*. The resulting residue was extracted into OEt_2 (100 mL) and cooled to -35 °C. Pivalyl chloride (780 mg, 6.47 mmol) was added at once to the chilled solution, which was subsequently allowed to warm to 25 °C and stirred for 16 h, at which point the color had settled to a light brown. Removal of volatiles *in vacuo* yielded a solid which was extracted into pentane (50 mL), filtered through Celite to remove salts, and stored at -35 °C, affording 4.03 g (several crops, 82 %) of beige, crystalline ^{t}BuC(O)-O-C≡Mo(N[R]Ar)$_3$. ^{1}H NMR (300 MHz, C_6D_6, 25 °C): δ = 6.67 ppm (s, 5), 6.09 (s, 4), 2.10 (s, 3), 1.50 (s, 1), 1.22 (s, C(CH_3)$_3$): ^{13}C NMR (125.66 MHz, C_6D_6, 25 °C): δ = 217.15 ppm (Mo≡COC(O)C(CH$_3$)$_3$, 173.7 (Mo(COC(O)C(CH$_3$)$_3$, 150.74 (aryl), 137.38 (aryl), 131.32 (aryl), 130.98 (aryl), 61.55 (6), 38.9 (Mo(COC(O)C(CH$_3$)$_3$, 33.84 (1, 2), 27.32 (Mo(COC(O)C(CH$_3$)$_3$, 21.88 (3): Anal. Calcd for $C_{42}H_{45}D_{18}MoN_3O_2$: C, 66.73; H, 8.40; N, 5.56. Found: C, 66.64; H, 8.24; N, 5.79.

4.8 X-ray structure of ^{t}BuC(O)-O-C≡Mo(N[R]Ar)$_3$.

Beige crystals were grown slowly from a pentane solution at -35 °C. The crystals were quickly moved from a scintillation vial to a microscope slide containing Paratone N (an Exxon product). Under the microscope a beige plate was selected and mounted on a glass fiber using wax. A total of 11877 reflections were collected ($-11 \leq h \leq 15$, $-20 \leq k \leq 21$, $-16 \leq l \leq 16$) in the θ range of 1.71 to 20.00° of which 3910 were unique (R_{int} = 0.0834). The structure was solved by direct methods in conjunction with standard difference Fourier techniques. All non-hydrogen atoms were placed in calculated ($d_{C\text{-}H}$ = 0.96 Å) positions. The largest peak and hole in the difference map were 1.201 and -0.601 e·Å^{-3}, respectively. No absorption correction was applied. The structure was refined isotropically for all atoms except Mo. R (based on F) = 0.0848, wR (based on F^2) = 0.2182, and GOF = 1.100 based upon $I > 2\sigma(I)$. Crystal data for $C_{42}H_{63}MoN_3O_2$: orthorhombic, space group = Pna2$_1$, z = 4, a = 14.198(8) Å, b = 19.721(8) Å, c = 14.995(7) Å, α = 90°, β = 90°, γ = 90°, V = 4199(4) Å^3, ρ_{calc} = 1.167 g·cm^{-3}, F(000) = 1576.

4.9 Synthesis of HC≡Mo(N[R]Ar)$_3$.

Solid sodium metal (353 mg, 15.35 mmol) was added to a 50 mL RB-flask and smeared along the walls so as to expose a large amount of clean metal surface. THF (25 mL) was then added to the flask, followed by 5 minutes of vigorous stirring at 25 °C. Solid beige ^{t}BuC(O)-O-C≡Mo(N[R]Ar)$_3$

(2.01g , 2.66 mmol) was then added at once and the reaction mixture was stirred vigorously for 3 hours, gradually turning dark orange. The volatiles were removed *in vacuo* and pentane (40 mL) was added to the resulting residue to extract the soluble products. This dark orange solution was filtered through Celite, concentrated to 10 mL, and quenched with acetonitrile (2.4 g, 61.5 mmol), which was added to the cold solution (chilled naturally by solvent evaporation). The mixture was allowed to warm gradually to 25 °C, followed by complete solvent removal *in vacuo*. A light orange solid remained and was collected on a sintered glass frit and washed thoroughly with acetonitrile until the washings were nearly colorless (4 X 5 mL). The insoluble beige powder which remained on the frit was recrystallized from OEt_2, affording 1.13 g (53 %) of analytically pure HC≡Mo(N[R]-Ar)$_3$. ^{1}H NMR (300 MHz, C_6D_6, 25 °C): δ = 6.64 ppm (s, 5), 6.00 (s, 4), 5.66 (d, Mo≡C*H*), $^1J_{CH}$ = 157 Hz) 2.07 (s, 3), 1.49 (s, 1). ^{13}C NMR (125.66 MHz, C_6D_6, 25 °C: δ = 287.5 ppm (Mo≡*C*H), 150.8 (aryl), 137.4 (aryl), 130.7 (aryl), 128.0 (aryl), 60.0 (6), 34.2 (1, 2), 21.8 (3). Anal. Calcd for $C_{37}H_{37}D_{18}N_3Mo$: C, 67.75; H, 8.45; N, 6.41. Found: C, 67.61; H, 8.29; N, 6.72.

4.10 Synthesis of [Li][C≡Mo(N[R]Ar)$_3$].

In a 20 mL scintillation vial 66.8 mg of HC≡Mo(N[R]Ar)$_3$ (0.1019 mmol) were dissolved in 2 mL of benzene. To this solution was added 3 mL of a 2:1 benzene–OEt_2 slurry of 6.9 mg *tert*-butyllithium. The solution was stirred for 3 h without a dramatic color change. The reaction volatiles were removed thoroughly *in vacuo* and the remaining light tan solid was extracted into 8 mL of pentane, filtered through Celite, and subsequently concentrated to 3 mL, initiating precipitation of a tan solid. The vial was stored at -35 °C for several hours and subsequent decanting of the supernatant afforded 42 mg (62 %) of a semi-crystalline, solvent-free [Li][C≡Mo(N[R]Ar)$_3$]. An independent experiment carried-out in C_6D_6 showed that [Li][C≡Mo(N[R]Ar)$_3$] formed virtually quantitatively and that isobutane was produced (0.85 ppm by ^{1}H NMR spectroscopy). Neopentyllithium effected a similarly clean conversion of HC≡Mo(N[R]Ar)$_3$ to [Li][C≡Mo(N[R]Ar)$_3$]. ^{1}H NMR (300 MHz, C_6D_6, 25 °C): δ = 6.69 ppm (s, 4), 6.63 (s, 5), 2.23(s, 3), 1.49 (s, 1). ^{13}C NMR (125.66 MHz, C_6D_6, 25 °C): δ = 470.1 ppm (sh s, Mo≡*C*Li). Anal. Calcd for $C_{37}H_{36}D_{18}N_3LiMo$: C, 67.15; H, 8.22; N, 6.35. Found: C, 67.65; H, 8.38; N, 6.50.

4.11 Synthesis of [K][C≡Mo(N[R]Ar)$_3$].

In a 20 mL scintillation vial equipped with a stir bar HC≡Mo(N[R]Ar)$_3$ (764.5 mg, 1.164 mmol) was dissolved in THF (8 mL) and cooled to -78 °C. While stirring, benzyl potassium (151.6 mg, 1.164 mmol) was added at once as an orange solid and reacted quickly on warming. The solution was stirred for 15 minutes, allowing it to reach room temperature, followed by removal of volatiles *in vacuo*. The resulting yellow solid was collected on a sintered frit and washed well with pentane to remove any remaining HC≡Mo(N[R]Ar)$_3$. The powder left behind was spectroscopically pure [K][C≡Mo(N[R]Ar)$_3$] (557 mg, 69 %). It was recrystallized by stirring in pentane and then adding THF dropwise until the material had just dissolved. Storing such a solution at -35 °C produced crystals which were appropriate for an X-ray diffraction study. ^{1}H NMR (300 MHz, C_6D_6, 25 °C): δ = 6.86 ppm (s, 4), 6.60 (s, 5), 2.22 (s, 3), 1.48 (s, 1). ^{1}H NMR (300 MHz, THF-d_8, 25 °C): δ = 6.38 ppm (sh s, 5), 6.25 (v br s, 4), 2.04 (sh s, 13), 1.31 (s (br, 1) ^{13}C NMR (125.66 MHz,

THF-d_8, 25 °C): δ = 502.3 ppm (br, Mo≡*C*K), 489.8 (br, Mo≡*C*K), 160 (br, aryl), 135.9 (aryl), 130.1 (aryl), 124.0 (aryl), 58.4 (6), 34.4 (1, 2), 21.8 (3). Anal. Calcd for $C_{37}H_{36}D_{18}N_3KMo$: C, 64.04; H, 7.84; N, 6.05. Found: C, 64.71; H, 7.59; N, 5.85.

4.12 X-ray structure of [K][C≡Mo(N[R]Ar)$_3$].

Yellow crystals were grown slowly from an OEt_2-pentane solution at -35 °C. The crystals were quickly moved from a scintillation vial to a microscope slide containing Paratone N (an Exxon product). Under the microscope a yellow plate was selected and mounted on a glass fiber using wax. An instrument failure caused prevented collection of a complete data set. The data collected was sufficient to solve the structure. A total of 1588 reflections were collected ($-7 \leq h \leq 8$, $-3 \leq k \leq 15$, $-2 \leq l \leq 20$) in the θ range of 2.56 to 23.31° of which 1518 were unique (R_{int} = 0.0370). The structure was solved by direct methods in conjunction with standard difference Fourier techniques. All non-hydrogen atoms were placed in calculated ($d_{C\text{-}H}$ = 0.96 Å) positions. The largest peak and hole in the difference map were 0.284 and -0.323 e·Å^{-3}, respectively. No absorption correction was applied. The structure was refined isotropically. R (based on F) = 0.0693, wR (based on F^2) = 0.1462, and GOF = 1.133 based upon $I > 2\sigma(I)$. Crystal data for $C_{37}H_{54}KMoN_3$: monoclinic, space group = $P2_1/c$, z = 4, a = 12.969(5) Å, b = 14.125(6) Å, c = 20.176(9) Å, α = 90°, β = 103.50(4)°, γ = 90°, V = 3594(3) Å^3, ρ_{calc} = 1.249 g·cm^{-3}, $F(000)$ = 1432.

4.13 Synthesis of [K(2,2,2-crypt)][C≡Mo(N[R]Ar)$_3$].

[K][C≡Mo(N[R]Ar)$_3$] (35.5 mg, 0.0512 mmol) was dissolved in THF (3 mL) to make a yellow solution. Solid white 2.2.2-cryptand (purchased as 2.2.2-Kryptofix from Aldrich), which had been previously dried by running a THF solution through a column of activated alumina, was added to the stirring solution at 25 °C. The solution remained yellow and was dried *in vacuo* after 10 minutes. The yellow solid which remained was insoluble in hydrocarbon, benzene, and OEt_2. Spectroscopic analysis in THF-d_8 confirmed a clean conversion to the salt [K(2,2,2-crypt)][C≡Mo(N[R]Ar)$_3$]. In THF-d_8, the anilido ligand resonances display much narrower linewidths at 25 °C in comparison to the precursor [K][C≡Mo(N[R]Ar)$_3$], consistent with formation of a discrete, monomeric salt in solution. The yellow material was easily recrystallized from a pentane–THF mixture and X-ray quality crystals were obtained, *albeit with difficulty*, from such a solution stored at -35 °C for several hours. ^{1}H NMR (300 MHz, THF-d_8, 25 °C): δ = 6.26 ppm (s, 5), 5.71 (v br s, 4), 3.58 (m, crypt), 3.53 (m, crypt), 2.53 (m, crypt), 1.92 (s, 3), 1.50 (s, 1) ^{13}C NMR (125.66 MHz, THF-d_8, 25 °C): δ = 482.8 ppm (s, Mo≡*C*), 157.7 (br, aryl), 135.4 (aryl), 129.5 (aryl), 123.9 (aryl), 71.5 (crypt), 68.8 (crypt), 58.7 (crypt), 57.9 (crypt), 55.2 (6), 35.4 (1, 2), 21.9 (3). Anal. Calcd for $C_{55}H_{72}D_{18}N_5O_6KMo$: C, 61.71 ; H, 8.47; N, 6.54. Found: C, 61.28; H, 8.21; N, 6.56.

4.14 ^{13}C NMR spectra of [K(2,2,2-crypt)][C≡Mo(N[R]Ar)$_3$].

A sample of yellow [K(2,2,2-crypt)][C≡Mo(N[R]Ar)$_3$] (35 mg, 0.0327 mmol) was dissolved in 0.8 mL of THF-d_8 (taken directly from a sealed ampule purchased from the Cambridge Isotope Laboratories) in an NMR tube under N_2 which was subsequently flame-sealed. ^{13}C NMR data were collected at temperatures ranging from +60 °C to -90 °C. A broad resonance centered ca. 485 ppm was observed at ambient temperature ($\Delta\nu_{1/2}$ = 1400 Hz at 25 °C) which broadened further upon warming. This resonance sharpened dramatically and shifted downfield as the temperature was lowered (ca. 500 ppm at -90 °C). The solution was recovered from the NMR tube and doped with 4 mg of HC≡Mo(N[R]Ar)$_3$ (0.0061 mmol). A ^{13}C NMR spectrum acquired of this mixture at 25 °C showed no resonances downfield of 150 ppm assignable to a ^{13}C≡Mo carbon atom, indicative of a fast proton exchange phenomenon.

An analogous sample of 54.1 mg [K(2,2,2-crypt)][C≡Mo(N[R]Ar)$_3$] was prepared in 0.8 mL of THF-d_8 which had been pre-dried by passing it through a short column of activated alumina, so as to minimize the presence of HC≡Mo(N[R]Ar)$_3$ impurity in the freshly prepared sample. A ^{13}C NMR spectrum of this solution showed an appreciably sharpened resonance compared to the sample in which the THF was not pre-dried over alumina ($\Delta\nu_{1/2}$ = 180 Hz at 25 °C). Furthermore, the addition of a small amount (ca. 4 mg) of benzylpotassium to this moderately "wet" solution of freshly dissolved [K(2,2,2-crypt)][C≡Mo(N[R]Ar)$_3$] effected a further sharpening of the ^{13}C≡Mo carbon atom resonance ($\Delta\nu_{1/2}$ = 53 Hz).

4.15 Synthesis of [K(benzo-15-crown-5)$_2$][C≡Mo(N[R]Ar)$_3$].

[K][C≡Mo(N[R]Ar)$_3$] (30.2 mg, 0.0435 mmol) was dissolved in THF (3 mL) to make a yellow solution. Solid white benzo-15-crown-5 (29.2 mg, 0.1088 mmol), which had been previously dried by passing a THF solution of it through a column of activated alumina, was added to the stirring solution at 25 °C. The solution remained yellow and was dried *in vacuo* after 10 minutes. The yellow solid which remained was insoluble in hydrocarbon, benzene, and ether. Spectroscopic analysis in THF-d_8 confirmed a clean conversion to the salt [K(benzo-15-crown-5)$_2$][C≡Mo(N[R]Ar)$_3$]. In THF-d_8, the anilido ligand resonances displayed much narrower linewidths at 25 °C by comparison to the precursor [K][C≡Mo(N[R]Ar)$_3$], consistent with formation of a discrete, monomeric salt in solution. The yellow material was easily recrystallized from a pentane–THF mixture and X-ray quality crystals were obtained from such a solution stored at -35 °C for several hours. ^{1}H NMR (300 MHz, THF-d_8, 25 °C): δ = 6.85 ppm (m, crown aryl), 6.60 (s, 5), 5.81(br s, 4), 5.5–4.1 (m, crown methylene), 2.06 (s, 3), 1.36 (s, 1). ^{13}C NMR (125.66 MHz, THF-d_8, 25 °C): δ = 502.8 (br, Mo≡C), 148.8 (aryl), 134.9 (aryl), 129.0 (aryl), 123.1 (aryl), 121.5 (aryl), 114.0 (aryl), 69.8 (crown), 69.2 (crown), 65.7 (6), 34.4 (1, 2), 21.0 (3). Anal. Calcd for $C_{65}H_{52}D_{18}KMoN_3O_{10}$: C, 63.44; H, 7.70; N, 3.42. Found: C, 62.83; H, 7.72; N, 3.36.

4.16 X-ray structure of [K(benzo-15-crown-5)$_2$][C≡Mo(N[R]Ar)$_3$].

Yellow crystals were grown slowly from a THF–pentane solution at -35 °C. The crystals were quickly moved from a scintillation vial to a microscope slide containing Paratone N (an Exxon product). Under the microscope a yellow plate was selected and mounted on a glass fiber using wax. A total of 23272 reflections were collected ($-15 \leq h \leq 15$, $-32 \leq k \leq 35$, $-12 \leq l \leq 19$) in the θ range of 1.28 to 20.00° of which 7288 were unique ($R_{int} = 0.0694$). The structure was solved by direct methods in conjunction with standard difference Fourier techniques. All non-hydrogen atoms were placed in calculated ($d_{C\text{-}H} = 0.96$ Å) positions. The largest peak and hole in the difference map were 0.419 and -0.794 e·Å^{-3}, respectively. No absorption correction was applied. The least squares refinement converged normally with residuals of R (based on F) = 0.0829, wR (based on F^2) = 0.1650, and GOF = 1.083 based upon $I > 2\sigma(I)$. Crystal data for $C_{65}H_{94}KMoN_3O_{10}$: monoclinic, space group = $P2_1/n$, $z = 4$, $a = 14.094(4)$ Å, $b = 31.815(8)$ Å, $c = 17.589(7)$ Å, $\alpha = 90°$, $\beta = 97.60(2)°$, $\gamma = 90°$, $V = 7818(4)$ Å^3, $\rho_{calc} = 1.030$ g·cm^{-3}, $F(000) = 2584$.

4.17 [K][C≡Mo(N[R]Ar)$_3$] + *i*-Pr$_2$NH.

The THF solvent used in this experiment was pre-dried as described above and passed through a short column of activated alumina just prior to usage. A solution of *i*-Pr$_2$NH (2.9 mg, 0.0287 mmol) in 1.5 mL of THF was added to a yellow stirring solution of [K][C≡Mo(N[R]Ar)$_3$] (19.4 mg, 0.0280 mmol) in 1.5 mL of THF at 25 °C. After 25 minutes ^{1}H NMR spectroscopy (C_6D_6) showed that no reaction had occurred. An additional 15 mg of *i*-Pr$_2$NH (0.1512 mmol) was then added to this sample directly. After 16 h ^{13}C NMR spectroscopy showed that HC≡Mo(N[R]Ar)$_3$ was present in significant quantity. A control sample of [K][C≡Mo(N[R]Ar)$_3$] stored in the same THF solvent over a 16 h period showed no HC≡Mo(N[R]Ar)$_3$ by ^{13}C NMR spectroscopy. In a separate experiment [K][C≡Mo(N[R]Ar)$_3$] (18.6 mg, 0.0268 mmol) and 5 eq of *i*-Pr$_2$NH were heated in 1 mL of THF at 50 °C for 72 h. ^{1}H and ^{13}C NMR spectroscopy showed that the solution contained 77 % [K][C≡Mo(N[R]Ar)$_3$] and 23 % HC≡Mo(N[R]Ar)$_3$ after this time period.

4.18 [K][C≡Mo(N[R]Ar)$_3$] + Toluene in THF

The THF solvent used in this experiment was pre-dried as described above and passed through a short column of activated alumina just prior to usage. [K][C≡Mo(N[R]Ar)$_3$] (0.0135 mg, 0.0195 mmol) was dissolved in a toluene–THF mixture (566 mg toluene and 100 mg THF) and stored in a 20 mL scintillation vial covered with tape so as to exclude light. After 48 h the yellow solution had turned beige. There was a small amount of white flocculent noticeable. ^{1}H and ^{13}C NMR spectroscopy (C_6D_6) showed HC≡Mo(N[R]Ar)$_3$ to be the only species detectable after this time period.

4.19 $[K][C{\equiv}Mo(N[R]Ar)_3]$ + PH_3CH in THF.

The THF solvent used in this experiment was pre-dried as described above and passed through a short column of activated alumina just prior to usage. Addition of 6.5 mg of a THF solution of PH_3CH (0.0266 mmol) to a yellow solution of 18.5 mg $[K][C{\equiv}Mo(N[R]Ar)_3]$ (0.0267 mmol) in THF resulted in a rapid color change to bright orange. The volatiles were removed after 20 minutes and spectroscopic analysis (^1H and ^{13}C NMR, C_6D_6) of the crude residue showed a mixture of $[K][C{\equiv}Mo(N[R]Ar)_3]$ (90 %) and $HC{\equiv}Mo(N[R]Ar)_3$ (10 %).

4.20 $HC{\equiv}Mo(N[R]Ar)_3$ + PH_3CK.

The THF solvent used in this experiment was pre-dried as described above and passed through a short column of activated alumina just prior to usage. A solution of PH_3CK was prepared by addition of 6.4 mg of PH_3CH (0.262 mmol) to a THF solution (1.0 mL) of benzylpotassium (3.4 mg, 0.262 mmol). The resuting solution was orange in color. A solution of 12.4 mg of $HC{\equiv}Mo(N[R]Ar)_3$ (0.0189 mmol) in 0.8 mL THF was then added to this orange solution at 25 °C. After 36 h the solution remained orange, albeit somewhat lighter in color. ^1H and ^{13}C NMR spectroscopy (C_6D_6) showed that 15 % $[K][C{\equiv}Mo(N[R]Ar)_3]$ and 85 % $HC{\equiv}Mo(N[R]Ar)_3$ were present at this time. *In a separate experiment:* A solution containing Ph_3CK was generated by mixing Ph_3CH (60.2 mg, 0.2474 mmol) and benzylpotassium (22 mg, 0.1670 mmol) in 4.104 g of THF. $HC{\equiv}Mo(N[R]Ar)_3$ (50 mg, 0.0762 mmol) was then dissolved in 1.889 g of the THF solution, i.e. in the appropriate amount of solution to expose the $HC{\equiv}Mo(N[R]Ar)_3$ to one molar equivalent of Ph_3CK. The solution turned from a rather intense orange to a lighter orange quickly upon dissolution of $HC{\equiv}Mo(N[R]Ar)_3$. After 20 minutes an aliquot was removed, thoroughly dried *in vacuo*, and triturated with hexane. Extraction of the resulting solid with C_6D_6 and subsequent spectroscopic analysis (^1H and ^{13}C NMR) showed $[K][C{\equiv}Mo(N[R]Ar)_3]$ and $HC{\equiv}Mo(N[R]Ar)_3$ to be present in approximately a 2:1 ration. A large amount of triphenylmethane was also present. The remaining THF solution was analyzed after a 24 h period and showed analogous spectra, indicating the reaction was complete withing the first 20 minutes.

4.21 $[K][C{\equiv}Mo(N[R]Ar)_3]$ + $PhC{\equiv}CH$ in THF.

The THF solvent used in this experiment was pre-dried as described above and passed through a short column of activated alumina just prior to usage. A solution containing 7.3 mg of phenylacetylene (0.0715 mmol) in 0.8 mL of THF was added to a solution containing 16 mg $[K][C{\equiv}Mo(N[R]Ar)_3]$ (0.0231 mmol) in 1 mL of THF at 25 °C. The initially yellow solution turned viscous and colorless instantaneously. The volatiles were removed and ^1H and ^{13}C NMR spectroscopy (C_6D_6) showed that $HC{\equiv}Mo(N[R]Ar)_3$ had been generated quantitatively.

4.22 Synthesis of $(Ar[R]N)_3Mo{\equiv}C\text{-}S\text{-}S\text{-}C{\equiv}Mo(N[R]Ar)_3$.

$[K][C{\equiv}Mo(N[R]Ar)_3]$ (287 mg, 0.4136 mmol) was partially dissolved in OEt_2 (10mL) and chilled to -35 °C. Yellow elemental sulfur (78mg, 2.432 mmol) was added in one portion as a solid, and the resulting heterogeneous mixture was allowed to warm to 25 °C. The reaction mixture, which had turned orange shortly after the reagents were mixed, was filtered through a medium porosity sintered glass frit after 35 minutes, removing a dark orange, caked solid to afford a bright orange filtrate. The caked solid was washed with 4 mL of a 1:1 pentane–toluene solution. Chilling the orange filtrate overnight at -35 °C gave an orange precipitate whose spectroscopic, chemical, and solubility properties were consistent with the neutral disulfide-bridged complex. *Notably, the orange solid was pentane soluble and did not react with chlorotrimethylsilane nor with benzo-15-crown-5.* ^{1}H NMR (300 MHz, C_6D_6, 25 °C): δ = 6.67 ppm (s, 5), 6.02 (v br s, 4), 2.08 (s, 3), 1.62 (s, 1). ^{13}CNMR (125.66 MHz, C_6D_6, 25 °C): δ = 253.8 ppm (s, Mo≡*C*-S), 150.7 (aryl), 137.5 (aryl), 130.9 (aryl), 62.77 (6), 34.23 (1, 2), 21.85 (3). Satisfactory microanalysis was not obtained for this complex despite several attempts. However, $(Ar[R]N)_3Mo{\equiv}C\text{-}S\text{-}S\text{-}C{\equiv}Mo(N[R]Ar)_3$ was easily converted to the desirable anionic complex $[Na][S\text{-}C{\equiv}Mo(N[R]Ar)_3]$by stirring a THF solution of $(Ar[R]N)_3Mo{\equiv}C\text{-}S\text{-}S\text{-}C{\equiv}Mo(N[R]Ar)_3$ over Na/Hg (*vide infra*).

4.23 Synthesis of $[Na][S\text{-}C{\equiv}Mo(N[R]Ar)_3]$and $[Na(benzo\text{-}12\text{-}crown\text{-}4)_2][S\text{-}C{\equiv}Mo(N[R]Ar)_3]$.

Yellow [K][**8**] (149 mg mg, 0.2147 mmol) was stirred in 8 mL of an OEt_2-benzene mixture (3:1) and chilled to -35 °C. Solid S_8 (40.5 mg, 1.26 mmol) was then added to the vigorously stirring solution at once. After 2 h the solution was filtered through Celite to remove a brown cake-like residue, dried, and then transferred to a 20 mL scintillation vial containing a 0.4 % Na/Hg amalgam (13.5 mg Na in 2.7 g Hg) and 5 mL of THF. The initially orange mixture turned light yellow within 30 minutes and after 1.5 h was filtered through Celite and dried to a solid. Spectroscopic data for this crude mixture were consistent with the clean formation of diamagnetic $[Na(THF)_x][S\text{-}C{\equiv}Mo(N[R]Ar)_3]$. ^{1}H NMR (300 MHz, C_6D_6, 25 °C): δ = 6.68 ppm (s, 5), 6.20 (br s, 4), 3.65 (m, THF), 2.19 (s, 3), 1.73 (s, 1), 1.44 (m, THF). ^{13}C NMR (125.66 MHz, C_6D_6, 25 °C): δ = 292.4 ppm (sh s, Mo≡*C*S), 153.7 (aryl), 135.7 (aryl), 130.0 (aryl), 125.2 (aryl), 61.3 (6), 33.9 (1, 2), 21.0 (3). The crude yellow solid was dissolved in 6 mL of a 1:1 OEt_2–benzene solution to which benzo-12-crown-4 (96.3 mg, 0.429 mmol) was added as a solid. A yellow salt precipitated from solution which was collected and recrystallized from 10 mL of a 3:2 pentane–THF mixture to give 139 mg (56 %) of crystalline $[Na(benzo\text{-}12\text{-}crown\text{-}4)_2][S\text{-}C{\equiv}Mo(N[R]Ar)_3]$. Microanalysis was obtained for this discrete salt. Anal. Calcd for $C_{61}H_{68}D_{18}MoN_3NaO_8S$: C, 63.24; H, 7.48; N, 3.63. Found: C, 63.61; H, 7.39; N, 3.60.

4.24 Synthesis of $[K][Se\text{-}C{\equiv}Mo(N[R]Ar)_3]$.

Yellow $[K][C{\equiv}Mo(N[R]Ar)_3]$ (190 mg, 0.274 mmol) was dissolved in 5 mL of a 10:1 OEt_2–THF mixture and chilled to -35 °C. Elemental selenium (105 mg, 1.329 mmol) was added at once as

a solid and the heterogeneous mixture was allowed to warm to 25 °C. Within 20 minutes a light flocculent had begun to precipitate from the solution. Stirring was continued for a total of 2 hours, after which time the solvent was removed *in vacuo*. The resulting yellow residue was washed thoroughly three times with 5 mL of pentane in order to remove HC≡Mo(N[R]Ar)$_3$, which was a significant reaction byproduct. The resulting yellow solid obtained was dried, then extracted with 7 mL of benzene, and filtered through Celite. Lyophilization of the frozen filtrate gave 118 mg (ca. 56 %) of spectroscopically pure [K][Se-C≡Mo(N[R]Ar)$_3$]. The material was easily recrystallized from a pentane–OEt_2 mixture. ^{1}H NMR (300 MHz, C_6D_6, 25 °C): δ = 6.73 ppm (s, 5), 6.17 (v br s, 4), 2.22 (s, 3), 1.83 (s, 1). ^{13}C NMR (125.66 MHz, C_6D_6, 25 °C): δ = 271.9 ppm (s, Mo≡*C*Se), 152.7 (aryl), 137.2 (aryl), 130.7 (aryl), 127.2 (aryl), 62.5 (6), 34.9 (1, 2), 22.1 (3). Anal. Calcd for $C_{37}H_{36}D_{18}KMoN_3Se$: C, 57.50; H, 7.04; N, 5.44. Found: C, 58.53; H, 7.29; N, 4.95.

4.25 Synthesis of [K(benzo-15-crown-5)$_2$][Se-C≡Mo(N[R]Ar)$_3$].

A yellow solution of [K][Se-C≡Mo(N[R]Ar)$_3$] (17.6 mg, 0.0228 mmol) in 2.5 mL of a 4:1 mixture of OEt_2–THF was added to a stirring solution of benzo-15-crown-5 (15.3 mg, 0.0570 mmol) in 2 mL of OEt_2. After 5 minutes the volatiles were removed *in vacuo* and upon addition of 2 mL of pure OEt_2 a yellow solid precipitated immediately. The supernatant was decanted and the solid was washed further with a 1:1 pentane–OEt_2 mixture (2 x 4 mL). Subsequent drying afforded 21 mg (ca. 70 %) of the discrete salt [K(benzo-15-crown-5)$_2$][Se-C≡Mo(N[R]Ar)$_3$]. Anal. Calcd for $C_{65}H_{76}D_{18}KMoN_3O_{10}Se$: C, 59.62; H, 7.23; N, 3.21. Found: C, 59.71; H, 7.18; N, 3.17.

4.26 X-ray structure of [K(benzo-15-crown-5)$_2$][Se-C≡Mo(N[R]Ar)$_3$].

Yellow crystals were grown slowly from a THF–pentane solution at -35 °C. The crystals were quickly moved from a scintillation vial to a microscope slide containing Paratone N (an Exxon product). Under the microscope a yellow plate was selected and mounted on a glass fiber using wax. A total of 38225 reflections were collected ($-21 \leq h \leq 14$, $-18 \leq k \leq 20$, $-34 \leq l \leq 43$) in the θ range of 1.49 to 20.00° of which 6337 were unique (R_{int} = 0.1077). The structure was solved by direct methods in conjunction with standard difference Fourier techniques. All non-hydrogen atoms were placed in calculated ($d_{C\text{-}H}$ = 0.96 Å) positions. The largest peak and hole in the difference map were 0.357 and -0.504 e·Å^{-3}, respectively. No absorption correction was applied. The least squares refinement converged normally with residuals of R (based on F) = 0.1044, wR (based on F^2) = 0.1878, and GOF = 1.548 based upon $I > 2\sigma(I)$. Crystal data for $C_{65}H_{93}KMoN_3O_{10}Se$: orthorhombic, space group = P*bca*, z = 8, a = 18.9868(7) Å, b = 18.1144(6) Å, c = 39.4714(14) Å, $\alpha = 90°$, $\beta = 90°$, $\gamma = 90°$, V = 13575.6(8) Å^3, ρ_{calc} = 1.263 g·cm^{-3}, $F(000)$ = 5432.

4.27 Synthesis of [K][Te-C≡Mo(N[R]Ar)$_3$].

Solid [K][C≡Mo(N[R]Ar)$_3$] (141.5 mg, 0.204 mmol) and elemental tellurium (45 mg, 0.353 mmol) were weighed into a 20 mL scintillation vial equipped with a stir bar. Approximately 5 mL of a 10:1 mixture of OEt_2–THF was added to the vial at -35 °C, and the heterogeneous mixture which

resulted was stirred vigorously for 14 hours at 25 °C. By this time the reaction mixture had turned to a yellow-brown color. The volatiles were removed *in vacuo* and the crude residue was extracted with 20 mL of pentane and filtered through a fine sintered glass frit, affording a yellow-brown filtrate and a yellow solid (somewhat discolored by the excess tellurium powder remaining on the frit). The yellow powder was spectroscopically pure [K][Te-C≡Mo(N[R]Ar)$_3$] and the filtrate contained a mixture of both HC≡Mo(N[R]Ar)$_3$ and the [K][Te-C≡Mo(N[R]Ar)$_3$] (^{1}H and ^{13}C NMR). Drying the filtrate *in vacuo* followed by re-extraction with 5 mL of pentane afforded, on standing at 25 °C, a second crop of yellow [K][Te-C≡Mo(N[R]Ar)$_3$]. This crop was combined with the main crop and the combined crude solids were extracted into 5 mL of benzene and filtered in order to remove residual tellurium powder. The yellow benzene filtrate was frozen and lyophilized to a constant weight of 78 mg (ca. 46%) of analytically and spectroscopically pure [K][Te-C≡Mo(N[R]Ar)$_3$]This material was easily recrystallized from a pentane–THF mixture. ^{1}H NMR (300 MHz, C_6D_6, 25 °C): δ = 6.73 ppm (s, 5), 6.16 (v br s, 4), 2.20 (s, 3), 1.84 (s, 1) ^{13}C NMR (125.66 MHz, C_6D_6, 25 °C): δ = 252.6 (s, Mo≡*C*Te), 152.6 (aryl), 137.2 (aryl), 130.7 (aryl), 127.3 (aryl), 68.2 (6), 34.7 (1, 2), 22.0 (3). Anal. Calcd for $C_{37}H_{36}D_{18}KMoN_3Te$: C, 54.09; H, 6.63; N, 5.11. Found: C, 54.44; H, 6.78; N, 4.99.

4.28 Generation of Me$_3$Si-C≡Mo(N[R]Ar)$_3$.

Yellow [K][C≡Mo(N[R]Ar)$_3$] (66.3 mg, 0.0955 mmol) was chilled to -35 °C in 3 mL of OEt$_2$. While stirring this slurry, ClSiMe$_3$ (18.0 mg, 0.248 mmol) was added to it as a chilled solution in 1 mL of OEt$_2$. The reaction mixture went homogeneous and turned to a slightly darker yellow-orange rapidly. The mixture was stirred for 30 minutes, after which time it was filtered through Celite and dried *in vacuo*. Extraction into C_6D_6 and spectroscopic analysis showed that two products, Me$_3$Si-C≡Mo(N[R]Ar)$_3$ and HC≡Mo(N[R]Ar)$_3$, had been formed in a 3:2 ratio, respectively. Spectroscopic data for Me$_3$Si-C≡Mo(N[R]Ar)$_3$: ^{1}H NMR (300 MHz, C_6D_6, 25 °C): δ = 6.66 ppm (s, 5), 5.90 (br s, 4), 2.10 (s, 3), 1.48 (s, 1), 0.54 (br s, Si*Me*$_3$). ^{13}CNMR (125.66 MHz, C_6D_6, 25 °C): δ = 345.6 ppm (s, Mo≡*C*-Si), 151.7 (aryl), 137.1 (aryl), 130.8 (aryl), 127.8 (aryl), 60.3 (6), 34.2 (1, 2), 21.9 (3). An effective means of separating Me$_3$Si-C≡Mo(N[R]Ar)$_3$ from HC≡Mo(N[R]Ar)$_3$ was not found.

4.29 Synthesis of Cl$_2$PC≡Mo(N[R]Ar)$_3$.

A cold solution of PCl$_3$ (89.1 mg, 0.6493 mmol) in 2 mL of OEt$_2$ was added to a cold, stirring yellow slurry of [K][C≡Mo(N[R]Ar)$_3$](450.5 mg, 0.6493 mmol) in 15 mL of OEt$_2$. A solid flocculent precipitated immediately and the solution color turned to a much darker yellow rapidly. Stirring was continued for one hour, after which time the mixture was filtered through Celite and dried *in vacuo*. The resulting brown–yellow residue was stirred vigorously in 4 mL of pentane, and then allowed to settle at -35 °C for several hours. A yellow solid settled out of the solution and was collected on a sintered glass frit. This solid was washed with pentane until the washings were colorless. This first crop was then passed through the sintered glass frit with OEt$_2$, which left behind an insoluble dark brown particulate. The resulting bright yellow filtrate was dried to afford a first pure crop weighing 197 mg. This procedure was repeated with the brownish filtrate to afford

a second pure crop of 65 mg, giving an overall yield of 262 mg (ca. 53 %). ^{1}H NMR (300 MHz, C_6D_6, 25 °C): δ = 6.64 (s, 5), 5.88 (v br s, 4), 2.04 (s, 3), 1.45 (s, 1) ^{13}C NMR (125.66 MHz, C_6D_6, 25 °C): δ = 294.6 (d, Mo≡*C*PCl$_2$), $^1J_{CP}$ = 144 Hz), 150.1 (aryl), 137.6 (aryl), 130.7 (aryl), 127.7 (aryl), 62.3 (6), 33.7 (1, 2), 21.8 (3). ^{31}P NMR (202.276 MHz, C_6D_6, 25 °C): 120.1 (d, Mo≡C*P*Cl$_2$), $^1J_{CP}$ = 144 Hz). Anal. Calcd for $C_{37}H_{36}D_{18}Cl_2MoP$: C, 58.72; H, 7.19; N, 5.55. Found: C, 58.64; H, 7.18; N, 5.50.

4.30 Synthesis of ClP(C≡Mo(N[R]Ar)$_3$)$_2$.

A cold yellow solution containing 94.5 mg [K][**8**] (0.1361 mmol) in 4 mL of OEt$_2$ was added via pipette to a stirring, chilled solution containing 103 mg of yellow Cl$_2$PC≡Mo(N[R]Ar)$_3$ (0.1361mmol) in 4 mL of OEt$_2$. As the solution warmed to ambient temperature the color turned deep orange. Stirring was continued for 3 h at 25 °C, after which time the reaction volatiles were removed. The remaining residue was extracted with 10 mL of pentane and filtered through Celite. The orange filtrate was stored at -35 °C for several hours, yielding a grey precipitate which did not redissolve in pentane. This was discarded, and the orange supernatant was concentrated to 4 mL and stored at -35 °C overnight. A tan-orange precipitate formed which was isolated and analyzed spectroscopically. This powder contained ca. 90 % ClP(C≡Mo(N[R]Ar)$_3$)$_2$ and ca. 10 % HC≡Mo(N[R]Ar)$_3$. Spectroscopic data for ClP(C≡Mo(N[R]Ar)$_3$)$_2$ was as follows: ^{1}H NMR (300 MHz, C_6D_6, 25 °C): δ = 6.71 (s, 5), 6.05 (v br s, 4), 2.14 (s, 3), 1.67 (s, 1) ^{13}C NMR (125.66 MHz, C_6D_6, 25 °C): δ = 301.4 {d, (Mo≡*C*)$_2$PCl, $^1J_{CP}$ = 149 Hz}, 151.4 (aryl), 137.1 (aryl), 131.2 (aryl), 130.7 (aryl), 62.0 (6), 34.2 (1, 2), 21.9 (3). ^{31}P NMR (202.276 MHz, C_6D_6, 25 °C): 129.7 {m, (Mo≡C)$_2$*P*Cl}.

4.31 Synthesis of K(benzo-15-crown-5)$_2$[S-CH$_2$CH$_2$C≡Mo(N[R]Ar)$_3$].

A homogeneuos yellow solution containing 98.6 mg of [K][**8**] (0.1421 mmol) in 3.5 mL of OEt$_2$–THF (15:1) was chilled to -35 °C. A pre-chilled solution of ethylene sulfide (11 mg, 0.183 mmol) in 3 mL of OEt$_2$ was then added dropwise to the stirring solution of [K][**8**]. Stirring was continued for 1 h at 25 °C, after which time the solution was a light peach color. Removal of the reaction volatiles *in vacuo* gave an oily residue with ^{13}C and ^{1}H NMR data consistent with a major new product [K][S-CH$_2$CH$_2$C≡Mo(N[R]Ar)$_3$] and ca. 30 % HC≡Mo(N[R]Ar)$_3$. ^{1}H NMR (300 MHz, C_6D_6, 25 °C): δ = 6.65 ppm (s, 5), 6.09 (v br s, 4), 4.30 (br m, SC*H*$_2$CH$_2$C≡Mo), 3.85 (br m, SCH$_2$C*H*$_2$C≡Mo), 2.13 (s, 3), 1.76 (s, 1) ^{13}C NMR (125.66 MHz, C_6D_6, 25 °C): δ = 304.0 (br, Mo≡*C*CH$_2$CH$_2$S$^-$K$^+$), 151.7 (aryl), 137.3 (aryl), 131.0 (aryl), 61.4 (6), 35.0-34.0 (1, 2, and overlapping methylene carbons), 22.0 (3). Attempts to effectively crystallize [K][S-CH$_2$CH$_2$C≡Mo-(N[R]Ar)$_3$] from pentane were not successful. However, addition of ca. 2 eq of benzo-15-crown-5 to the crude product mixture in OEt$_2$–THF (10:1) effected fast precipitation of the yellow discrete salt complex K(benzo-15-crown-5)$_2$[S-CH$_2$CH$_2$C≡Mo(N[R]Ar)$_3$]. Decanting the supernatant and subsequent pentane washing of the remaining solid effectively removed the HC≡Mo(N[R]Ar)$_3$ impurity. Recrystallization from pentane–THF afforded 52 mg of crystalline K(benzo-15-crown-5)$_2$[S-CH$_2$CH$_2$C≡Mo(N[R]Ar)$_3$]. Anal. Calcd for $C_{67}H_{80}D_{18}N_3KMoO_{10}S$ C, 62.35; H, 7.65; N, 3.26. Found: C, 61.87; H, 7.59; N, 3.25.

4.32 $Cl_2PC{\equiv}Mo(N[R]Ar)_3$ + $Cp_2Zr(H)(Cl)$. Generation of $H_2PC{\equiv}Mo(N[R]Ar)_3$.

A yellow solution containing 99.6 mg of $Cl_2PC{\equiv}Mo(N[R]Ar)_3$ (0.1316 mmol) in 7 mL of benzene was added quickly to a stirring slurry of $Cp_2Zr(H)(Cl)$ in 3 mL of benzene at 25 °C. A purplish color resulted within ca. 10 minutes and after 1 h the volatiles were removed *in vacuo*. The resulting residue was extracted with 12 mL of pentane and filtration removed a pinkish–white residue (Cp_2ZrCl_2). The filtrate dried to a constant weight of 95.6 mg. Recrystallization of this solid from 3 mL of pentane produced 47.1 mg of a solid which was seemingly off-white in color but contained a small amount of intensely colored blue-purple impurities. Complete spectroscopic analyses (^1H, ^{13}C, and ^{31}P NMR) of this complex were consistent with its formulation as $H_2PC{\equiv}Mo(N[R]Ar)_3$, but an analytically pure sample has not yet been obtained. ^1H NMR (300 MHz, C_6D_6, 25 °C): δ = 6.64 (s, 5), 6.60 (br s, 4), 5.40 (br d, $Mo{\equiv}CPH_2$, $^1J_{PH}$ = 175 Hz), 2.07 (s, 3), 1.49 (s, 1). ^{13}C NMR (125.66 MHz, C_6D_6, 25 °C): δ = 288.9 (m, $Mo{\equiv}CPH_2$), 151.4 (aryl), 137.4 (aryl), 130.6 (aryl), 128.0 (aryl), 62.4 (6), 34 (1, 2), 21.9 (3). ^{31}P NMR (202.276 MHz, C_6D_6, 25 °C): δ = -81.7 ppm (br m, $Mo{\equiv}CPH_2$, $^1J_{PH}$ = approx. 175 Hz).

4.33 $[K][C{\equiv}Mo(N[R]Ar)_3]$ + $Mo(N[R]Ar)_3$ under N_2.

Solid yellow $[K][C{\equiv}Mo(N[R]Ar)_3]$ (51 mg, 0.0735 mmol) and solid orange $Mo(N[R]Ar)_3$ (47.2 mg, 0.0735 mmol) were weighed into a chilled vial to which 4 mL of cold OEt_2 (-35 °C) was added at once. The initially orange solution darkened within 10 minutes stirring as it was allowed to warm. An aliquot after 5 minutes was inspected by FTIR and showed a broad stretch centered at 1727 cm^{-1}. Over a 70 minute period the reaction solution darkened to a deep red and a second FTIR spectrum acquired at this time showed that the broad ν_{NN} stretch at 1727 cm^{-1} had dramatically increased in intensity. The reaction volatiles were removed *in vacuo* and a ^1H NMR spectrum of the crude residue showed two products in a 1:1 ratio, one being $HC{\equiv}Mo(N[R]Ar)_3$ and the other assigned as $[K][(N_2)Mo(N[R]Ar)_3]$. A ^{13}C NMR spectrum showed one signal for the carbide carbon atom at 287.5 ppm, consistent with $HC{\equiv}Mo(N[R]Ar)_3$ as the only carbide-carbon containing product.

References

[1] Holt, E. M.; Whitmire, K. H.; Shriver, D. F. *J. Organomet. Chem.*, **1981**, *213*, 125.

[2] Chisholm, M. H.; Hammond, C. E.; Johnston, V. J.; Streib, W. E.; Huffman, J. C. *J. Am. Chem. Soc.*, **1992**, *114*, 7056.

[3] Peters, J. C.; Odom, A. L.; Cummins, C. C. *J. Chem. Soc., Chem. Commun.*, **1997**, 1995.

[4] Evans, D. F. *J. Chem. Soc.*, **1959**, 2003.

[5] Sur, S. K. *J. Magnetic Resonance*, **1989**, *82*, 169.

[6] Landrum, G. A., YAEHMOP: Yet Another Extended Molecular Orbital Package, version 2, 1997. This package is available on the WWW at URL: http://overlap.chem.cornell.edu:8080/yaehmop.html

[7] Peters, J. C.; Johnson, A. R.; Odom, A. L.; Wanandi, P. W.; Davis, W. M.; Cummins, C. C. *J. Am. Chem. Soc.*, **1996**, *118*, 10175.

[8] Simões, J. A. M.; Greenberg, A.; Liebman, J. F. *Energetics of Oganic Free Radicals (Search Series)*; Ed.; Chapman & Hall: New York, **1996**, vol. *4*.

[9] Kochi, J. K. *Free Radicals. Volume 1*; J.K. Kochi, Ed.; John Wiley and Sons: **1973**.

[10] Nikishin, G. I.; Vinogradov, M. G.; Kereselidge, R. V. *Bull. Adam. Sci. USSR*, **1967**, 1570.

[11] Schorigin, P. *Chem. Ber.*, **1924**, *57*, 1627.

[12] Hartwig, W. *Tetrahedron*, **1983**, *39*, 2609.

[13] Nugent, W. A.; Mayer, J. M. *Metal-Ligand Multiple Bonds*; John Wiley and Sons: New York, 1988.

[14] Schrock, R. R.; Seidel, S. W.; MoschZanetti, N. C.; Shih, K. Y.; O'Donoghue, M. B.; Davis, W. M.; Reiff, W. M. *J. Am. Chem. Soc.*, **1997**, *119*, 11876.

[15] Schrock, R. R.; Seidel, S. W.; MoschZanetti, N. C.; Dobbs, D. A.; Shih, K. Y.; Davis, W. M. *Organometallics*, **1997**, *16*, 5195.

[16] Shih, K.-Y.; Totland, K.; Seidel, S. W.; Schrock, R. R. *J. Am. Chem. Soc.*, **1994**, *116*, 12103.

[17] Jamison, G. M.; Bruce, A. E.; White, P. S.; Templeton, J. L. *J. Am. Chem. Soc.*, **1991**, *113*, 5057.

[18] Churchill, M. R.; Rheinghold, A. L.; Wasserman, H. J. *Inorg. Chem.*, **1981**, *20*, 3392.

[19] Manna, J.; Kuk, R. J.; Dallinger, R. F.; Hopkins, M. D. *J. Am. Chem. Soc.*, **1994**, *116*, 9793.

[20] Sharp, P. R.; Holmes, S. J.; Schrock, R. R.; Churchill, M. R.; Wasserman, H. J. *J. Am. Chem. Soc.*, **1981**, *103*, 965.

[21] Chisholm, M. H.; Folting, K.; Hoffman, D. M.; Huffman, J. C. *J. Am. Chem. Soc.*, **1984**, *106*, 6794.

[22] Schlosser, R. R.; Hartmann, J. *Angew. Chem. Int. Ed. Engl.*, **1973**, *12*, 508.

[23] Weiss, E. *Angew. Chem. Int. Ed. Engl.*, **1993**, *32*, 1501.

[24] Laplaza, C. E.; Johnson, M. J. A.; Peters, J. C.; Odom, A. L.; Kim, E.; Cummins, C. C.; George, G. N.; Pickering, I. J. *J. Am. Chem. Soc.*, **1996**, *118*, 8623.

[25] Laplaza, C. E.; Davis, W. M.; Cummins, C. C. *Angew. Chem. Int. Ed., Engl.*, **1995**, *34*, 2042.

[26] Wu, G.; Rovnyak, D.; Johnson, M. J. A.; Zanetti, N. C.; Musaev, D. G.; Morokuma, K.; Schrock, R. R.; Griffin, R. G.; Cummins, C. C. *J. Am. Chem. Soc.*, **1996**, *118*, 10654.

[27] Casey, C. P.; Meszaros, M. W.; Fagan, P. J.; Bly, R. K.; Marder, S. R.; Austin, E. A. *J. Am. Chem. Soc.*, **1986**, *108*, 4043.

[28] Casey, C. P.; Gohdes, M. A.; Meszaros, M. W. *Organometallics*, **1986**, *5*, 196.

[29] March, J. M. *Advanced Organic Chemistry, 4th Ed.*; John Wiley & Sons: New York, 1992.

[30] Buchwald, S. L.; LaMaire, S. J.; Nielsen, R. B.; Watson, B. T.; King, S. M. *Tetrahedron Lett.*, **1987**, *28*, 3895.

[31] Holmes, S. J.; Schrock, R. R.; Churchill, M. R.; Wasserman, H. J. *Organometallics*, **1984**, *3*, 476.

[32] Jamison, G. M.; White, P. S.; Templeton, J. L. *Organometallics*, **1991**, *10*, 1954.

[33] List, A. K.; Hillhouse, G. L.; Rheingold, A. L. *Organometallics*, **1989**, *8*, 2010.

[34] Broadhurst, P. V. *Polyhedron*, **1985**, *4*, 1801.

[35] Clark, G. R.; Marsden, K.; Rickard, C. E. F.; Roper, W. R.; Wright, L. J. *J. Organomet. Chem.*, **1988**, *338*, 393.

[36] Clark, G. R.; James, S. M. *J. Organomet. Chem.*, **1977**, *134*, 229.

[37] Johnson, A. R.; Davis, W. M.; Cummins, C. C.; Serron, S.; Nolan, S. P.; Musaev, D. G.; Morokuma, K. *J. Am. Chem. Soc.*, **1998**, *120*, 2071.

[38] Bühl, M.; van Eikema Hommes, N. J. R.; von Ragué Schleyer; Fleischer, U.; Kutzelnigg, W. *J. Am. Chem. Soc.*, **1991**, *113*, 2459.

[39] Pangborn, A. B.; Giardello, M. A.; Grubbs, R. H.; Rosen, R. K.; Timmers, F. J. *Organometallics*, **1996**, *15*, 1518.

Acknowledgements

The rapid pace of these past four years was not ideally suited to taking adequate time in thoughtfully thanking those individuals to whom I am grateful. I will take a moment to do so now.

I entered graduate school searching for a place to learn the craft of inorganic chemistry, particularly in the synthesis of new inorganic complexes. I gambled on Professor Kit Cummins, my research mentor, to guide me towards that endeavor. Kit exceeded my expectations and I am grateful for his friendship, his idealistic approach to chemistry, and to his enthusiasm for inorganic synthesis, an enthusiasm which he in turn triggered in me. I have been proud to be a member of his research group and to contribute to our group's efforts. To my delight, Kit surrounded himself with some very young yet talented individuals during his first year as a professor. Kit, Mike Fickes, Adam Johnson, Marc Johnson, Catalina Laplaza, Sheree Stokes, and Aaron Odom welcomed me warmly into the Cummins Group and enhanced my growth as a chemist in every possible way. I am thankful for Cati's untapping of $Mo(N[R]Ar)_3$, the complex around which my entire thesis is centered, and to Aaron's help with an array of X-ray structures contained herein. Aaron provided me with a sound example of the many qualities which every productive chemist should have. Marc and Adam, who like myself bought stock in $Mo(N[R]Ar)_3$, made my work an enjoyably shared experience. With time, I came to greatly value and respect Marc's intellectual agility and his strict adherence to academic honesty. Mike and Sheree, aside from having adept hands and heaps of generosity to offer to all of us, provided me with encouragement and close friendship throughout this process. Newer group members such as Luis Baraldo, Jane Brock, Steve Klei, and Daniel Mindiola added a well-needed refreshment to the latter part of my graduate experience. I wish to especially thank Luis Baraldo and Daniel Mindiola for their enthusiastic help with electrochemistry and X-ray crystallography, respectively.

I am lucky to have had the Schrock group, particularly my classmates Myra O'Donoghue and Robert Baumann and Professor Schrock himself, in close proximity. My own work has greatly benefited from my interactions with them and from the work done in their labs. I am also indebted to Dr. Bill Davis for his friendship and for mounting and solving the structure of the terminal carbide complex presented in Chapter 3. Professor Nocera arrived at MIT recently and his presence immediately impacted me and my group in a very positive way. Professor Alan Davison and Lynn Davison embraced Kit and his young band of chemists generously, and in so doing, buffered our group through many of its growing pains. I eagerly continue to embrace them.

I wisely accepted Dietrich Steinheubel, Robert Baumann, Dan LeCloux, and Mike Fickes as my mates when I arrived here in Boston. It was their input which I often sought in defining the direction and worth of my research, as well as my life in general. The staff at a nearby pub, especially my favorite waitress Dr. Tracey Slater, are to be thanked for providing Dietrich, Dan, Robert, Mike and myself with an inviting environment in which to unwind. While we took our issues to many a pub, it is at the Miracle that many of our ideas were generated - most of which never worked.

I am grateful to the University of Chicago, in particular to Professors Gregory Hillhouse and his late colleague Jeremy Burdett, for initially sparking my interest in inorganic chemistry and for giving me some solid tools with which to begin this long process. Greg continuously provides me with his friendship and reminds me that chemical research is but one of our most important responsibilities. Professor J. J. Turner, my inorganic mentor at Nottingham, remains my quiet

standard of a great scientist and a true gentleman. I have missed both Greg and Jim dearly these past few years.

Finally, I thank my family. I am grateful to my brother Jonathan and my second dad, Robert Mendelson, for being a part of my life and the lives of people for whom I deeply care. This is also true of my extended family. As for my parents, Mayleen Mendelson and James Peters, I have constantly asked them for their patience and for their understanding. They have given both to me unwaiveringly. I thank my mom and dad for being the only people I will ever encounter who ask of me nothing and yet give me everything. I am grateful simply to be their son. And I am happy to dedicate the work of my thesis to them.